Title
Effect of Environmental Variables on the Flammability of Fire Resistant Materials

Author
Osorio, Andres Felipe

Publication Date
2014

Peer reviewed|Thesis/dissertation

Effect of Environmental Variables on the Flammability of Fire Resistant Materials

by

Andres Felipe Osorio

A dissertation submitted in partial satisfaction of the
requirements for the degree of
Doctor of Philosophy

in

Engineering – Mechanical Engineering

in the

Graduate Division

of the

University of California, Berkeley

Committee in charge:

Professor A. Carlos Fernandez-Pello, Chair
Professor Jyh-Yuan Chen
Professor Scott Stephens

Fall 2014

Effect of Environmental Variables on the Flammability of Fire Resistant Materials

Abstract

Effect of Environmental Variables on the
Flammability of Fire Resistant Materials

by

Andres Felipe Osorio

Doctor of Philosophy in Engineering – Mechanical Engineering

University of California, Berkeley

Professor A. Carlos Fernandez-Pello, Chair

This work investigates the effects of external radiation, ambient pressure and microgravity on the flammability limits of fire-resistant (FR) materials. Future space missions may require spacecraft cabin environments different than those used in the International Space Station, 21%O_2, 101.3kPa. Environmental variables include flow velocity, oxygen concentration, ambient pressure, micro or partial-gravity, orientation, presence of an external radiant flux, etc. Fire-resistant materials are used in astronauts, firefighter, and racecar driver suits, cable harnesses, airplane components, etc. However, their fire resistant characteristics, including flammability limits may depend on the environmental conditions and require further study.

The addition of an external radiant flux is able to extend the flammability limits of materials. Based on the results, there is a Limiting Oxygen Concentration (LOC) above which flame spread occurs without the aid of an external radiant flux. Below this critical oxygen concentration flame spread may occur if there is an external radiant flux large enough to allow the fabric to continue the pyrolysis process. Experiments with four different kinds of fabrics showed that FR material content affects the value of the minimum external radiant flux for flame spread. As FR material content increases, so does the value of the minimum external radiant flux.

Regarding the effect of ambient pressure, pressures above 70 kPa result in small changes in the LOC. However, as ambient pressure drops below 70 kPa reducing ambient pressure results in an increase in the LOC. This flammability behavior can be phenomenologically explained in terms of factors such as heat transfer between the flame and unburned solid, buoyancy induced flows, and chemical kinetics. A reduction in ambient pressure decreases the heat transfer from the flame to the unburned fuel while at the same time reducing buoyancy induced flows and the associated heat losses. Examining the Flame/No-Flame spread boundaries in terms of the ambient pressure and oxygen partial pressure revealed a nearly linear relationship between p and p_{O_2}. The reduction in p_{O_2} as a function of p suggests

that is possible for materials to exhibit significantly different flammability behavior when following a constant oxygen partial pressure curve, like for example normoxic atmospheres similar to those suggested for future spacecraft.

The combination of microgravity and/or addition of an external radiant flux are able to extend the flammability limits of ETFE insulated wires. Under no external radiant flux microgravity conditions resulted in a 6% decrease in the Limiting Oxygen Concentration (LOC) for opposed flame spread. When microgravity conditions were combined with an external radiant flux of 25 kW/m^2 the decrease in the LOC was 12%. Microgravity limits heat losses, making possible to reduce the oxygen concentration and flame temperature while maintaining a critical solid decomposition rate. External radiation is able to further compensate for reductions in flame temperature, resulting in a noticeable reduction between the $1g$ and μg LOC. The $1g$ and μg LOC values of ETFE insulated wires were also compared to those of polyethylene (PE) insulated wires. This comparison showed that μg results in a bigger change in the LOC of ETFE than PE. This observation is explained in terms of thermal parameters, critical mass flux and chemical kinetic effects.

Adoption of testing methodologies similar to those described in the present work can produce flammability maps that provide more information than Pass/Fail methods while presenting a clearer picture of the flammability of materials. The results of this work are important given that the flammability of materials is routinely tested without considering the effect of environmental variables, which according to the results presented in this dissertation, may not be indicative of the absolute flammability limits of materials.

Para la familia Osorio y
la familia Gonzalez

Table of Contents

List of Figures

List of Tables

Nomenclature

Letters

c	generic constant
g	gravity
h	elevation above sea level
k	thermal conductivity
l_b	burn length
l_f	flame length
l_h	heated length
l_p	pyrolysis length
$\dot{m}$	mass loss rate
n	reaction order
p	pressure
p_{O_2}	oxygen partial pressure
$\dot{q}''$	heat flux per unit area
$\dot{q}''_{MAX}$	external radiant flux at sample leading edge
$\dot{q}''_{MIN}$	minimum external radiant flux required for flame spread
$\dot{q}''_{cond}$	gas-phase conduction heat flux from the flame
$\dot{q}''_{conv}$	convective heat flux
$\dot{q}''_{core}$	heat flux to/from wire core
$\dot{q}''_{ext}$	external radiant flux

$\dot{q}''_{fr}$	radiant flux from the flame to the solid
$\dot{q}''_{sr}$	reradiation from the solid
$\dot{q}''_{tot}$	total heat flux
s	solid thickness
t	time
t_{chem}	chemical time
t_{ig}	ignition time
t_{mix}	mixing time
t_p	pyrolysis time
u	flow velocity parallel to the fuel surface
u_∞	forced flow free stream velocity
v	flow velocity normal to the fuel surface
A	pre-exponential factor in Arrhenius rate equation
Cp	specific heat
Da	Damkohler number
E_a	activation energy
Gr	Grashof number
Pr	Prandtl number
Re	Reynolds number
$\dot{Q}'$	heat release rate per unit length
T	temperature
T_o	solid initial temperature
T_p	pyrolysis temperature
V_f	flame spread rate

Y_i	mass fraction of specie i

Greek Symbols

β	volumetric thermal expansion coefficient
δ	boundary layer thickness
λ	lapse rate
μg	microgravity
$\dot{\omega}$	reaction rate
ρ	density
ΔH_c	heat of combustion
ΔH_p	heat of pyrolysis
ΔLOC	change in LOC due to μg

Subscripts

f	adiabatic flame
a	air
cr	critical
f	flame
g	gas
ig	ignition
on	moment sample wire ignites
p	pyrolysis
s	solid
F	fuel

O	oxidizer
∞	ambient condition

Abbreviations

FR	fire-resistant
HF	hydrogen fluoride
PE	polyethylene
UL	Underwriters Laboratories
HRR	Heat Release Rate
HRP	heat release parameter
ISS	International Space Station
JEM	Japanese Experiment Module
LOC	Limiting Oxygen Concentration
LOI	Limiting Oxygen Index
MOC	Maximum Oxygen Concentration
NFR	non fire-resistant
PLC	programmable logic controller
SEA	Space Exploration Atmospheres
TGA	Thermogravimetric Analysis
ETFE	ethylene tetrafluoroethylene
FIST	Forced Ignition and Flame Spread Test
JAXA	Japanese Aerospace Exploration Agency
PTFE	polytetrafluoroethylene
PMMA	polymethylmethacrylate
PP/GL	polypropylene/fiber glass
ULOI	Upward Limiting Oxygen Index

Acknowledgments

First of all, I would like to thank my parents because their unselfishness, unconditional support, and love have given my brother and I opportunities I could had never dreamed of. I will always be grateful for the sacrifices my parents have made to give us the the best opportunities in life. To my brother, Ruben, for always being there for me. For helping me move again and again despite living in Orlando, for listening when I need someone to listen, and for telling me things even when I do not want to hear them. To Katie, for being supportive, caring and a motivation to me. For being with me through the many ups and downs, joys and frustrations that a Ph.D. can be.

At UC Berkeley I have had the chance to learn from great professors, Professors Ömer Savaş, J.Y. Chen, Robert Dibble, and Scott Stephens. Thank you for helping me grow personally and academically, writing recommendation letters, and even for reviewing this dissertation. I also want to thank my research advisor, Professor Carlos Fernandez-Pello, who first took me as a summer undergraduate student and then giving me the opportunity to return as a graduate student. For equipping me with the necessary tools to succeed in graduate school and showing me that is possible have fun while doing research. For teaching me the "80/20 rule" and that sometimes it is "better to be lucky than good". Thank you for being the best advisor I could ask for and a great friend that I look up to.

During my time at the Combustion and Fire Processes Lab (CFPL) I have met a great number of individuals who have made a contribution to my work and made my time in the lab very memorable. To Sara McAllister for showing me what a great place UC Berkeley is, and how exciting research can be. To Sonia Fereres for helping me get started with my research and answering the many questions I have had over the years. To David Rich for his willingness to listen and provide insightful comments and suggestions. To Laurence Bernard and Shuhei Takahashi for being exceptional friends and opening my eyes about studying abroad. To the great undergraduate students that have helped me over the years, Andrew Ajirogi, Mathew Fisher, Debra Zepeda, Janna Rodriguez, Debera Hsiao, and Davis Tran. Thank you for your help with building experiments, cutting samples, sewing igniters, etc. I have truly enjoyed working with each of you.

To MaryAnne Peters for taking care of us in the lab and making sure everything runs smoothly. To other lab members, Casey Zak, Daniel Murphy, Shmuel Link, James Urban, Sarah Scott, Jennifer Jones, Dylan Bethel, Danielle Kirchmeyer, Chris Ategeka, Greg Noel, Anna Matala, Rory Hadden, Heinrik Hindborg, Romina Rodriguez, Colin Silla and Michelle Ma. Thank you for making the lab a great place to be and a place where I enjoyed working. To fellow Hesse Hall residents Scott McCormick, Michael Neufer, Pete Graham and Alex Jordan. Thank you for your assistance with everything related to Hesse Hall. It was a pleasure to be a GSI for ME 107 and ME 140 with your help.

I would like to thank Professor Osamu Fujita from Hokkaido University. Thank you for allowing me to join the Laboratory of Space Utilization (LSU) during my stay and giving me the opportunity to work on an extremely interesting project. To Ken Mizutani for being a great friend and an excellent coworker, and to the other members of the laboratory, who welcomed me and always helped me navigate life in Japan.

To my close friend and fellow Ph.D. candidate, Jaime Duarte. Numerous times we have confided about graduate school, life and what will come next. It is good to know someone who is going through the same process and understands your victories and disappointments. To friends outside the lab, Pablo, Jessica, Hans, Wendy, Roxana, Varada, Carlos, Kevin and Melanie. All of you are very special friends to me and I am thankful for your friendship. To friends back in Orlando, Omar, Vani, Albert, and David. You make me look forward to each visit and and make feel like nothing has changed there. To Jaime, Diego, and Juan, for showing me that distance and time do not matter in true friendships.

Finally, to the institutions and financial support that has made this research possible. Starting from the SUPERB REU program and its directors Beatriz Lopez-Flores and Meltem Erol, the UC Berkeley Chancellor's Fellowship, the NSF Graduate Fellowships Research Program (GRFP) Grant DGE1106400, NASA Grants NNX08BA77A and NNX12AN67A, NSF East Asia and Pacific Summer Institute (EAPSI), JAXA grant for the third phase utilization of JEM/ISS, and the Alfred P. Sloan Foundation Minority Ph.D. Program. A special mention to Dr. David L. Urban, Dr. Gary Ruff and Dr. Paul Ferkul from NASA Glenn Research Center. Thank you for your reviews, ideas, and suggestions related to this research.

CHAPTER 1

INTRODUCTION

1.1 Problem Overview

There is enough evidence to suggest that humans used fire 400,000 years ago, with some evidence suggesting its use as early as 1.5 million years ago[1, 2]. The use of fire by humans resulted in significant advancements such as an increased caloric intake thanks to cooking of food[3] and manufacturing of more efficient hunting tools through heat treatment of stones[4]. Though times have changed and humanity has come a long way since the stone age, fire still remains an important part in modern life. In the same way that harnessing fire has had a positive impact, fire can also take a more destructive personality and result in undesired consequences such as property destruction and loss of life. The need to better understand fire, its potential applications, and how to better protect against its negative consequences has captured the interest of many bright minds throughout time.

Our understanding of fire has greatly improved over the years[5], and according to Emmons[6] fire research holds a promising future. This improved knowledge about fire, in combination with government policies has resulted in steady decrease in the total number of fire incidents and fire related deaths over the last three decades[7]. One scenario in which reducing the risk of fires remains extremely important is space exploration. Future space exploration missions by NASA and other space agencies together with commercial space exploration have the potential to encourage the design of a new generation of spacecrafts and increase the number of humans traveling to space. An increased human presence in space also poses many challenges, particularly in fire safety. Fire in a spacecraft environment represents a particularly dangerous situation given the combined effects of extended periods of time, confined space, and microgravity.

The current fire safety strategy in space exploration relies on selecting materials not likely to be flammable inside a spacecraft. In an ideal situation it would be possible to test the flammability of materials used in a spacecraft directly in space, however this is

an expensive and very unlikely possibility. A more reasonable alternative is to develop testing methodologies intended to represent worst-case scenarios that can provide some useful information regarding the flammability behavior of a particular material in space. One of such testing methodologies is NASA Standard 6001, which establishes guidelines for testing the flammability, odor, and offgassing characteristics of materials used in spacecraft[8]. In this standard, criteria such as burn length, burn propagation, self-extinguish and dripping behavior are used to determine if a material can be considered for use in a spacecraft, or if additional considerations are required.

On earth flammability standards are used to regulate a wide number of products including building materials, textiles, furnishings, and consumer electronics to name a few. These standards are developed by a combination of government agencies, and international standards and certification organizations such as ASTM International or Underwriters Laboratories (UL) among others. The main purpose of these standards is to characterize and classify the behavior of products during a fire. Standardized testing makes possible to determine important flammability indicators such as ignition delay time, minimum oxygen concentration for sustained burning, critical heat flux for ignition, flame spread rate, etc. These indicators can be used to make inferences regarding the behavior of materials during a fire. An actual prediction is a difficult task given that each fire is unique and may not necessarily replicate the conditions stipulated in standardized testing methodologies.

The primary goal of this research is to understand the effect that environmental variables such as oxygen concentration, environmental pressure, external radiation, and microgravity have on the flammability limits of fire-resistant (FR) materials used in space applications. One important aspect of the present research is the use of FR materials that have been used in space applications. Traditionally, well characterized materials such as polymethylmethacrylate (PMMA), or polyethylene (PE) insulated wires have been used, whereas only a few number of studies have used FR materials actually used in space applications. In this research, experiments under a different combination of environmental variables are used to determine flammability maps in terms of the minimum conditions that result in flame spread over FR materials. Characterizing flammability behavior in each possible scenario is a taunting task. However, a better understanding of the relationship between environmental variables and material flammability can greatly benefit fire safety in both space and earth applications.

1.2 Background

In space exploration as well as more traditional earth instances it is impossible to completely eliminate the risk a fire, however there are alternative methods for reducing the risk of a fire to an acceptable level. One method that is routinely used in space applications is limiting the potential fuel sources through the use of FR materials. As their name indicates, FR materials are not expected to be flammable in the expected cabin environment because they

may be difficult to ignite, or once ignite self-extinguish. Some examples include the use of FR fabrics for astronaut spacesuits, FR wire insulations, FR polymeric materials, etc. Fire-resistant materials are not only reserved for space applications, firefighters and race car drivers use suits made of Nomex, aircraft interiors and tray tables are made Kydex, a FR polymeric material, to name a few examples.

Determining whether materials are flammable in a selected environment is difficult since flammability can be easily affected by numerous variables. For example, two identical samples may exhibit different flammability behaviors as a result of exposure to different environmental conditions. Environmental conditions is a general term used to describe variables such as oxygen concentration, ambient pressure, surrounding air velocity, material orientation, and gravity ,among others. Some of these conditions may enhance the flammability, some others may decrease it, and in occasions they may result in an initial decrease followed by an increase, or vice versa.

There is also the pending issue of defining flammability. Flammability may be interpreted as the ease of ignition, the ability for flames to propagate, or a combination of both. Depending on the application one definition may be more convenient than another. For example, in order to reduce potential source of fires one may be interested in studying the ease of ignition of materials, whereas in buildings one may be more interested in the rate at which flames propagate. NASA flammability testing uses an upward flame propagation test in order to assess the flammability of materials used in space applications[8]. Flame spread in FR materials is a complex process that involves solid and gas phase combustion, subject to the surrounding environment. The following sections will introduce relevant literature pertaining flame spread, the relationship between flammability and environmental variables, and a brief review of fire-resistant materials.

1.2.1 Flame Spread in Thin Fuels

Flame spread in solid fuels has been extensively studied as evidenced by the comprehensive reviews in[9–13]. Flame spread can be viewed as a solid ignition process in which the flame acts as both, the heat source for the solid pyrolysis and the pilot[10]. A propagating flame will transfer heat to a region ahead of the pyrolysis front of the flame heating the fuel to its pyrolysis temperature. The time required to bring the heated region to its pyrolysis temperature is analogous to the ignition time in a solid. Thus, the flame spread rate can be interpreted as the ratio of the heated region ahead of the flame to the solid ignition time, i.e. $V_f = l_h/t_{ig}$. Depending on the flame, flow and fuel thickness characteristics l_h and t_{ig} will take on different forms.

Generally speaking, flame spread can be categorized in terms of the fuel thickness and the direction of flame propagation with respect to the oxidizer flow as shown in Figure 1.1. The classification in terms of solid fuel thickness is based on the limiting cases of heat

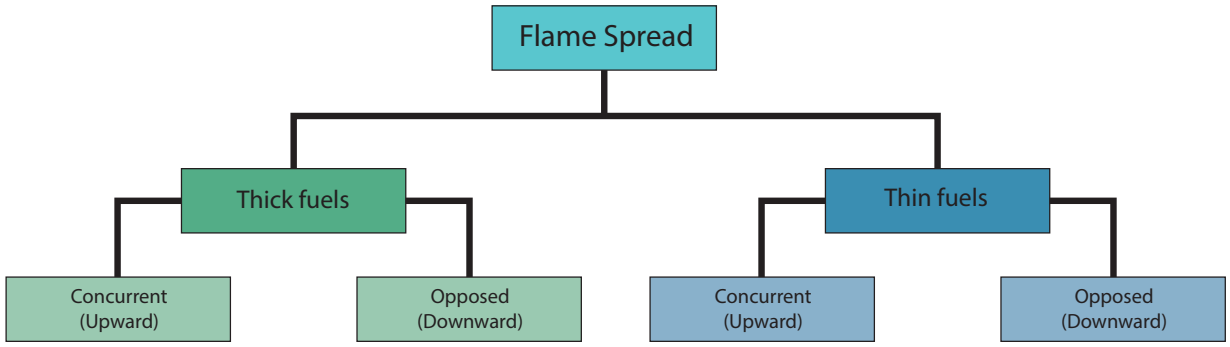

Figure 1.1: Generalized classification of flame spread over solid fuels.

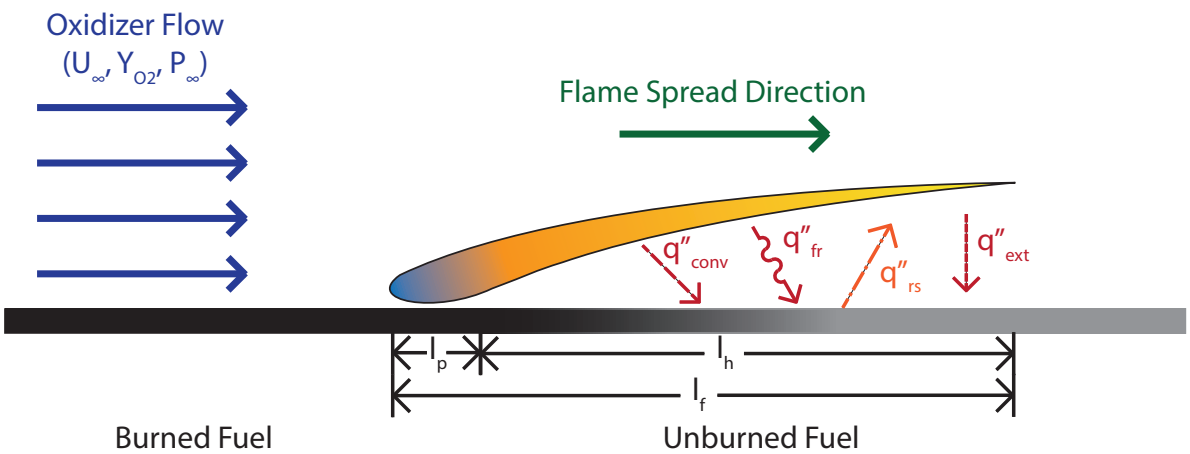

Figure 1.2: Schematic of concurrent flame spread in solids.

transfer to the solid fuel. For thermally thick fuels, the thickness is greater than the heat penetration layer at a particular time[10], whereas in thermally thin fuels it is assumed that temperature across the fuel thickness is uniform[9]. Within a particular fuel category flame spread can once again be broken into two categories, concurrent and opposed flame spread, which are schematically shown in Figure 1.2 and Figure 1.3. In concurrent flame spread flames propagate in the same direction as the flow, while in opposed flame spread they propagate against the flow. It is worth mentioning that the flow can be forced flow or buoyancy driven flow, since the fundamental process is the same except that forced flow expressions are replaced by natural convection ones.

The first and perhaps one of the most known flame spread theories is the deRis[14] model. Recognizing the importance of heat transfer from the flame to the solid fuel deRis made specific assumptions that allowed him to analytically solve the flame spread problem.

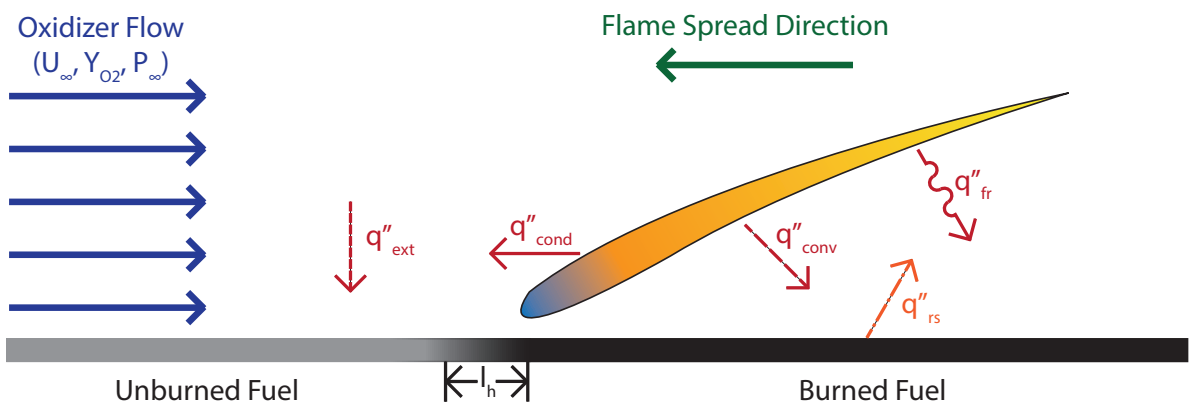

Figure 1.3: Schematic of opposed flame spread in solids.

In the deRis model it is assumed that the gas phase has constant properties and a uniform velocity profile, also known as the Oseen flow assumption, i.e. $u = u_\infty$, $v = 0$. The solid fuel is treated as a vaporizing solid that does not vaporize until reaching a vaporization temperature, T_v, and that once it reaches this temperature it continues to vaporize at this constant temperature. Mass transfer is assumed to occur by convection parallel to the fuel surface and by diffusion perpendicular to the fuel surface. The combustion reaction results in a diffusion flame that is assumed to occur infinitely fast in the gas phase only. Solving the corresponding governing equations results in the following expression for flame spread in thermally thin fuels:

$$V_f = \sqrt{2}\left(\frac{k_s}{\rho_s Cp_s s}\right)\left(\frac{k_s}{k_g}\right)\left(\frac{k_g \rho_g Cp_g}{k_s \rho_s Cp_s}\right)^{1/2}\frac{T_f - T_v}{T_v - T_o} \tag{1.2.1}$$

where V_f is the flame spread rate, k is the thermal conductivity, ρ is the density, Cp is the heat capacity, s is the fuel thickness, T_f is the flame temperature and T_∞ the ambient temperature. Subscripts s and g denote solid and gas respectively.

A similar expression was obtained by Williams[15] using the fundamental fire spread equation shown in Equation 1.2.2. In this equation, q is the total heat transferred from the flame to the solid, and Δh is the thermal enthalpy change between the fuel at ignition and ambient conditions. Equation 1.2.2 can be applied over a wide range of applications by properly specifying q. In this model it is assumed that gas phase conduction is the dominant heat transfer mode resulting in an expression analogous to Equation 1.2.1. This assumption is valid given that for thin fuels the path for heat transfer through the solid phase is limited[9]

and was verified by the heat flux calculations conducted by Hirano et al.[16].

$$q = \rho_s V_f \Delta h \tag{1.2.2}$$

The biggest limitation of the deRis[14], Williams[15] and similar models is that they fail to incorporate chemical effects. For low flow velocities and/or high oxygen concentrations and temperatures the chemical time is very short and heat transfer to the solid dominates rendering chemical kinetic effects negligible. On the other hand, for high flow velocities and/or low oxygen concentrations and temperatures the delay of the gas phase chemical reaction takes over. Accounting for chemical effects results in the flame spread expressions obtained by Fernandez-Pello and Williams[17] and Fernandez-Pello[10]. The flame spread expressions in [10] still retain a similarity to Equation 1.2.1 although they incorporate more elaborate expressions of the heat transfer from the flame to the solid and ignition time.

1.2.2 Environmental Variables

Material flammability does not only depend on the nature of the material and its physical and chemical properties, but also on its surrounding environment. For example, two identical samples may exhibit different flammability behaviors as a result of exposure to different environmental conditions. Environmental conditions is a general term used to describe variables such as external radiant heating, oxygen concentration, ambient pressure, oxidizer flow velocity, material orientation, and gravity among others. For example, a material may be considered fire resistant if it does not burn in ambient conditions, i.e. $P = 101.3\ kPa$, $[O_2]$=21%. However, this does not imply that the material is fire resistant for all conditions. Increasing the oxygen concentration, exposing the material to an external heat source, or reducing gravity to name a few are possible changes in the environmental variables that can turn fire resistant materials into flammable ones. In normal ambient conditions, Nomex, a fabric used for firefighters clothing, race car driver suits and astronauts suits is fire-resistant. But if the oxygen concentration is raised high enough flames can spread along the surface of the fabric as seen in Figure 1.4.

1.2.2.1 Oxygen Concentration

Oxygen concentration is one of the most studied environmental variables given that without oxygen combustion cannot take place. Numerous studies including [18–23] to name a few, have investigated the effect of oxygen concentration on flame spread. As Fernandez-Pello and Hirano point out in [9] early research on the combined effects of oxidizer flow velocity and oxygen concentration resulted in contradicting results. According to some researchers flame spread rate remained nearly constant for low velocities up to a limiting velocity, and beyond this velocity the flame spread rate decreases sharply. However, some other researchers found that flame spread increased with increasing oxidizer flow velocity. In experiments with thick

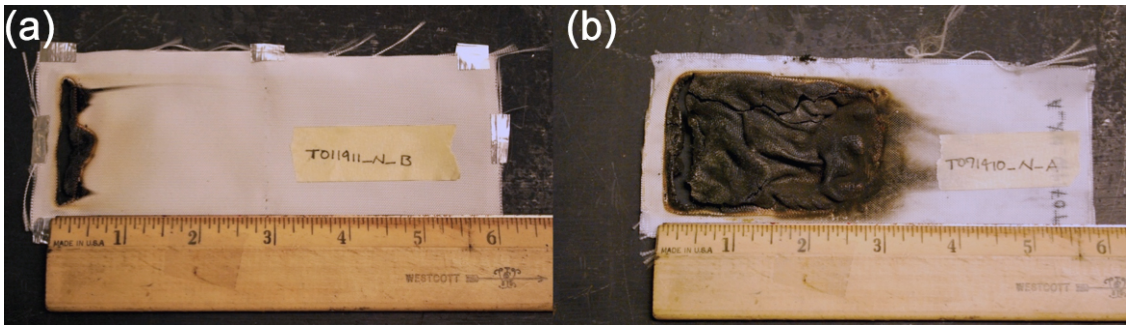

Figure 1.4: Example of the effect of environmental variables in the flammability of Nomex HT90-40. In (a) $[O_2]$=21% whereas in (b) $[O_2]$=40%. $p = 101.3\ kPa$ in both cases.

PMMA samples, Lastrina et al.[20] were able to observe the apparently contradictory results, however it was not until the work of Fernandez-Pello et al.[18] that a more comprehensive investigation was conducted. Fernandez-Pello et al.[18] conducted opposed flame spread experiments with thick PMMA sheets and thin paper sheets over a wide range of oxidizer flow velocities and oxygen concentrations.

When analyzing the results Fernandez-Pello et al.[18] noted that the observed behavior could not be explained in terms of heat transfer alone. Instead, they proposed that flame spread is controlled by heat and mass transfer processes in addition to chemical kinetic effects. Moreover, they suggested that by considering the extreme cases it was possible to understand their combined effect. The approach taken by Fernandez-Pello et al.[18] consisted on correlating the non-dimensional flame spread rate, $\overline{V_f}$, to the Damkohler number, Da. Plotting the experimental results in terms of the non-dimensional spread rate and Da showed that the results 'correlate extremely well' as evidenced by the results in Figure 1.5 and Figure 1.6. Altenkirch et al.[24] also observed a similar correlation in experiments with thin paper sample over a wide range of oxygen concentrations, ambient pressures and gravity conditions.

Correlating $\overline{V_f}$ to Da was an important step towards understanding the interaction between thermal and chemical kinetic effects. For low Da numbers, that is low oxygen concentrations and high oxidizer flow velocities, chemical kinetic effects dominate flame spread. As Da increases, chemical kinetic effects start becoming less important to the point that at high Da, high oxygen concentration or low flow velocity, the reaction rate is fast and thermal effects dominate flame spread.

Oxygen concentration can also affect the solid decomposition. Hirata et al.[25] studied the solid decomposition of PMMA in pure nitrogen and air environments. Their results showed that at low temperatures degradation in air increases the stability of PMMA, whereas at high temperatures it destabilizes PMMA by shifting the peak mass loss rate to a lower

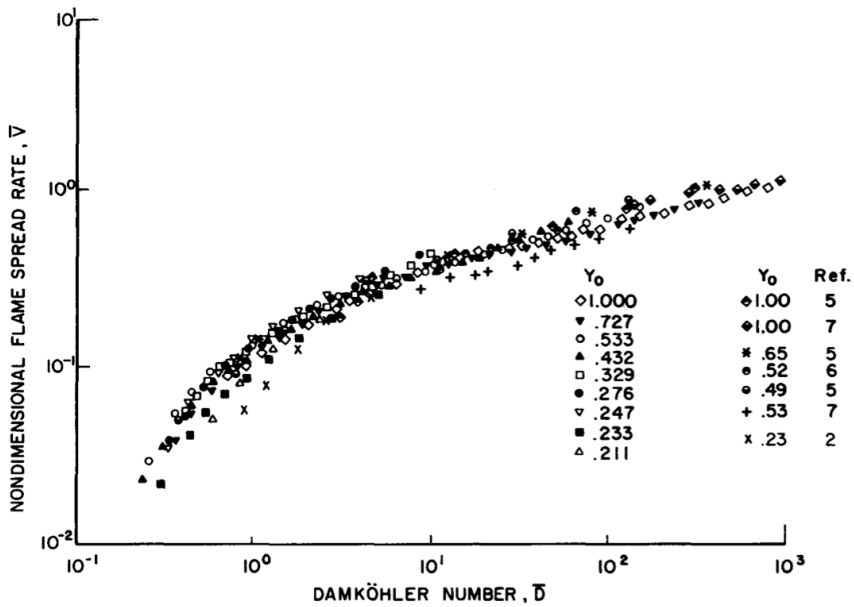

Figure 1.5: Non-dimensional flame spread rate over thick PMMA sheets (Fernandez-Pello et al.[18]).

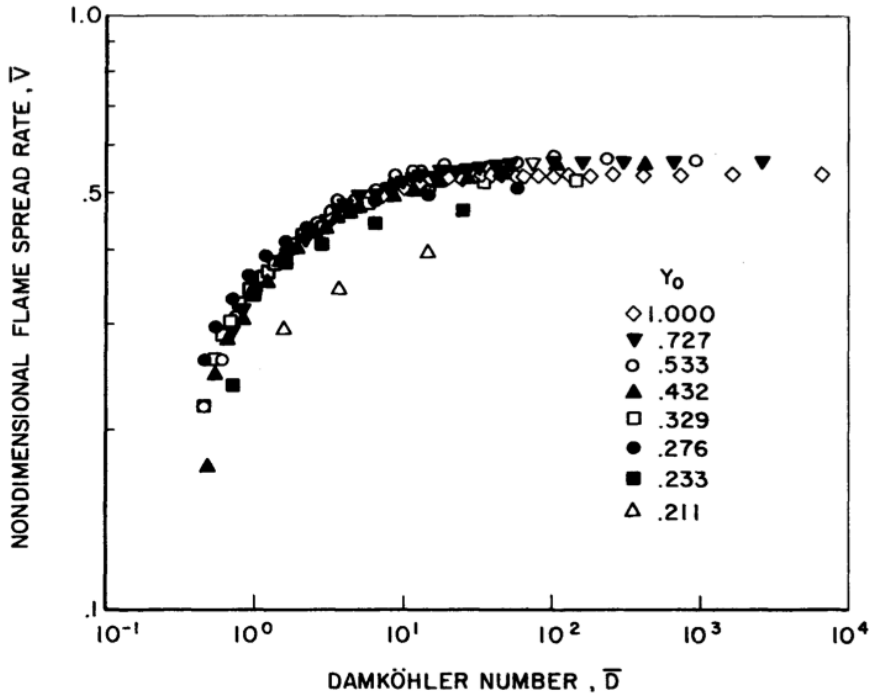

Figure 1.6: Non-dimensional flame spread rate over thin paper sheets (Fernandez-Pello et al.[18]).

temperature when compared to degradation in pure nitrogen. Kashiwagi and Ohlemiller[26] conducted similar solid degradation experiments with PMMA and PE under different levels of external radiation and oxygen concentrations. Results from these experiments showed that external radiant fluxes and oxygen concentration affect the mass loss rate of PMMA and PE. Based on these results Kashiwagi and Ohlemiller concluded that transient solid decomposition cannot be described just in terms of surface temperature, but that oxidative chemical reactions need to be included among others. One example of such models is the one developed by Lautenberger and Fernandez-Pello[27]. This generalized pyrolysis model provides good agreement with the experimental results of Kashiwagi and Ohlemiller[26] and other more complex solid decomposition cases including charring and intumescent materials.

1.2.2.2 Ambient Pressure

There are numerous situations in which it is desired to know how changes in ambient pressure may affect the flammability of materials. Within the field of material flammability several studies have focused on understanding how ambient pressure affects ignition delay time and flame spread. Restricting to the flammability of thin materials, Altenkirch[24] was among the first researchers to investigate the role of environmental variables, including ambient pressure, in flame spread over thin materials. His results showed that flame spread had a slight dependence on ambient pressure, but most importantly showed that flame spread could be analyzed in terms of a non-dimensional spread rate and Damkohler number in the same way that was proposed by Fernandez-Pello[18]. In his work, Altenkirch concluded that changes in ambient pressure affect buoyancy and the rate at which the gas phase reaction proceeds.

The design of the next generation of space exploration vehicles has resulted in a renewed interest in the effect of reduced ambient pressure on the flammability of materials[22, 28–37]. The effect of ambient pressure in the flammability of materials has been studied using different approaches. Kleinhenz and T'ien[28], Olson et al.[31] and Olson and Miller[33] studied the effect of ambient pressure on the flame spread characteristics and of thin fuels and determined flammability boundaries in terms of ambient pressure and limiting oxygen concentration for flame spread. Their findings showed that flame spread has a weak dependence on ambient pressure and revealed that downward propagating flames spread faster than upward propagating ones. These results were also used to develop flammability boundaries in terms of ambient pressure and oxygen concentration. Such boundaries showed that a reduction in ambient pressure results in an increase in the minimum oxygen concentration required for flame spread. Moreover, by defining the Limiting Oxygen Index (LOI) and Maximum Oxygen Concentration (MOC) in terms of NASA Standard 6001 pass rate, Olson et al.[31] and Olson and Miller[33] were able to quantify the effects of ambient pressure, oxygen concentration and microgravity on the flammability limits of materials.

Nakamura and Aoki[22] studied the flammability of thin cellulosic sheets irradiated with

a CO_2 laser and found that the flammability boundary in terms of the oxygen partial pressure showed a nearly linear decrease with a reduction in ambient pressure. During the experiments they observed that as ambient pressure was reduced ignition occurred further away from the fuel surface and that ignition was observed for ambient pressures below 20 kPa. Nakamura et al.[32] followed this work by studying flame spread over electrical wires in reduced ambient pressures. The results from this work differed from previous reduced ambient pressure studies in that flame spread rate did not decrease when ambient pressure was reduced. A possible explanation for such behavior was given in terms of the effect of pressure on the flame edge length and conductive wire length. Depending on their relative lengths two flame spread modes were proposed, *flame driven* and *wire driven*. When the flame edge length is greater, the primary heat input source is the flame. On the other side, when the conductive wire length is greater, heat conduction through the solid is the main mode of heat input.

Hirsch et al.[29, 30] studied the flammability limits of different kinds of common polymeric thin materials used in aerospace applications. The materials studied included rigid plastics, fabrics, composites/laminates and foams. Flammability limit experiments were conducted in three different ambient pressures, 48.2, 85.3 and 101.3 kPa. The flammability boundaries followed a behavior similar to that found by Nakamura and Aoki[22], a nearly linear decrease in the oxygen partial pressure with a reduction in ambient pressure. One interesting finding was that materials with higher initial limits showed a greater decrease in the oxygen partial pressure when ambient pressure was reduced.

At UC Berkeley the FIST project has studied the effect of ambient pressure on the flammability of thick PMMA sheets. McAllister[34, 35] studied the ignition delay characteristic of PMMA in reduced ambient pressures and found that the ignition delay time had a "U-shaped" dependence on ambient pressure. This non-monotonic behavior was explained in terms of three regimes, a transport controlled regime near atmospheric conditions, a chemical kinetic regime at at low ambient pressures, and an overlap regime where both, transport and chemical kinetic effects are important. The decrease in the ignition delay time was attributed to a reduction in the convective heat losses of the sample, which results in an increase in the net heat flux at the sample surface. Fereres[36, 37] continued the PMMA piloted ignition work in reduced ambient pressures and experimentally and numerically studied the critical mass flux at the moment of ignition. Results showed that the critical mass flux at ignition decreases with a reduction in ambient pressure. Therefore, as ambient pressure is reduced smaller amounts of fuel and oxygen are required to attain a flammable mixture suggesting that a reduction in ambient pressure increases the flammability of materials.

1.2.2.3 External Radiant Flux

Heating and gasification of a solid fuel require the presence of a heat flux whether it may be conductive, convective, radiative or a combination of all. The total heat flux at the surface raises the temperature of the solid to the point that it starts decomposing into vapor

fuel. Vaporized fuel produced at the solid surface mixes with an oxidizer gas and if the temperature is high enough a combustion reaction occurs. Though not completely accurate, it can be assumed that pyrolysis occurs at a constant surface temperature called the pyrolysis temperature, T_p[10]. A propagating flame must supply enough heat to the solid in order to raise the surface temperature to T_p and overcome any heat losses such as conduction through the solid, convective heat losses and surface reradiation. This balance between total heat input and output gives basis for the use of a critical heat flux for ignition. In piloted ignition, heat fluxes below this critical value will not result in ignition, whereas heat fluxes greater or equal than this critical value result in ignition of the fuel if an ignition source is present.

An external radiant flux may come in the form of nearby flames, heated walls, hot smoke layers etc. and its presence enhances flame spread rate due to an increase in the solid temperature. The effect of an external radiant flux on the flame spread over solid fuels has received significant attention as pointed out in [9, 10]. Some examples include the works of Fernandez-Pello in upward[38] and downward [39] flame spread subject to an external radiant flux, and Quintiere et al.[40] in flames subject to external irradiance. Based on these results it has been concluded that for low radiant flux values the addition of external radiation is reduced to the correct estimation of the surface temperature, whereas at high heat fluxes fuel gasification and gas-phase kinetics make estimating the effect of an external radiant flux more difficult. Depending on the magnitude of the external radiant flux the flame spread rate may be constant, acceleratory, or none. When an external radiant flux balances the solid heat losses the flame spread rate is constant, if it is greater than the heat losses the flame spread rate accelerates, and in some other cases a flame may not spread until a minimum external radiant flux is provided.

Accounting for the presence of an external radiant flux has led to development of flammability tests that determine the critical heat flux for ignition or the minimum heat flux for flame spread. Such tests allow the development of flammability diagrams that capture the piloted ignition and flame spread characteristics of solid fuels. For example, ASTM E 1321[41] is an standardized flammability test to determine material properties related to the piloted ignition and lateral flame spread when exposed to an external radiant flux. Similar standards exists for determining the minimum heat flux for flame spread in attic floor insulations[42] and horizontal floors[43]. An apparatus based on ASTM E 1321, referred as FIST has been developed at UC Berkeley under NASA sponsorship[44]. This apparatus was originally designed to test piloted ignition and opposed flame spread characteristics under varied environmental conditions and produce flow dependent flammability diagrams. Protocols for flammability testing under external radiant fluxes can be used to determine heat release rate, peak heat release rate, and other important material properties in complex fire-resistant materials such as foams, fabrics[45] among others.

1.2.2.4 Microgravity

Fire in microgravity (μg) is different to fire in normal gravity ($1g$) due to the elimination of natural convection and changes in transport processes that make diffusion dominant. A candle burning in $1g$ will appear very different than in μg as it can be seen in Figure 1.7[46]. A $1g$ candle flame will be elongated and have a bright orange color, whereas in μg it will be spherical shape and have a blue color. Microgravity can affect more than the physical appearance of flames and as a result a significant number of researchers have studied combustion in microgravity environments. Since the focus of this work is flammability limits for flame spread, the remainder of this section will introduce literature specific to flame spread over thin fuels in microgravity environments. For a more generalized take of microgravity combustion the reader is referred to the reviews of Law and Faeth[47], Kono et al.[48], and Ronney[49]. Though not completely up to date, these reviews showcase the variety of microgravity combustion research projects and major findings up until the late 1990's.

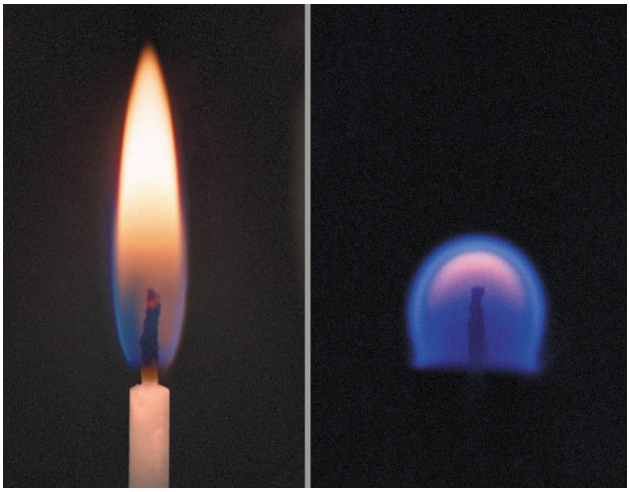

Figure 1.7: Candle flame in normal (Left) and microgravity (Right) conditions[46].

Microgravity flame spread in thin and thick fuels has been extensively studied experimentally and through the use of numerical simulations[31, 33, 50–59]. Current understanding of flame spread over solid fuels in microgravity is based on the experimental work by Olson et al.[54] and Olson[55] and the numerical simulations of Bhattacharjee et al.[50] and Bhattacharjee and Altenkirch[51].

Olson and collaborators (Olson et al.[54] and Olson[55]) conducted opposed flame spread experiments using thin fuels and identified two types of extinction, a "quenching" and a "blowoff" limit. The "blowoff" limit had been previously identified by Altenkirch[24] and Fernandez-Pello and Hirano[9] had previously identified the existence of the "blowoff" limit

and attributed it to the decrease of the Damkohler number below a certain critical value. The "quenching" limit is unique to microgravity and is a result of limited oxygen transport to the flame when the oxidizer flow velocity is reduced below values typically attained in $1g$. Limited oxygen supply found along the "quenching" limit reduces the reaction rate and results in increased heat losses that eventually lead to extinction of the flame.

Bhattacharjee et al.[50] and Bhattacharjee and Altenkirch[51] further investigated the existence of the "quenching" limit and the effect of radiation heat losses in microgravity opposed flame spread. Using numerical simulations they noted that inclusion of surface radiation resulted in better agreement with drop tower experiments. Furthermore, they concluded that surface radiation results in a decrease in the net heat transfer to the solid fuel and the flame spread rate. For the case of low oxidizer flow velocities the propagating flame has more time to "feel" the radiation losses, which reinforced the existence of the "quenching" limit described by Olson and collaborators.

Existence of the "quenching" and "blowoff" limits has been used to explain the non-monotonic behavior between flame spread rate and oxidizer flow velocity observed in microgravity flame spread experiments. This non-monotonic behavior is common in opposed flame spread and is responsible for a peak in the flame spread rate as a function of oxidizer flow velocity[55, 58] and a minima in the oxygen concentration extinction boundary for opposed flame spread[55, 60]. The location of this peak can be said to occur at the intersection of the "quenching" and "blowoff" extinction limits[60]. This peak tends to occurs in oxidizer flow velocities ranging from 5 to 30 cm/s[31, 54, 55, 58, 60] which is similar to spacecraft ventilation velocities. This unfortunate coincidence enhances the flammability of materials and increases the risk of a fire onboard a spacecraft.

Additional flame spread experiments with thin materials have reported that opposed flame spread rates are higher than those of concurrent flame spread[31, 33] suggesting that during a fire in microgravity flames are more likely to spread downward. Specifically for flames spreading over electrical cables, Kikuchi et al.[59] and Fujita et al.[58] concluded that curvature effects in smaller diameter wires, initial wire temperature, and enhanced oxygen diffusion serve to increase the flame spread rate. Umemura et al.[53] also found that in electrical wires the metallic conductor acts as both a heat source ahead of the flame and a heat sink directly below it. In contrast to flame spread studies, only a limited number have dealt with the effects of microgravity and other variables on the flammability limits of materials[31, 60–62]. These researchers have found that microgravity conditions enhance the flammability limits of materials, and that when combined to additional variables such as Joule heating and oxidizer flow velocity, among others, it is possible to further reduce the ignition limits of materials.

1.2.3 Fire Resistant Materials

Fire-resistant (FR) materials are routinely used to satisfy fire safety regulations around the world [63–65] and even in space exploration[8]. Labeling a material as fire-resistant does not mean it will not ignite or that it is not flammable, instead it means that in standard room conditions the materials will not ignite, or once ignited it exhibits self-extinguish behavior. Fire resistance can be accomplished through physical action, chemical action, or a combination of both[64, 65]. Physical action mechanisms include: cooling of the fuel below its ignition temperature, shielding of the fuel from the flame or dilution of the fuel vapors. Chemical action mechanisms affect the gas-phase and solid-phase reactions. In the gas phase, scavenging of H and OH radicals hinder chain branching reactions that are key to combustion. In the solid phase chemical action can lead to melting of dripping of the material and formation of char insulation that in combination to intumescent layers reduce heat and mass transfer to the virgin material. The overview of fire resistance mechanisms is intended to provide context for the investigation of the flammability limits of FR materials and will not be an area of focus of the present work, for more information on FR materials consult Refs.[64, 65].

1.3 Contribution of the Current Research

Research in material flammability has primarily focused on studying piloted ignition and flame spread characteristics, and in more recent times flammability limits. Very often the fuels selected constitute non fire-resistant materials with a relatively simple composition such as PMMA sheets, thin cellulosic paper sheets or PE insulated wires. Despite the fact that FR materials have allowed gaining a fundamental understanding of piloted ignition, flame spread and flammability limits, the fact is that they are rarely used in practical situations. On the other hand, fire-resistant (FR) materials are often used in order to satisfy fire safety requirements, and in the case of space exploration the use of FR materials represents the best method for reducing the risk of an onboard fire.

A unique aspect of this research is the selection of FR materials proposed or currently used in aerospace applications. At this time it is unclear whether FR materials behave the same way when ambient conditions change, i.e reduction of ambient pressure, elimination of gravity, and therefore it is important to understand how ambient conditions affect the flammability of FR materials. The present work aims to expand on the current understanding of FR material flammability by investigating the effects of environmental variables on the flammability of FR materials. This objective is accomplished by (1) conducting small-scale flame spread experiments with FR materials over a wide range of ambient conditions, and (2) the development of flammability boundaries in terms of the Flame/No-Flame spread limit. Flammability boundaries constitute an improvement over flammability indices such as LOI, MOC, etc. because they are able to capture the flammability of a material over a range of conditions instead that at a single point. This dissertation is structured into

an introductory and literature review chapter, three chapters focusing on the FR material flammability limits, and a conclusions and future work chapter.

Chapter 2 presents experiments focused on the relationship between an external radiant flux and oxygen concentration in concurrent flame spread over both fire-resistant (FR) and non fire-resistant (NFR) fabrics. The experiments are conducted in a modified version of the FIST apparatus that used an non-uniform external radiant flux similar to ASTM E 1321[41] for varied oxygen concentration and oxidizer flow velocity conditions. Fire-resistant and non fire-resistant fabrics are used to study the effects of fabric composition as well as evaluate candidate materials for possible large-scale microgravity flammability experiments. Results are reported in terms of Flame/No-Flame Spread boundaries constructed using $\dot{q}''_{MIN}$ as a function of oxygen concentration. The results of this chapter are discussed in terms of a modified expression for flame spread in thin fuels.

Chapter 3 focuses on the effect of reduced ambient pressure and the Limiting Oxygen Concentration (LOC) for flame spread in FR and NFR fabrics. Reduced ambient pressure experiments are carried out inside a 105 L chamber that allows conducting concurrent and opposed flame spread experiments in horizontal and vertical orientations. In this chapter flammability boundaries are developed in terms of ambient pressure and LOC for each of the four possible flame spread configurations. These results are alternatively presented in terms of the oxygen partial pressure, p_{O_2}, revealing a nearly linear reduction in p_{O_2} when ambient pressure decreases. A discussion is provided regarding the observed shapes of the flammability boundaries, the effects of ambient pressure, flame spread configuration and the implications of a reduction in p_{O_2} when ambient pressure is reduced.

Chapter 4 describes the design of an experimental apparatus for testing of opposed flame spread in electrical cables for use in parabolic flight experiments. The apparatus allows controlling the oxidizer flow velocity, oxygen concentration, ambient pressure, and features a set of external radiant heaters. In addition, this chapter reports a set of flammability limits experiments conducted with ethylene tetrafluoroethylene (ETFE) insulated wires subject to an external radiant flux in normal ($1g$) and microgravity (μg) conditions. These results are used to develop $1g$ and μg flammability maps that are used to discuss the effect of microgravity conditions on the flammability of FR insulated wires. Finally, the results with ETFE insulated wires are compared to previously obtained results by Takahashi et al.[60] using PE insulated wires. The comparison between ETFE (FR) and PE (NFR) is the first one of its kind and is used to analyze the effect of μg in the flammability limits of FR and NFR materials.

Figure 1.8: Wire flame spread apparatus onboard parabolic flight aircraft.

1.4 References

[1] Steve Weiner et al. "Evidence for the Use of Fire at Zhoukoudian, China". In: *Science* 281.5374 (1998), pp. 251–253. DOI: 10.1126/science.281.5374.251.

[2] John A.J. Gowlett and Richard W. Wrangham. "Earliest fire in Africa: Towards the Convergence of Archaeological Evidence and the Cooking Hypothesis". In: *Azania: Archaeological Research in Africa* 48.1 (2013), pp. 5–30. DOI: 10.1080/0067270X.2012.756754.

[3] Chris Organ et al. "Phylogenetic Rate Shifts in Feeding Time during the Evolution of Homo". In: *Proceedings of the National Academy of Sciences* (2011). DOI: 10.1073/pnas.1107806108.

[4] John Webb and Marian Domanski. "Fire and Stone". In: *Science* 325.5942 (2009), pp. 820–821. DOI: 10.1126/science.1178014.

[5] Howard W. Emmons. "The Growth of Fire Science". In: *Fire Safety Journal* 3.3 (1981), pp. 95–106. DOI: 10.1016/0379-7112(81)90036-9.

[6] Howard W. Emmons. "The Further History of Fire Science". In: *Combustion Science and Technology* 40.1 – 4 (1984), pp. 167–174. DOI: 10.1080/00102208408923804.

[7] NFPA Fire Analysis and Research Division. *Trends and Patterns of U.S. Fire Losses in 2012*. Nov. 2013. URL: http://www.nfpa.org/~/media/Files/Research/NFPA%20reports/Overall%20Fire%20Statistics/ostrends.pdf.

[8] *Flammability, Odor, Offgassing, and Compatibility Requirements and Test Procedures for Materials in Environments that Support Combustion, NASA STD 6001*. 1998. URL: http://www.nasa.gov/centers/johnson/pdf/485934main_NASA-STD-(I)-6001A%20Released.pdf.

[9] A.C. Fernandez-Pello and T. Hirano. "Controlling Mechanisms of Flame Spread". In: *Combustion Science and Technology* 32.1 – 4 (1983), pp. 1–31. DOI: 10.1080/00102208308923650.

[10] C. Fernandez-Pello, in: G. Cox (Ed.) *Combustion Fundamentals of Fire*. San Diego, CA: Academic Press, 1995. ISBN: 0121942309.

[11] James G. Quintiere. *Fundamentals of Fire Phenomena*. West Sussex, England: John Wiley & Sons, Ltd, 2006. ISBN: 9780470091135.

[12] Dougal Drysdale. *An Introduction to Fire Dynamcis*. Third Edition. West Sussex, United Kingdom: John Wiley & Sons, Ltd, 2011. ISBN: 9781119975465.

[13] Indrek S. Wichman. "Theory of Opposed-Flow Flame Spread". In: *Progress in Energy and Combustion Science* 18.6 (1992), pp. 553–593. DOI: 10.1016/0360-1285(92)90039-4.

[14] J.N. De Ris. "Spread of a Laminar Diffusion Flame". In: *Symposium (International) on Combustion* 12.1 (1969), pp. 241–252. ISSN: 0082-0784. DOI: 10.1016/S0082-0784(69)80407-8.

[15] F.A. Williams. "Mechanisms of Fire Spread". In: *Symposium (International) on Combustion* 16.1 (1977), pp. 1281–1294. DOI: 10.1016/S0082-0784(77)80415-3.

[16] Toshisuke Hirano, Stanley E. Noreikis, and Thomas E. Waterman. "Measured Velocity and Temperature Profiles Near Flames Spreading Over a Thin Combustible Solid". In: *Combustion and Flame* 23.1 (1974), pp. 83–96. DOI: 10.1016/S0010-2180(74)80029-5.

[17] A.C. Fernandez-Pello and F.A. Williams. "A Theory of Laminar Flame Spread Over Flat Surfaces of Solid Combustibles". In: *Combustion and Flame* 28 (1977), pp. 251–277. DOI: 10.1016/0010-2180(77)90032-3.

[18] A.C. Fernandez-Pello, S.R. Ray, and I. Glassman. "Flame Spread in an Opposed Forced Flow : The Effect of Ambient Oxygen Concentration". In: *Symposium (International) on Combustion* 18.1 (1981). Eighteenth Symposium (International) on Combustion, pp. 579–589. DOI: 10.1016/S0082-0784(81)80063-X.

[19] Robert F. McAlevy and Richard S. Magee. "The Mechanism of Flame Spreading Over the Surface of Igniting Condensed-Phase Materials". In: *Symposium (International) on Combustion* 12.1 (1969), pp. 215–227. DOI: 10.1016/S0082-0784(69)80405-4.

[20] F.A. Lastrina, R.S. Magee, and R.F. McAlevy. "Flame Spread Over Fuel Beds: Solid-Phase Energy Considerations". In: *Symposium (International) on Combustion* 13.1 (1971). Thirteenth symposium (International) on Combustion Thirteenth symposium (International) on Combustion, pp. 935–948. DOI: 10.1016/S0082-0784(71)80094-2.

[21] Y. H. C. Chao and A. C. Fernandez-Pello. "Concurrent Horizontal Flame Spread: The Combined Effect of Oxidizer Flow Velocity, Turbulence and Oxygen Concentration". In: *Combustion Science and Technology* 110 – 111.1 (1995), pp. 19–51. DOI: 10.1080/00102209508951915.

[22] Y. Nakamura and A. Aoki. "Irradiated Ignition of Solid Materials in Reduced Pressure Atmosphere with Various Oxygen Concentrations for Fire Safety in Space Habitats". In: *Advances in Space Research* 41.5 (2008), pp. 777–782. DOI: 10.1016/j.asr.2007.03.027.

[23] Shuhei Takahashi et al. "Behavior of Flame Spread on Thin PMMA near Extinction Limit at Low Oxygen Level". In: *Trans. JSASS Aerospace Tech. Japan* 10.ists28 (2012), Ph_9–Ph_13. DOI: 10.2322/tastj.10.Ph_9.

[24] R.A. Altenkirch, R. Eichhorn, and P.C. Shang. "Buoyancy Effects on Flames Spreading Down Thermally Thin Fuels". In: *Combustion and Flame* 37 (1980), pp. 71–83. DOI: 10.1016/0010-2180(80)90072-3.

[25] T. Hirata, T. Kashiwagi, and J.E. Brown. "Thermal Oxidative Degradation of Poly(methyl methacrylate): Weight Loss". In: *Macromolecules* 18 (1985), pp. 1410–1418. DOI: 10.1021/ma00149a010.

[26] Takashi Kashiwagi and Thomas J. Ohlemiller. "A Study of Oxygen Effects on Nonflaming Transient Gasification of PMMA and PE during Thermal Irradiation". In: *Symposium (International) on Combustion* 19.1 (1982), pp. 815–823. DOI: 10.1016/S0082-0784(82)80257-9.

[27] Chris Lautenberger and Carlos Fernandez-Pello. "Generalized pyrolysis model for combustible solids". In: *Fire Safety Journal* 44.6 (2009), pp. 819–839. DOI: 10.1016/j.firesaf.2009.03.011.

[28] Julie Kleinhenz and James S. T'ien. "Combustion of Nomex III Fabric in Potential Space Habitat Atmospheres: Cyclic Flame Spread Phenomenon". In: *Combustion Science and Technology* 179.10 (2007), pp. 2153–2169. DOI: 10.1080/00102200701386172.

[29] David B. Hirsch et al. "Oxygen Concentration Flammability Thresholds of Selected Aerospace Materials Considered for the Constellation Program". In: (2007). URL: http://ntrs.nasa.gov/archive/nasa/casi.ntrs.nasa.gov/20070018178_2007017304.pdf.

[30] David Hirsch, Jim Williams, and Harold Beeson. "Pressure Effects on Oxygen Concentration Flammability Thresholds of Polymeric Materials for Aerospace Applications". In: *Journal of Testing and Evaluation* 36.1 (2008), p. 100975. DOI: 10.1520/jte100975.

[31] Sandra L. Olson, Gary A. Ruff, and Fletcher J. Miller. "Microgravity Flame Spread in Exploration Atmospheres: Pressure, Oxygen, and Velocity Effects on Opposed and Concurrent Flame Spread". In: *38th International Conference on Environmental Systems*. San Francisco, CA: SAE International, June 2008. DOI: 10.4271/2008-01-2055.

[32] Yuji Nakamura et al. "Flame Spread over Electric Wire in Sub-Atmospheric Pressure". In: *Proceedings of the Combustion Institute* 32.2 (2009), pp. 2559–2566. DOI: 10.1016/j.proci.2008.06.146.

[33] S.L. Olson and F.J. Miller. "Experimental Comparison of Opposed and Concurrent Flame Spread in a Forced Convective Microgravity Environment". In: *Proceedings of the Combustion Institute* 32.2 (2009), pp. 2445–2452. DOI: 10.1016/j.proci.2008.05.081.

[34] Sara McAllister et al. "Piloted Ignition Delay of PMMA in Space Exploration Atmospheres". In: *Proceedings of the Combustion Institute* 32.2 (2009), pp. 2453–2459. ISSN: 1540-7489. DOI: 10.1016/j.proci.2008.05.076.

[35] Sara McAllister et al. "The Combined Effect of Pressure and Oxygen Concentration on Piloted Ignition of a Solid Combustible". In: *Combustion and Flame* 157.9 (2010), pp. 1753–1759. DOI: 10.1016/j.combustflame.2010.02.022.

[36] Sonia Fereres et al. "Mass Flux at Ignition in Reduced Pressure Environments". In: *Combustion and Flame* 158.7 (2011), pp. 1301–1306. DOI: 10.1016/j.combustflame.2010.11.013.

[37] Sonia Fereres et al. "Understanding Ambient Pressure Effects on Piloted Ignition through Numerical Modeling". In: *Combustion and Flame* 159.12 (2012), pp. 3544–3553. DOI: 10.1016/j.combustflame.2012.08.006.

[38] A. C. Fernandez-Pello. "Upward Laminar Flame Spread Under the Influence of Externally Applied Thermal Radiation". In: *Combustion Science and Technology* 17.3 – 4 (1977), pp. 87–98. DOI: 10.1080/00102207708946818.

[39] A. C. Fernandez-Pello. "Downward Flame Spread Under the Influence of Externally Applied Thermal Radiation". In: *Combustion Science and Technology* 17.1 – 2 (1977), pp. 1–9. DOI: 10.1080/00102209708946807.

[40] James G. Quintiere, Margaret Harkleroad, and Yuji Hasemi. "Wall Flames and Implications for Upward Flame Spread". In: *Combustion Science and Technology* 48.3-4 (1985), pp. 191–222. DOI: 10.1080/00102208608923893.

[41] ASTM Standard E1321-13, (2013). *Standard Test Method for Determining Material Ignition and Flame Spread Properties*. West Conshohocken, PA: ASTM International, 2013. DOI: 10.1520/E1321-13. URL: http://www.astm.org.

[42] ASTM Standard E970-14, (2014). *Standard Test Method for Critical Radiant Flux of Exposed Attic Floor Insulation Using a Radiant Heat Energy Source*. West Conshohocken, PA: ASTM International, 2014. DOI: 10.1520/E0970-14. URL: http://www.astm.org.

[43] ASTM Standard E648-10, (2010). *Standard Test Method for Critical Radiant Flux of Floor-Covering Systems Using a Radiant Heat Energy Source*. West Conshohocken, PA: ASTM International, 2010. DOI: 10.1520/E0648-10E01. URL: http://www.astm.org.

[44] J. L. Cordova et al. "Oxidizer Flow Effects on the Flammability of Solid Combustibles". In: *Combustion Science and Technology* 164.1 (2001), pp. 253–278. DOI: 10.1080/00102200108952172.

[45] T.M. Kotresh et al. "Effect of Heat Flux on the Burning Behaviour of Foam and Foam/Nomex III Fabric Combination in the Cone Calorimeter". In: *Polymer Testing* 25.6 (2006), pp. 744–757. DOI: 10.1016/j.polymertesting.2006.05.009.

[46] NASA. *Glen Research Center — Aerospace Research and Development*. [Online; accessed 06/11/2014]. 2014. URL: http://spinoff.nasa.gov/spinoff1999/ard4.htm.

[47] C.K. Law and G.M. Faeth. "Opportunities and Challenges of Combustion in Microgravity". In: *Progress in Energy and Combustion Science* 20.1 (1994), pp. 65–113. DOI: 10.1016/0360-1285(94)90006-X.

[48] Michikata Kono et al. "Current State of Combustion Research in Microgravity". In: *Symposium (International) on Combustion* 26.1 (1996), pp. 1189–1199. DOI: 10.1016/S0082-0784(96)80335-3.

[49] Paul D. Ronney. "Understanding Combustion Processes through Microgravity Research". In: *Symposium (International) on Combustion* 27.2 (1998), pp. 2485–2506. DOI: 10.1016/S0082-0784(98)80101-X.

[50] S. Bhattacharjee et al. "A Theoretical Description of Flame Spreading over Solid Combustibles in a Quiescent Environment at Zero Gravity". In: *Combustion Science and Technology* 69.1 – 3 (1990), pp. 1–15. DOI: 10.1080/00102209008951599.

[51] S. Bhattacharjee and R.A. Altenkirch. "The Effect of Surface Radiation on Flame Spread in a Quiescent, Microgravity Environment". In: *Combustion and Flame* 84.1 – 2 (1991), pp. 160–169. DOI: 10.1016/0010-2180(91)90045-D.

[52] Kuldeep Prasad et al. "Effect of Wind Velocity on Flame Spread in Microgravity". In: *Proceedings of the Combustion Institute* 29.2 (2002), pp. 2553–2560. DOI: 10.1016/S1540-7489(02)80311-X.

[53] Akira Umemura et al. "Physical Model Analysis of Flame Spreading along an Electrical Wire in Microgravity". In: *Proceedings of the Combustion Institute* 29.2 (2002), pp. 2535–2543. DOI: 10.1016/S1540-7489(02)80309-1.

[54] Sandra L. Olson, Paul V. Ferkul, and James S. T'ien. "Near-Limit Flame Spread Over a Thin Solid Fuel in Microgravity". In: *Symposium (International) on Combustion* 22.1 (1989), pp. 1213–1222. DOI: 10.1016/S0082-0784(89)80132-8.

[55] S. L. Olson. "Mechanisms of Microgravity Flame Spread Over a Thin Solid Fuel: Oxygen and Opposed Flow Effects". In: *Combustion Science and Technology* 76.4 – 6 (1991), pp. 233–249. DOI: 10.1080/00102209108951711.

[56] George W. Sidebotham and Sandra L. Olson. "Microgravity Opposed-Flow Flame Spread in Polyvinyl Chloride Tubes". In: *Combustion and Flame* 154.4 (2008), pp. 789–801. DOI: 10.1016/j.combustflame.2008.05.014.

[57] S.L. Olson et al. "Flame Spread Over Thin Fuels in Actual and Simulated Microgravity Conditions". In: *Combustion and Flame* 156.6 (2009), pp. 1214–1226. DOI: 10.1016/j.combustflame.2009.01.015.

[58] Osamu Fujita, Katsuhiro Nishizawa, and Kenichi Ito. "Effect of Low External Flow on Flame Spread over Polyethylene-insulated Wire in Microgravity". In: *Proceedings of the Combustion Institute* 29.2 (2002), pp. 2545–2552. DOI: 10.1016/S1540-7489(02)80310-8.

[59] Masao Kikuchi et al. "Experimental Study on Flame Spread over Wire Insulation in Microgravity". In: *Symposium (International) on Combustion* 27.2 (1998), pp. 2507–2514. DOI: 10.1016/S0082-0784(98)80102-1.

[60] Shuhei Takahashi et al. "Extinction Limits of Spreading Flames over Wires in Microgravity". In: *Combustion and Flame* 160.9 (2013), pp. 1900–1902. DOI: 10.1016/j.combustflame.2013.03.029.

[61] Osamu Fujita et al. "Ignition of Electrical Wire Insulation with Short-term Excess Electric Current in Microgravity". In: *Proceedings of the Combustion Institute* 33.2 (2011), pp. 2617–2623. DOI: 10.1016/j.proci.2010.06.123.

[62] Yoshitomo Takano et al. "Ignition Limits of Short-term Overloaded Electric Wires in Microgravity". In: *Proceedings of the Combustion Institute* 34.2 (2013), pp. 2665–2673. DOI: 10.1016/j.proci.2012.06.064.

[63] *16 CFR Volume 2 Chapter II Subchapter D - Flammable Fabrics Act Regulations*. 2012. URL: http://www.gpo.gov/fdsys/pkg/CFR-2012-title16-vol2/pdf/CFR-2012-title16-vol2-chapII-subchapD.pdf.

[64] G. Camino, L. Costa, and M.P. Luda di Cortemiglia. "Overview of fire retardant mechanisms". In: *Polymer Degradation and Stability* 33.2 (1991), pp. 131–154. DOI: 10.1016/0141-3910(91)90014-I.

[65] J. Troitzsch. "Overview of flame retardants". In: *Chemistry today* 16 (1998). URL: http://www.aerofiltri.it/DC_pdf/AS_A_OoFR.pdf.

CHAPTER 2

EXTERNAL RADIATION

2.1 Introduction

Radiation heat transfer refers to the exchange of energy in the form of electromagnetic waves as a result of changes in electron configurations of the elements or atoms that make up matter[1]. Thermal radiation is an important process in many aspects of daily life. It is the reason the earth receives energy from the sun, it is an essential part in photosynthesis, and it holds a promising future as a source of renewable energy. In engineering applications thermal radiation is an important heat transfer mechanism, particularly at high temperatures such as those associated with combustion processes. Whereas conduction and convection heat transfer are proportional to the difference in temperature between two bodies, thermal radiation is proportional to the difference between the fourth power of their absolute temperatures[2]. For example, in wildland fires thermal radiation can account for up to 20% of the total heat released by the fire and constitutes the majority of the heat felt by a person standing in front of the fire. A person fully surrounded by tall flames can be expected to experience a total radiant flux of up to 100 kW/m^2. To put this in perspective, the radiant flux of a clear summer day is 1 kW/m^2, and a person starts feeling pain when the radiant flux exceeds 2 kW/m^2[3].

Due to the role that thermal radiation plays in the spread of fires, external radiant heat sources have been incorporated into standardized flammability tests. Standardized flammability tests such as ASTM E 1321[4], ASTM E 970[5], and ASTM E 648[6] incorporate an external radiant flux as a way of measuring flammability and flame spread characteristics of materials. ASTM E 1321 uses an inclined radiant heater panel to create a decreasing radiant flux distribution over vertically oriented samples, this test is used to predict the time to ignition, t_{ig}, and flame spread rate, V_f, in vertical surfaces. ASTM E 970 is similar to ASTM E 1321 and is primarily concerned with the critical heat flux for flame spread of insulation installed on the floor of building attics. Insulation materials are required to have a critical radiant flux greater or equal to 0.12 W/cm^2(1.2 kW/m^2), which is slightly greater

than the thermal radiation from the sun in a clear summer day. ASTM E 648 also uses a decreasing radiant flux distribution to critical radiant flux at which flames extinguish in horizontally mounted floor-covering systems. In ASTM E 1321 the maximum radiant flux depends on the material, whereas for ASTM E 970 and ASTM E 648 the maximum radiant flux is about 12 kW/m^2.

Similarly to the critical radiant flux, oxygen concentration has also been used as way to characterize the flammability of materials. The minimum oxygen concentration at which a material is able to support a flame, more commonly referred as the Limiting Oxygen Index (LOI), has been used a indicator of the flammability of materials[7, 8]. Materials with LOI values of less than 21% are flammable in standard atmospheric conditions (non fire-resistant); while materials with LOI values greater than 21% are generally regarded as fire-resistant. ASTM D 2863[7] is a test method for determining the LOI of a wide range of materials such including structurally self-supporting materials and thin materials such as fabrics and films. Usage of LOI values facilitates relative material flammability rankings, something that cannot be accomplished using *Pass/Fail* flammability standards such as NASA Standard 6001[9]. NASA Standard 6001 Test 1 is an upward flame propagation test that uses a *Pass/Fail* criteria to characterize material flammability in space applications. In some instances the LOI and a similar index, the Maximum Oxygen Concentration (MOC), have been defined in terms of NASA Standard 6001 Test 1. In such instances the LOI has been defined as the maximum oxygen concentration at which a material passes NASA Standard 6001 Test 1 approximately half the time, and the MOC is defined as the maximum oxygen concentration for with a material always passes NASA Standard 6001 Test 1[10, 11].

An extensive amount of work conducted in normal and reduced gravity have characterized the ignition and flame spread characteristics of thick and thin fuels under varying conditions of external heat flux, oxygen concentration, pressure, and forced flow velocity, see Chapter 1. However, only a reduced number of studies have focused on studying the flammability FR materials following testing methods similar to NASA Standard 6001. Particularly relevant to the present work are the studies of [8, 10, 11] regarding the limiting oxygen concentrations, flammability and flame spread characteristics of FR fabrics. Kleinhenz and T'ien[8] conducted upward and downward LOI experiments using a Nomex III blend (92% Nomex, 5% Kevlar, and 3% P-140) and found that the LOI in upward and downward flame spread were 24% and 28% respectively. Their results showed that even though Nomex III is flammable over what is often termed Space Exploration Atmospheres (SEA), a term used to describe low pressure and elevated oxygen concentration ambient conditions that have been selected as candidates for future spacecraft designs. Another interesting finding in their research was the fact that as sample width increased the LOI decreased.

Continuing work with FR materials, Hirsch et al.[10] conducted LOI and MOC experiments following the NASA Standard 6001 Test 1 with several materials that were intended for use in the NASA Constellation Program. Materials tested included rigid plastics, fabrics,

composites/laminates and foams. Their results showed that for an ambient pressure of 0.7 atm, Nomex HT90-40 had LOI and MOC value of less than 30%, which is in agreement to results from other researchers[8, 11]. Olson et al.[11] studied the effect of environmental variables such as pressure, oxygen concentration and microgravity (μg) on the flame spread in Kimwipes and LOI and MOC of selected FR materials. The results showed that μg results in a decrease in both the LOI and MOC. For the case of Nomex HT90-40, in normal gravity ($1g$) and with an ambient pressure of 1 atm the LOI for upward flame spread is 25.4%, whereas in μg it reduces to 23.0%. The MOC showed no variation between $1g$ and μg conditions, and it had a value of 22.0%. Similar experiments with the FR fabric Ultem 1000 in an ambient pressure of 0.7 atm showed that the LOI reduced from 26.5% in $1g$ to 24.0% in μg, and that the MOC reduced from 24.0% in $1g$ to 23.0% in μg. This reduction in LOI and MOC was attributed to the elimination of natural convection in μg and the reduction of convective heat losses in the unburned fuel. The reduction in heat losses allows the flame to transfer the same amount of heat to the unburned fuel despite the lower heat release due to a reduced oxygen concentration.

This chapter will present experiments aimed to determine the effects of environmental variables, specifically external radiant flux, oxidizer flow velocity, and oxygen concentration on the minimum conditions for concurrent flame spread over two fire-resistant and two non fire-resistant cotton based fabrics. In the current experiments concurrent flame spread was selected since it is analogous to upward flame spread, thus allowing for reasonable comparisons with NASA Standard 6001 or similar flammability standards. The two FR fabrics selected are Nomex HT90-40, and a Nomex/Nylon/Cotton fabric blend. Nomex is a family of aromatic polyamide polymers that create a strong flexible polymer chain with a high degree of heat resistance. In normal atmospheric conditions Nomex does not melt or drip but chars when exposed to high temperatures[12] which contributes to its FR characteristics and makes it suitable for use in space suits, firefighter clothes, and race car driver uniforms. The two non fire-resistant cotton based fabrics used in this chapter haven been suggested for use in large scale μg fire safety experiments and the results reported here constitute part of their flammability characterization.

The basic approach used in the experiments is to combine the concepts of a critical radiant flux and minimum oxygen concentration for sustained flaming in order to produce flammability maps of both FR and NFR materials. Studies on the flammability of FR materials are limited and so far have not accounted for the presence of an external radiant flux. An external radiant flux may increase the range of oxygen concentrations over which a FR material is flammable. Moreover, this research will show that flammability indices such as the LOI, MOC, etc. are not constant, but instead depend on ambient conditions, i.e. radiant heat flux, ambient pressure, etc. The study of the minimum conditions for concurrent flame spread over FR in terms of a critical radiant flux and oxygen concentration is a novel approach to investigate the flammability of materials since it is able to capture the relationship between ambient conditions and flammability limits.

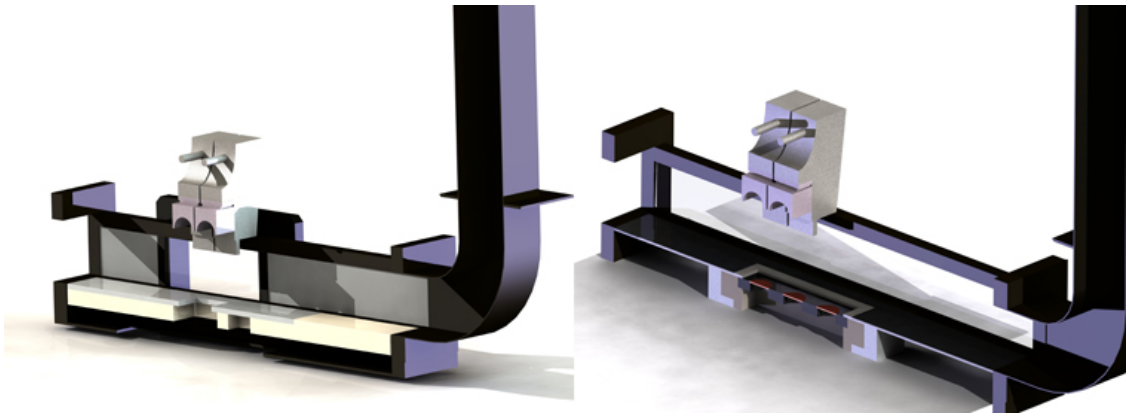

Figure 2.1: Comparison between original and modified FIST apparatus. Left: Original FIST apparatus used by Rich et al.[13]. Right: Modified FIST apparatus used in the current experiments. Modifications to the original FIST tunnel include a new floor section that accommodates longer test samples, a bottom insulation block, and reposition of external radiant heaters.

2.2 Experiment Description

Concurrent flame spread experiments were conducted in modified version of the FIST apparatus that has been developed at UC Berkeley under NASA sponsorship[13]. The original version of the FIST apparatus was used to perform critical mass flux measurements at piloted ignition for polymethylmethacrylate (PMMA) and polypropylene/fiber glass (PP/GL) subject to a uniform external radiant flux. The samples used in the original FIST apparatus were 30 mm wide, 30 mm long and 10 mm thick. In comparison, the fabrics used in this research are much thinner ($\sim$0.3 mm versus 10 mm), longer (152 mm versus 30 mm) and hence prompted a redesign of the bottom section of the apparatus. A comparison between the original and the modified FIST apparatus is shown in Figure 2.1.

The modified FIST is shown schematically in Figure 2.2 and consists of a small-sale combustion tunnel 560 mm long with a rectangular cross-section 127 mm by 100 mm. The floor of the tunnel is made up of a 3.2 mm aluminum plate covered by a 1.6 mm ceramic insulation sheet. The bottom surface of the tunnel has a rectangular cut-out 50.8 mm wide and 152.4 mm long. Sample dimensions were chosen in accordance to 16 C.F.R. Part 1610[14], which stipulates the methodology for testing flammability of clothing textiles sold in the United States. Other standardized flammability tests have similar sample dimensions; for example, NASA Standard 6001 Test 1[9] uses 300 mm by 64 mm samples sizes, and ASTM D 2863[7] uses samples 80 to 150 mm long and 10 mm wide. Experiment samples are attached to an aluminum sample holder that is mounted to the tunnel floor allowing the sample to sit flushed to bottom surface of the tunnel. Ignition of the test samples is

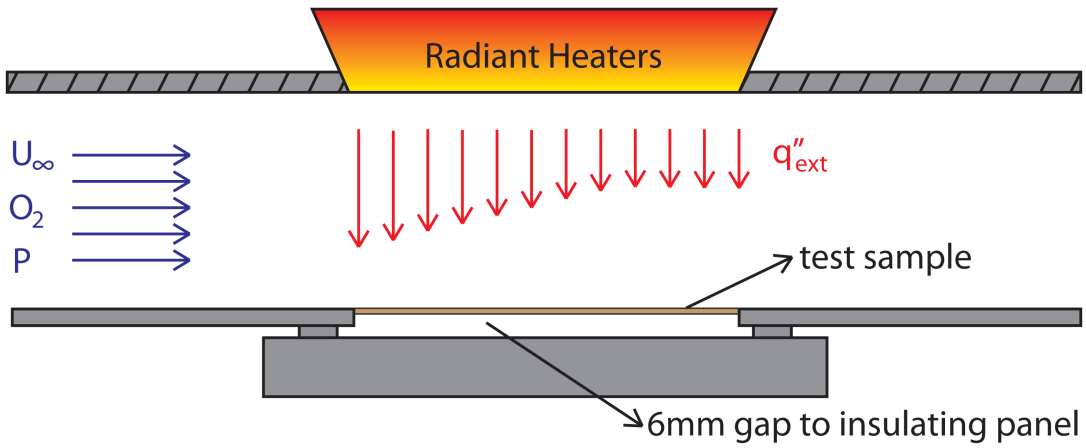

Figure 2.2: Experiment schematic.

accomplished using a 29 AWG Kanthal wire woven across the upstream edge of the fabric sample. An insulation block made of a 12 mm thick Pyrex glass mounted inside a 29 mm thick Marinite insulation board is placed below the sample holder in order to prevent entrainment of air once the sample is ignited.

Tests were conducted with a single layer of Nomex HT90-40 (Stern and Stern Industries Inc., Hornell, NY, USA), a 29% Cotton/ 31% Nylon/ 40% Nomex fabric blend (Magnafabrics, Denton, NC, USA) and two cotton fabrics labeled as *Fabric 1* and *Fabric 2* with densities of 3 and 5 mg/cm^2 respectively. The cotton based fabrics were provided by NASA as candidates for large-scale fire experiments in μg environments. Sidewalls of the tunnel are made of 6mm quartz windows for optical access, and the top surface of the tunnel is fitted with two parabolic radiant heaters (Research Inc., Eden Prairie, MN USA).

The radiant heaters emit in the near IR region with a peak wavelength emission between 1.15 and 1.80 microns, and are capable of producing a peak heat flux of 40 kW/m^2 at the leading edge of the experiment sample. The two radiant heaters were positioned in such a way that they created a non-uniform radiant flux distribution similar to the one used in ASTM E 1321[4], ASTM E 970[5] and ASTM E 648[6]. The radiant heaters provided an approximately uniform heat flux distribution along the sample width and decaying heat flux distribution along sample length with the maximum radiant flux, $\dot{q}''_{MAX}$, occurring at the leading edge of the sample as shown in Figure 2.3. Heat flux measurements were conducted using a Schmidt-Boelter heat flux sensor (Medtherm, Huntsville, AL USA).

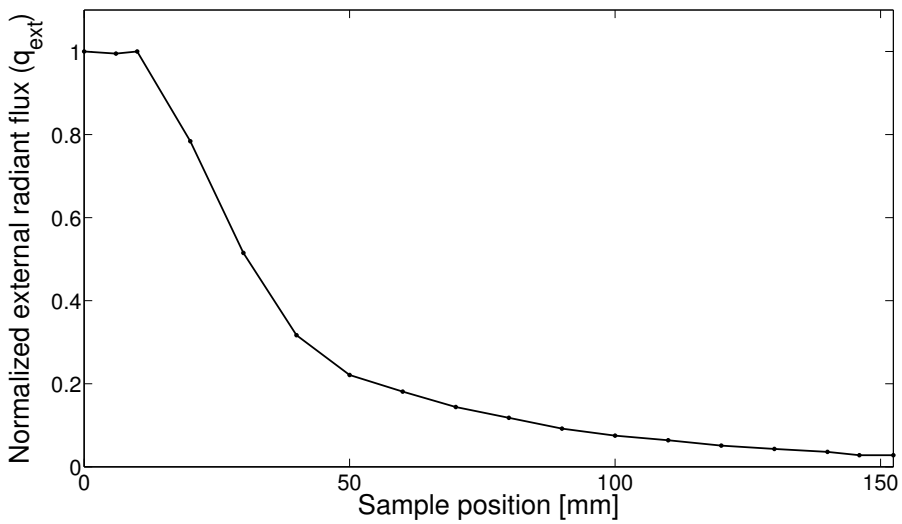

Figure 2.3: Normalized external radiant flux distribution along sample length.

The oxidizer flow velocity and oxygen concentration were set using a combination of critical nozzles and hot wire anemometry. The flow bench used in the experiments allowed attaining oxidizer flow velocities, u_∞, ranging from 0.5 to 1.5 m/s and oxygen concentrations ranging from 14% to 40%. Oxygen concentrations were set using the mass flow rates of the compressed air and pure oxygen or nitrogen, and verified using an oxygen sensor (Apogee Instruments, Logan, UT, USA) mounted upstream of the tunnel section. The modified FIST apparatus including the external radiant heaters is shown in Figure 2.4.

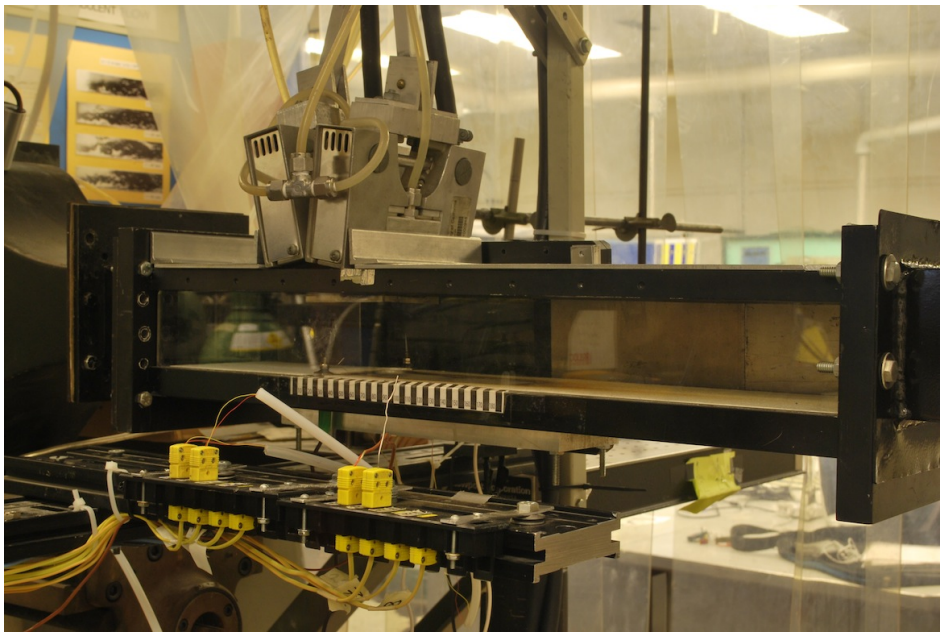

Figure 2.4: Modified FIST apparatus with external radiant heaters.

2.3 Experimental Procedure

The decaying radiant flux distribution allows to experimentally determine the minimum heat flux for flame spread, $\dot{q}''_{MIN}$, by relating the flame propagation distance to the imposed heat flux distribution. Figure 2.5 provides and example of the process of determining $\dot{q}''_{MIN}$ for concurrent flame spread to occur. In this particular experiment the oxidizer flow velocity was 1.0 m/s with an oxygen concentration of 31%. The flame spread length was measured to be 57mm. Based on the known heat flux distribution this gives a value of $8.5kW/m^2$ for $\dot{q}''_{MIN}$.

A test beings by adjusting the oxidizer flow velocity and oxygen concentration using the calibrated flow bench. Once the flow has stabilized and the oxidizer flow velocity and oxygen concentration have been verified the external radiant heaters were turned on and allowed to irradiate the samples so that sample surface temperature reached a steady-state. Depending on the nature of the fabric different irradiation times were used. For the case of Nomex HT90-40 the preheating period was 180s, and for the Cotton/Nylon/Nomex fabric blend and cotton based fabrics (*Fabric 1*, *Fabric 2*) a shorter, 120s preheating period was used. In the fabric blend and cotton based fabrics it was observed that preheating periods longer than 120s resulted in some charring and release of smoke, therefore it was concluded that a 120s preheating period would result in a steady-state sample surface temperature without noticeable charring or smoke release.

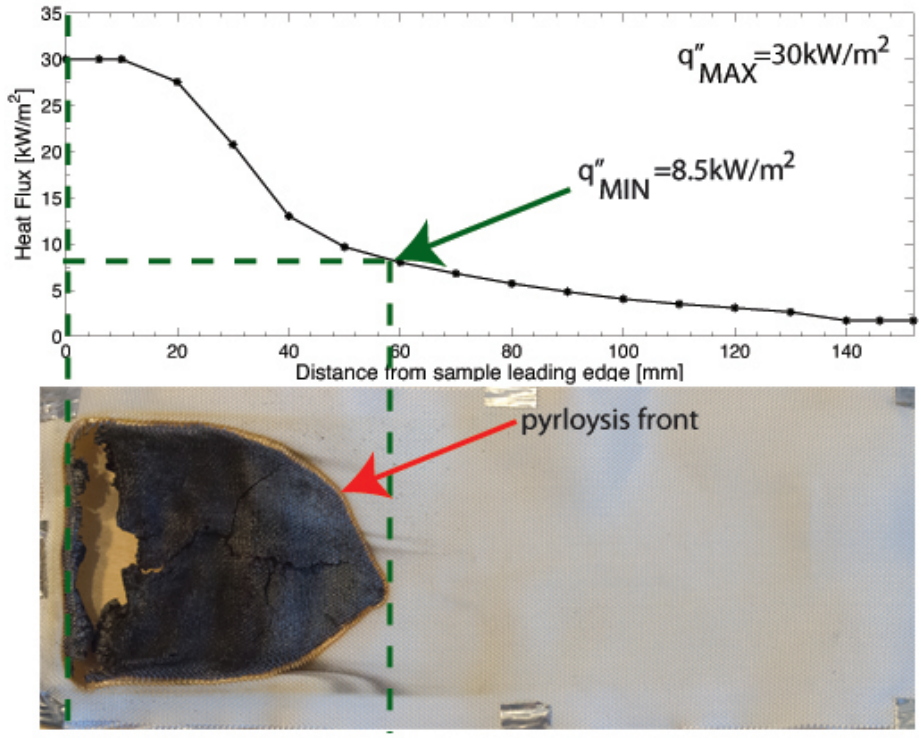

Figure 2.5: Relationship between flame spread and minimum heat flux for flame spread. Oxidizer flow velocity was 1.0 m/s, O_2 concentration 31% and $\dot{q}''_{MAX}$ 30 kW/m^2.

Steady-state sample surface temperatures were verified by sewing type-K thermocouples to the top and back surface of the fabrics at different locations downstream of the sample leading edge. An example of back surface sample temperature for Nomex HT90-40 subject to a peak radiant flux of 30 kW/m^2 is shown in Figure 2.6. In this figure it can be seen that Nomex HT90-40 achieves an approximate steady state surface temperature within the 180s preheating period. Although it is possible for some pyrolysis of the fabric to occur prior to ignition, sample the surface temperatures are below 500^oC, which is the temperature at which significant mass loss in Nomex is observed[12, 15]. The fact that no significant decomposition occurs at the observed sample surface temperatures was verified using TGA tests. The tests conducted with samples of Nomex HT90-40 showed that no significant decomposition occurred below 420^oC as seen in Figure 2.7. Similar considerations were taken for the other fabrics used in the reported experiments.

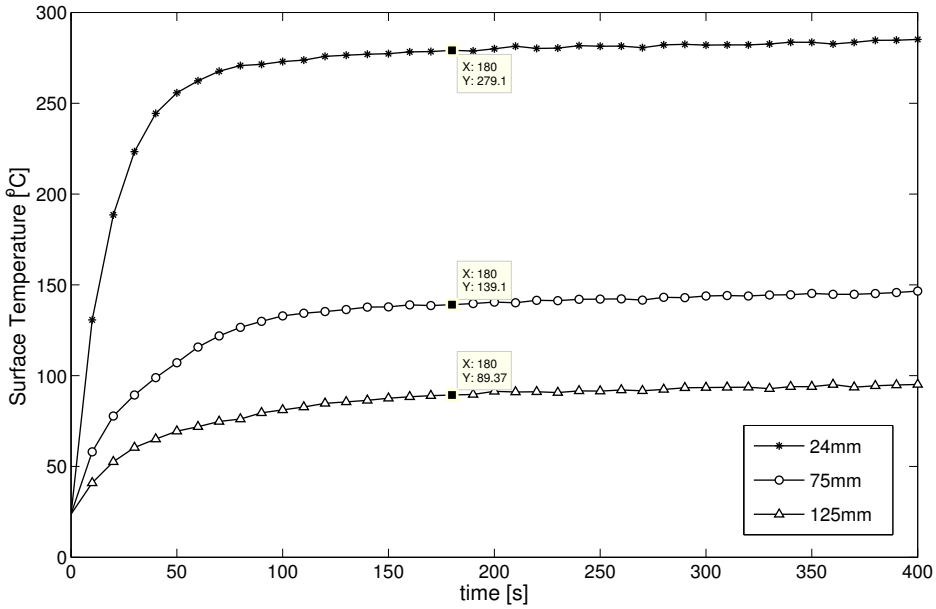

Figure 2.6: Temperature trace for Nomex HT90-40 exposed to $\dot{q}''_{MAX} = 30kW/m^2$. Type-K thermocouples were sewn at 24, 75 and 125 mm from the sample leading edge.

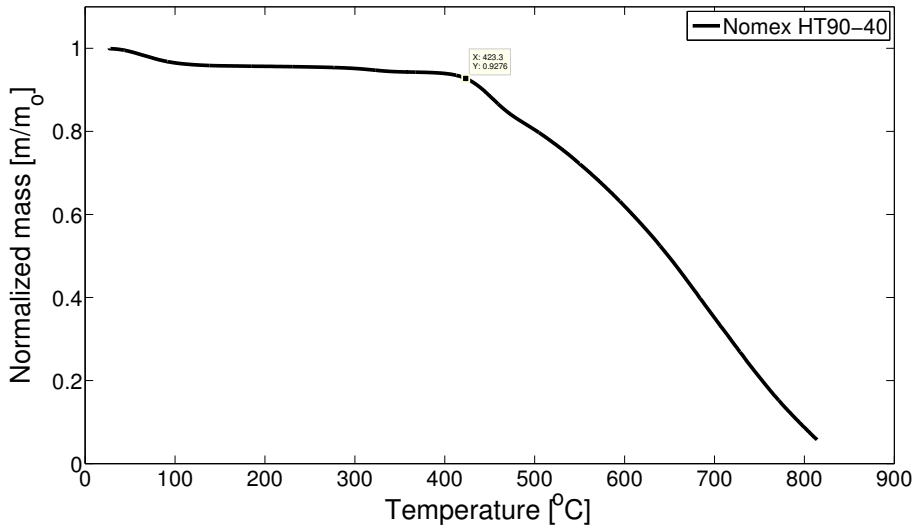

Figure 2.7: Nomex HT90-40 sample mass loss curve from TGA tests.

2.4 Results

The minimum radiant flux for flame spread, $\dot{q}''_{MIN}$, was determined using a minimum of three different maximum radiant flux values, $\dot{q}''_{MAX}$. Selecting different $\dot{q}''_{MAX}$ values allowed to verify that $\dot{q}''_{MIN}$ was independent of sample surface temperature. For a particular set of flow conditions different $\dot{q}''_{MAX}$ values resulted in different flame spread lengths, however $\dot{q}''_{MIN}$ was approximately the same. An example of experimental data of Nomex HT90-40 with an oxidizer flow velocity of 0.5 m/s is shown in Figure 2.8. As the value of $\dot{q}''_{MAX}$ increases, the external radiant flux applied to the fabric sample increases resulting in a longer flame spread distance to reach the same minimum radiant flux for flame spread. Increasing $\dot{q}''_{MAX}$ from 30 to 40 kW/m^2 resulted in longer flame spread distances for all oxygen concentrations tested. The constant nature of $\dot{q}''_{MIN}$ can be observed from the horizontal alignment of the different flame spread distances for a combination of oxygen concentration and external radiation. For any given combination of external radiant flux, oxygen concentration and oxidizer flow velocity at least two experiments are conducted and the reported values of $\dot{q}''_{MIN}$ correspond to the average of no less than six experiments.

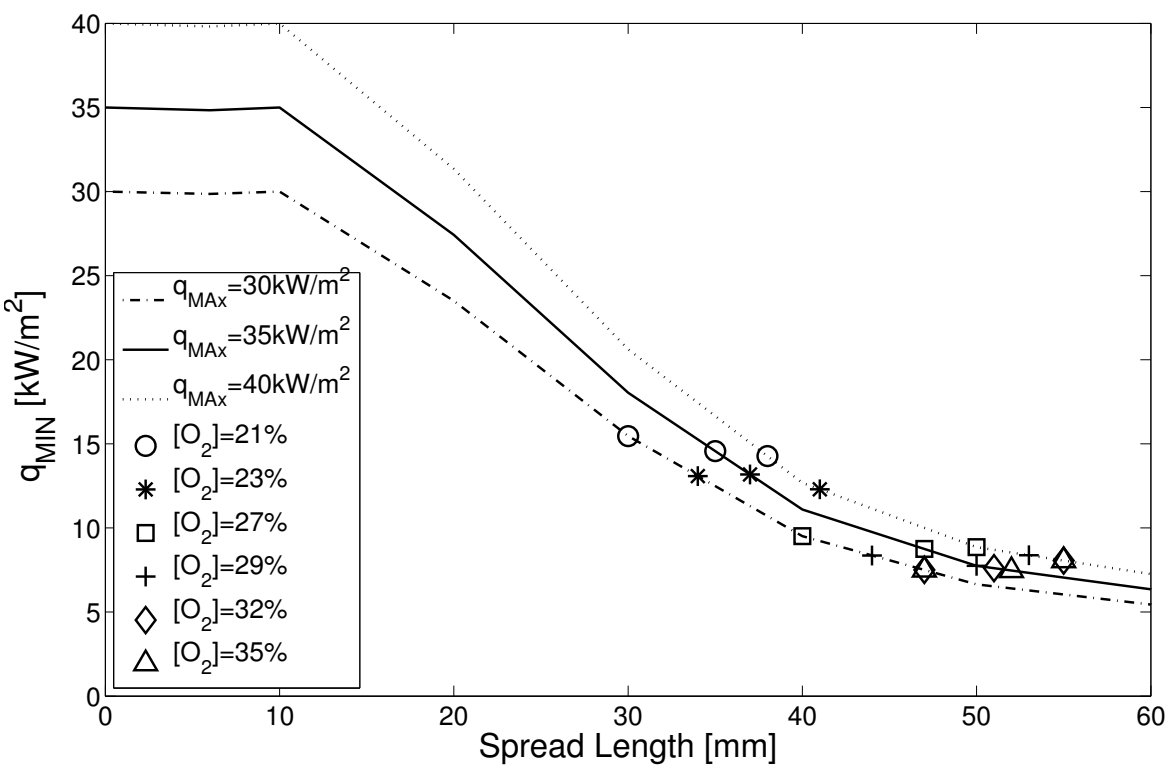

Figure 2.8: Experimental data for Nomex HT90-40 and oxidizer flow velocity of 0.5 m/s.

2.4.1 Nomex HT90-40

An example of flame spread over a Nomex HT90-40 is presented in Figure 2.9. For this experimented the oxidizer flow velocity was 0.5 m/s, the oxygen concentration was 40%, and the maximum external radiant flux had a value of 40 kW/m^2. Prior to ignition of the sample fabric at $t = 0s$, the external radiant heaters were allowed to irradiate the test sample for $180s$. Shortly after the igniter wire was turned on, a flame appeared over the sample and started spreading. As the flame spread over the surface, Nomex HT90-40 swelled resulting in observable wrinkles along the sample surface. As the fabric burned it left behind a char residue, which burned out at a slower rate than the flame spread rate. The green line in Figure 2.9 represents the approximate location of the flame front.

Figure 2.10 presents $\dot{q}''_{MIN}$ measurements for Nomex HT90-40 as a function of oxygen concentration for selected oxidizer flow velocities, with the data markers in the figure indicating the experimentally determined limit between flame and no flame spread. During the experiments three maximum external radiant flux values of 30, 35 and $40kW/m^2$ were used in combination with oxygen concentrations ranging from 21% to 40% and oxidizer flow velocities of 0.5, 0.7 and 1.0 m/s resulting in forced flow conditions over the sample.

From the results the general trend is that as oxygen concentration increases the minimum external radiant flux for flame spread, $\dot{q}''_{MIN}$ decreases. When the oxygen concentration was 21%, a large variation in the value of $\dot{q}''_{MIN}$ was observed primarily due to the variability in flame spread distances observed for different $\dot{q}''_{MAX}$ values. In the region near the leading edge of the sample the gradient of the external radiant flux is steep, and therefore small changes in flame spread distance can result in large differences in $\dot{q}''_{MIN}$. It is also possible that the flame spread distance may have been influenced by heat from the igniter wire. As the oxygen concentration was further increased, the spread in the data is reduced as a result of longer and more consistent flame spread distances.

Increasing the oxygen concentration between 22% and 35% resulted in a small reduction in the value of $\dot{q}''_{MIN}$. The reduction in $\dot{q}''_{MIN}$ was gradual until reaching 35%, at which point a large variation in the data appeared. Additional repetitions in oxygen concentrations of 35% and 37% also showed variation in $\dot{q}''_{MIN}$. In the experiments with 35% and 37% some repetitions would result in partial burning of the test sample, while others would result in flame spread that propagated over the entire sample. Once the oxygen concentration reached 40% the variation disappeared and all experiments had a $\dot{q}''_{MIN}$ of less than 1 kW/m^2.

Different oxidizer flow velocities of 0.5, 0.7 and 1.0 m/s were used to investigate the effect of flow velocity in the minimum heat flux for flame spread. The results revealed that for the range of velocities tested the oxidizer flow velocity does not have a significant influence in the value of $\dot{q}''_{MIN}$. Except for oxygen concentrations around 21% and between 35% and 37%, the values of $\dot{q}''_{MIN}$ appear to be independent of the oxidizer flow velocity selected.

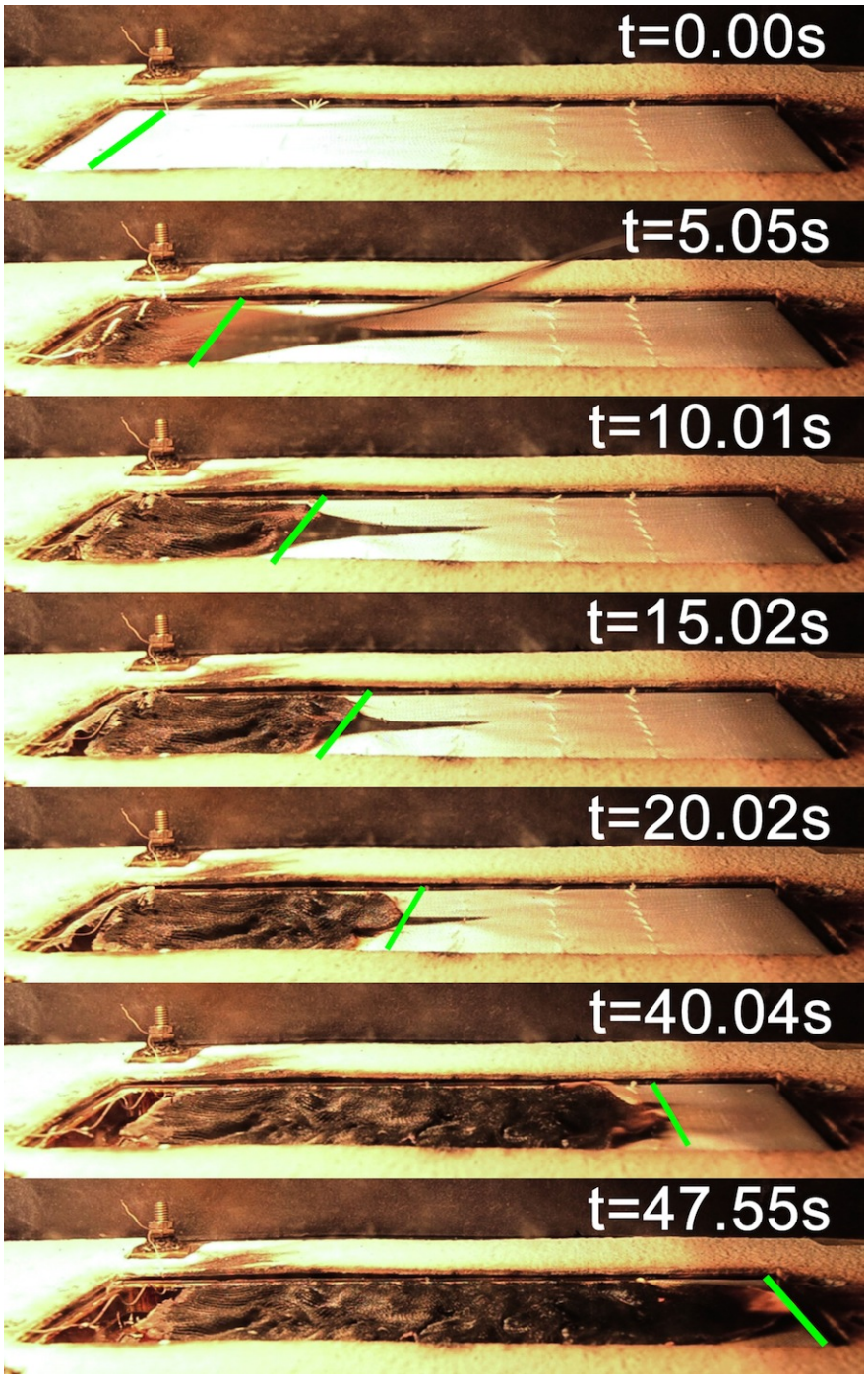

Figure 2.9: Flame spread over Nomex HT90-40.

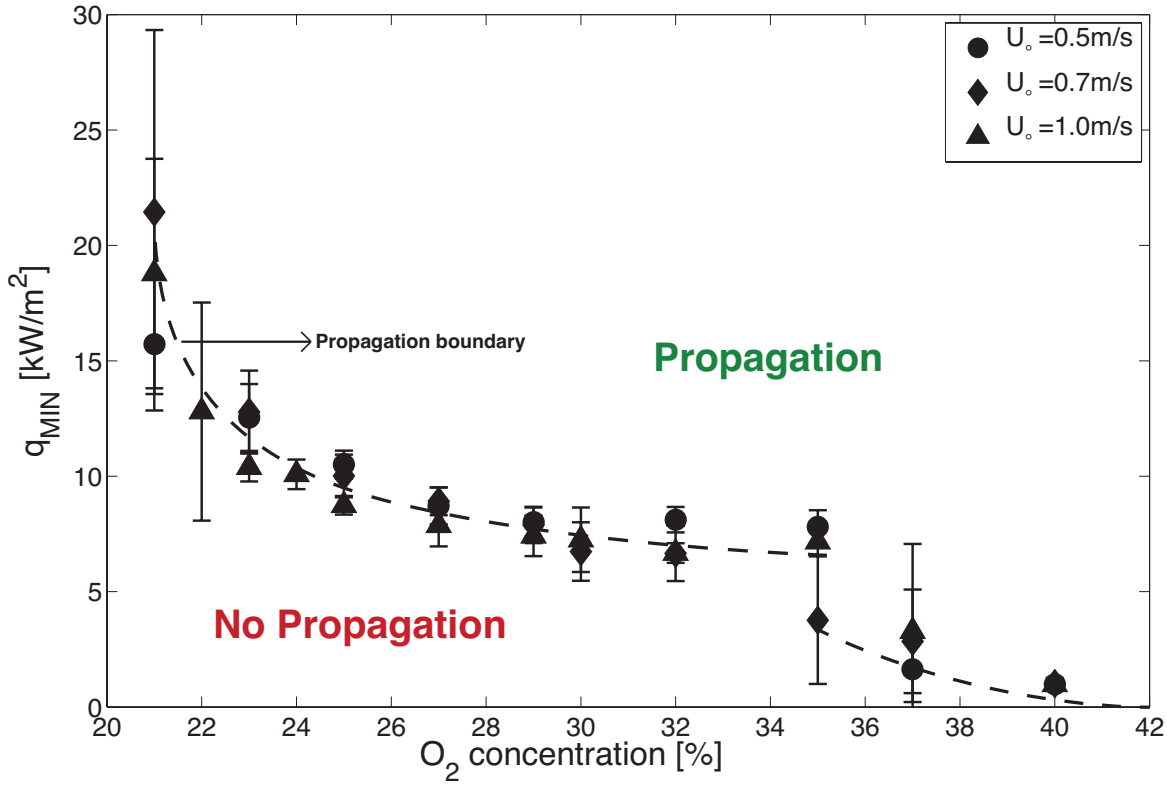

Figure 2.10: $\dot{q}''_{MIN}$ vs. [O_2] for Nomex HT90-40 in oxidizer flow velocities of 0.5, 0.7 and 1.0 m/s.

2.4.2 Cotton/Nylon/Nomex Fabric Blend

A fabric blend made of 29% Cotton/31% Nylon/40% Nomex was used to study how fabric composition affected the value of the minimum external radiant flux for flame spread. Preliminary experiments showed that maximum external radiant flux values, $\dot{q}''_{MAX}$, greater than 25 kW/m^2 resulted in offgassing and charring of the fabric blend. Once charring occurred, ignition of the fabric blend proved to be difficult. Therefore, in order to avoid off gassing and/or charring, $\dot{q}''_{MAX}$ was limited to a maximum value of 25 kW/m^2. Overall, it was found that the fabric blend followed a trend similar to the one observed in experiments with Nomex HT90-40, $\dot{q}''_{MIN}$ decreased as oxygen concentration increased.

The main difference between Nomex HT90-40 and the fabric blend was the oxygen concentration at which no external radiant flux is needed for flame spread. Whereas in Nomex HT90-40 the $\dot{q}''_{MIN} = 0kW/m^2$ point corresponded to an oxygen concentration of 40%, in the case of the fabric blend the corresponding oxygen concentration was 19%. As the oxygen concentration was further reduced the value of $\dot{q}''_{MIN}$ increased and once the oxygen concen-

tration reached 15%, $\dot{q}''_{MIN}$ had an average value of 14 kW/m^2 for an oxidizer flow velocity of 0.5 m/s, and 12 kW/m^2 for an oxidizer flow velocity of 1.5 m/s. A limited number of experiments were conducted in oxygen concentrations below 15% since it was determined that oxygen concentrations below 15% fall below the hypoxic limit at 1 atm and do not represent likely conditions in earth or space applications.

Similar to the work conducted with Nomex HT90-40, the effect of the oxidizer flow velocity in $\dot{q}''_{MIN}$ was also tested using the Cotton/Nylon/Nomex fabric blend. Experiments with oxidizer flow velocities of 0.5 and 1.5 m/s showed more noticeable differences in the fabric sample $\dot{q}''_{MIN}$ values. It was observed that as oxidizer flow velocity increased $\dot{q}''_{MIN}$ decreased. Although the increasing the oxidizer flow velocity resulted in more noticeable differences than in the case of Nomex HT90-40, the differences are small and suggest that oxidizer flow velocity does not affect significantly the value of $\dot{q}''_{MIN}$ for the range oxidizer flow velocities covered. Results of $\dot{q}''_{MIN}$ as a function of oxygen concentration for oxidizer flow velocities of 0.5 and 1.5 m/s are shown in Figure 2.11.

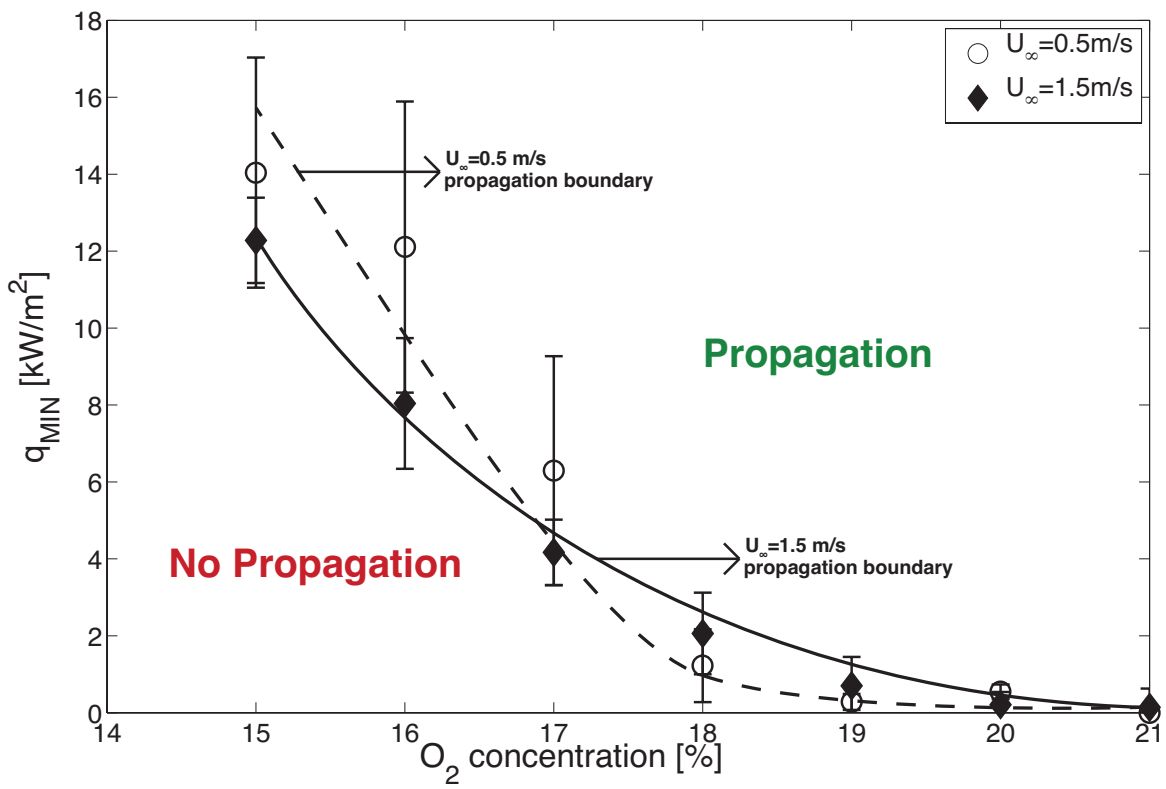

Figure 2.11: $\dot{q}''_{MIN}$ vs. $[O_2]$ for Cotton/Nylon/Nomex fabric blend in oxidizer flow velocities of 0.5 and 1.5 m/s.

2.4.3 Cotton Based Fabrics

The minimum external radiant flux for flame spread was used to study the flammability behavior of two non fire-resistant cotton based fabrics that have been suggested as potential fuels for large-scale flammability experiments in microgravity. The two fabrics referred as *Fabric 1* and *Fabric 2*, had densities of 3 and 5 mg/cm^2 respectively. The two cotton based fabrics allowed investigating the effect of fabric density on $\dot{q}''_{MIN}$. A maximum external radiant flux of 25 kW/m^2 was used in all experiments with the cotton based fabrics. A constant oxidizer flow velocity of 1 m/s was used in all experiments given that changes in oxidizer flow velocity in Nomex HT90-40 and the Cotton/Nylon/Nomex fabric blend resulted in small changes in $\dot{q}''_{MIN}$.

Results showed that for oxygen concentrations greater than 17% no external radiant flux is required for flame spread in *Fabric 1* and *Fabric 2*. As the oxygen concentration was reduced, addition of an external radiant flux was required in order to observe flame spread matching the trend observed in Nomex HT90-40 and the Cotton/Nylon/Nomex blend. During the experiments it was observed that once the flame propagated over the sample surface and extinguished, it gave way to a smoldering front that propagated at a slower rate that consumed the material. The value of $\dot{q}''_{MIN}$ for the cotton based fabrics was calculated using the distance at which the smoldering front stopped propagating because the smoldering front was able to consume the fabric. Based on the observed results, fabric density plays a minor role in the value of $\dot{q}''_{MIN}$, with larger densities requiring higher external radiant flux values.

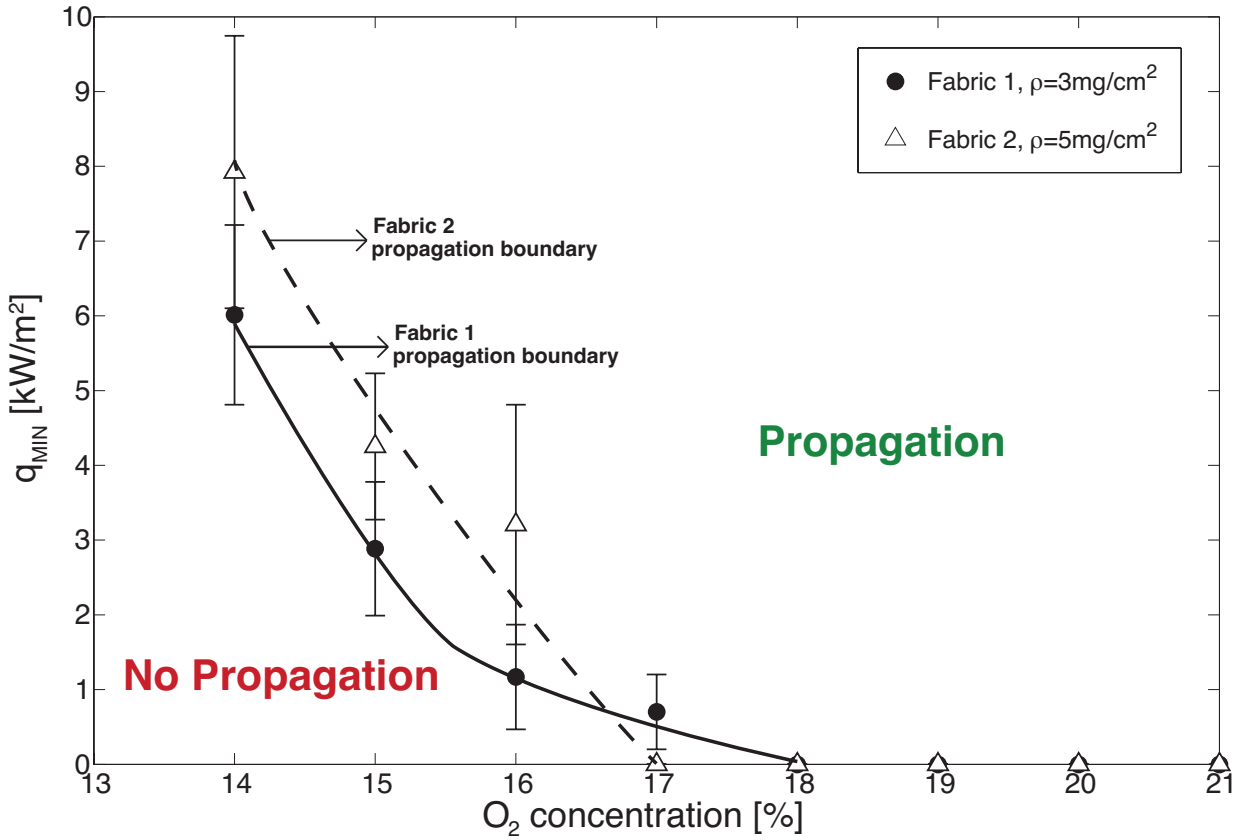

Figure 2.12: $\dot{q}"_{MIN}$ vs. $[O_2]$ for three cotton based fabrics in oxidizer flow velocities of 1.0 m/s.

2.5 Analysis

Flame spread over thin fire-resistant (FR) materials is a complex process that involves both, the solid and the gas phase. In solid phase processes such as charring and intumescence alter chemical and physical properties of the fuel to slow the rate at which solid fuel is decomposed, and ultimately slow or eliminate flame spread. In the gas phase, dilution and radical quenching can slow the gas-phase reaction rate, which can reduce the reaction rate and the amount of heat transferred to the unburned fuel. For the above reasons, the development of an analytical solution for flame spread over FR materials is difficult. Acknowledging the complexity of the problem at hand, it is possible to phenomenologically interpret the results using the flame spread formulation developed by Fernandez-Pello[16] for thin fuels.

In this formulation, flame spread is seen as a series of continuous piloted ignition events for which the flame acts as both, the pilot and source of heat for the pyrolysis process. The

flame spread rate, V_f, is calculated as the ratio of the heated length, l_h, to the solid ignition time, t_{ig}. The heated length is the region between the pyrolysis front, l_p, and the flame length, l_f, i.e. $l_h = l_f - l_p$. For an schematic of l_f, l_p and l_h refer to Figure 1.2 in Chapter 1. The ignition time is given by the sum of the pyrolysis time, mixing time, and chemical time, that is $t_{ig} = t_p + t_{mix} + t_{chem}$ and represents the time required to raise the temperature of the heated length to the point the solid decomposes and eventually ignites. Under low oxidizer flow velocities and/or high oxygen concentrations conditions it is reasonable to assume that the time required to bring the solid fuel to its pyrolysis temperature is the most relevant time scale for the ignition of a solid fuel. For a thin solid, the pyrolysis time, t_p, is given by

$$t_p = \frac{\rho_s Cp_s s(T_p - T_o)}{\dot{q}''_{tot}} \tag{2.5.1}$$

In Equation 2.5.1, $\dot{q}''_{tot}$ is the net heat flux at the fuel surface including radiative, convective and conductive heat fluxes. Combining expressions for t_p and l_h, Fernandez-Pello[16] proposed the following expression for concurrent flame spread over thin fuels

$$V_f \approx \frac{\left[(k_g \rho_g Cp_g u_\infty / l_p)^{1/2} (T_f - T_p) + \dot{q}''_{fr} - \dot{q}''_{sr} + \dot{q}''_{ext}\right] (l_f - l_p)}{\rho_s Cp_s s(T_p - T_o)} \tag{2.5.2}$$

When exposed to heat, charring materials such as wood or Nomex produce a char layer that limits heat and mass transfer to the unburned portion of the fuel. As the char layer builds up it acts as an insulation layer that limits the amount of heat reaching the unburned fuel, which in turn reduces the rate at which the solid heats up. Since solid pyrolysis follows an Arrhenius behavior, a reduction in the solid fuel temperature will reduce the solid decomposition rate. Once the temperature drops below a critical value, the decomposition rate falls off rapidly and it is not able to sustain a flame. In experiments with thick wood slabs Saito et al.[17] noted that charring introduced a time-dependent mass loss rate, $\dot{m}''$. The authors noted that the time dependent mass loss rate will depend on the pyrolysis characteristics of the material. An approximate expression for the time dependent mass loss rate proposed by Saito et al. assumes a uniform mass loss rate per unit area, $\dot{m}'' = \dot{m}''_o$, during a fixed pyrolysis time and zero otherwise, see Equation 2.5.3.

$$\dot{m}''(t) = \begin{cases} \dot{m}''_o & \text{if } t \leq t_p \\ 0 & \text{if } t > t_p \end{cases} \tag{2.5.3}$$

The introduction of a time dependent solid decomposition implies that as a charring material burns, both the l_p and l_f change. Hence the most straightforward method to

incorporate the charring behavior of Nomex into Equation 2.5.2 is to include an expression for the time-dependent flame length. Quintiere and Harkleroad[18] and Hasemi[19] proposed an alternative method for estimating l_f in upward propagation using the heat release rate per unit width of fuel, $\dot{Q}'$. A modified version for forced flow can be used to express l_f as

$$l_f = c\left(\frac{\dot{Q}'}{Cp_g T_f \rho_g u_\infty}\right) \tag{2.5.4}$$

where $\dot{Q}'$ can be calculated by integrating the mass loss rate over the time dependent pyrolysis length and multiplying it by the heat of combustion, ΔH_c,

$$\dot{Q}' = \int_{l_b(t)}^{l_p(t)} \dot{m}''(t)\Delta H_c dx \tag{2.5.5}$$

In Equation 2.5.5, the time dependence of l_b and l_p is a result of the char layer build up. Initially, char build up is small allowing unrestricted heat transfer to the fabric, but as the char layer builds up the solid decomposition drops resulting in smaller flames. Once the insulating layer is thick enough, heat transfer from the flame to the unburned solid is not enough to maintain a propagating flame and the flame extinguishes, i.e. $l_p = l_b$.

Assuming that the heat needed to bring the solid to the pyrolysis temperature is small compared to the heat needed to pyrolyse the fuel, ΔH_p, and that the material behaves as thermally thin, $\dot{m}''_o$ can be calculated using Equation 2.5.6. In this equation $\dot{q}''_{tot}$ is the total amount of heat transferred from the flame to the solid fuel, i.e. conduction, convection and radiation, $\dot{q}''_{sr}$ is the heat reradiated by the solid, and $\dot{q}''_{ext}$ is the external radiant flux, if present. The charring behavior of the material will also appear through changes in ΔH_p as the sample composition changes due to preferential pyrolysis of blended materials and char layer build up. Therefore, as the value of ΔH_p increases the pyrolysis rate of the material will decrease.

$$\dot{m}''_o = \frac{\dot{q}''_{tot} - \dot{q}''_{sr} + \dot{q}''_{ext}}{\Delta H_p} \tag{2.5.6}$$

Combining Equation 2.5.4, Equation 2.5.5, Equation 2.5.6 and replacing into Equation 2.5.2 a modified expression for flame spread over thin charring materials such as Nomex takes the form of Equation 2.5.7. This expression can be used to phenomenologically explain

the effects of external radiation, oxygen concentration, fabric composition, and oxidizer flow velocity in the minimum conditions for flame spread in FR materials.

$$V_f \approx \frac{\left[\left(\frac{k_g \rho_g Cp_g u_\infty}{l_p}\right)^{1/2} (T_f - T_p) + \dot{q}''_{fr} - \dot{q}''_{sr} + \dot{q}''_{ext}\right]\left[\left(\frac{\int_{l_b}^{l_p} \frac{\dot{q}''_{fr} - \dot{q}''_{sr} + \dot{q}''_{ext}}{\Delta H_p} \Delta H_c dx}{Cp_g T_f \rho_g u_\infty}\right) - l_p\right]}{\rho_s Cp_s s(T_p - T_o)} \tag{2.5.7}$$

2.5.1 Oxygen Concentration and External Radiant Flux

Flame spread over solid is characterized by the development of a non-premixed flame with the reaction zone is concentrated near stoichiometric conditions. In addition, it is assumed that the chemical reaction is fast in comparison to the mixing and solid decomposition processes. Under this assumption changes in oxygen concentration will mainly result in changes in the flame temperature, T_f. This relationship between $[O_2]$ and T_f is important because the flame acts as a heat source making the total amount of heat transferred from the flame to the solid fuel a function of T_f. An increase in oxygen concentration will result in a greater convective, $\dot{q}''_{conv}$, and radiative, $\dot{q}''_{fr}$, heat transfer to the solid fuel since $\dot{q}''_{conv} \propto T_f$ and $\dot{q}''_{fr} \propto T_f^4$. As both, $\dot{q}''_{conv}$ and $\dot{q}''_{fr}$ increase, t_p decreases resulting in faster solid decomposition rates that result in longer pyrolysis and flame lengths.

When the oxygen concentration is high enough, $\dot{q}''_{tot}$ can provide enough heat to drive the solid pyrolysis without any additional external heat transfer. In the experiments this corresponds to the oxygen concentration at which $\dot{q}''_{MIN} = 0kW/m^2$. For the case of Nomex HT90-40 the lowest oxygen concentration at which no external radiant flux was required for flame spread was 37%, which is significantly higher than the LOI values obtained by [8, 10, 11]. The difference in oxygen concentrations can be attributed to differences in the testing configuration. Whereas in ASTM D 2863[7] (LOI Test Method) both sides of the sample are exposed to an oxidizer, in the current experiments only the top surface of the fabric was exposed to an oxidizer flow. Another difference constitutes the ignition source used in the experiments, both NASA Standard 6001 Test 1[9] and ASTM D 2863 uses a chemical igniter, i.e. flame, and the present experiments use an ignition wire. It is important to note that present results are not attempting to recreate LOI or MOC tests, but instead the focus is to understand how oxygen concentration and addition of an external radiant flux affect flame spread over fire-resistant and non fire-resistant fabrics.

For oxygen concentrations below the $\dot{q}''_{MIN} = 0\ kW/m^2$ limit the reduction in $[O_2]$ and subsequently T_f mean that the heat transfer from the flame alone cannot maintain flame

spread. Below this limit there exists an unbalance between the heat required to maintain an adequate pyrolysis rate and the heat released by the propagating flame. The addition of an external radiant heat flux allows overcoming this unbalance and extends the range of oxygen concentrations over which flame spread can occur. With decreasing oxygen concentration the heat transfer deficit increases resulting in an increase in $\dot{q}''_{MIN}$ as observed in the results with all the fabrics tested.

It is also possible that oxygen concentration has an effect in the solid fuel pyrolysis. As shown by Hirata et al.[20]. In weight loss experiments with PMMA, Hirata et al. found that the degradation of PMMA occurred faster in air than in pure nitrogen environments and concluded that degradation in environments containing oxygen had two distinct effects. At low temperatures oxygen increases the stability to PMMA, and at high temperatures destabilizes it. Assuming similar behavior for Nomex HT90-40 would help explaining the variation in $\dot{q}''_{MIN}$ observed in oxygen concentrations around 35%.

2.5.2 Oxidizer Flow Velocity

The effect of the oxidizer flow velocity will appear through convective heat flux, which in according to Equation 2.5.7 is approximately equal to

$$\dot{q}''_{conv} = \left(\frac{k_g \rho_g C p_g u_\infty}{l_p} \right)^{1/2} (T_f - T_p) \tag{2.5.8}$$

In the above expression, $\dot{q}''_{conv} \sim {u_\infty}^{1/2}$, similar to the solution for laminar flow heat transfer over a flat plate. In laminar flow over a flat plate, increasing u_∞ decreases the thermal boundary layer thickness, δ_t, since $\delta_t \sim \mathrm{Re}^{-1/2}$. At the fabric surface, $\dot{q}''_{conv}$ will be proportional to $\dot{q}''_{conv} \sim (T_f - T_p)/\delta_t$. Therefore, increasing u_∞ will decrease δ_t and result in an increase in $\dot{q}''_{conv}$. Assuming that $\dot{q}''_{tot}$ remains constant, an increase in $\dot{q}''_{conv}$ would lower the amount of external radiant flux required to sustain flame spread. In the results with Nomex HT90-40, the effect of the oxidizer flow velocity is not very evident, but for the case of the Cotton/Nylon/Nomex blend the results support the phenomenological explanation that increasing u_∞ decreases $\dot{q}''_{MIN}$.

The small variation in $\dot{q}''_{MIN}$ for Nomex when u_∞ changed can be attributed to the fact that oxygen concentration, through the increase in T_f plays a more significant role than u_∞ given the small of range of velocities tested. It is possible that due to the charring and intumescent characteristics of Nomex HT90-40, changes in $\dot{q}''_{conv}$ as the sole result of changing u_∞ are small compared to the total heat flux required for pyrolysis of the solid fuel. The lower Nomex content of the Cotton/Nylon/Nomex fabric blend does not result in the same amount of char or intumescence and $\dot{q}''_{conv}$ accounts for a more significant portion of the total heat flux required to sustain the decomposition of the solid fuel.

2.5.3 Fabric Characteristics

Fabric characteristics can affect flame spread in multiple ways. Different types of materials will have different physical and thermal properties such as thickness, s, specific heat Cp, density ρ_s, and pyrolysis temperature, T_p, to name a few. Each of these properties will have an effect on the flame spread rate, V_f, and $\dot{q}''_{MIN}$. The important issue is to understand which characteristics are more likely to affect V_f and $\dot{q}''_{MIN}$. Looking at the results of the cotton based fabrics, it is observed that changing the fabric density resulted in a small change in $\dot{q}''_{MIN}$. Equation 2.5.7 suggests that increasing ρ_s will increase the amount of energy required to bring the solid to its pyrolysis temperature and with it the minimum external radiant flux required for flame spread. However, the difference in the values is small, and much like the oxidizer flow velocity it can be concluded that although material density may affect $\dot{q}''_{MIN}$ it is not as important as the effect of oxygen concentration.

Experiments with the different fabrics showed that fabric composition has a more significant effect on flame spread and the value of $\dot{q}''_{MIN}$. Results showed that materials with a higher Nomex content required higher oxygen concentrations in order to observe unassisted flame spread ($\dot{q}''_{MIN} = 0\ kW/m^2$), see Table 2.1. From the experiments it was also noted that for a particular oxygen concentration, a higher Nomex content resulted in higher $\dot{q}''_{MIN}$ values. The differences in $\dot{q}''_{MIN}$ are a direct result of differences in the charring and intumescence characteristics of materials. As FR materials such as Nomex are replaced by NFR materials such as Cotton or Nylon, the fabric's ability to develop an insulation layer diminishes allowing the pyrolysis process to be sustained at lower oxygen concentrations.

Material	$[O_2]$at $\dot{q}''_{MIN} = 0\ kW/m^2$
Nomex HT90-40	37%
Cotton/Nylon/Nomex	19%
Fabric 1	18%
Fabric 2	18%

Table 2.1: Oxygen concentrations for unassisted flame spread.

2.6 Conclusions

This chapter introduced experiments conducted to evaluate the minimum conditions for flame spread in both fire-resistant (FR) and non fire-resistant (NFR) materials. The primary focus consisted in experimentally determining the minimum external radiant flux required for concurrent flame spread, $\dot{q}''_{MIN}$, as a function of variables such as oxygen concentration, oxidizer flow velocity, and fabric composition. The response of $\dot{q}''_{MIN}$ to different environmental conditions allows obtaining more detailed information about the flammability behavior of

materials over a wide range on conditions. Experiments with two FR and two NFR fabrics under different combinations of external radiant flux, oxygen concentration, and oxidizer flow velocity suggest the following:

1. In concurrent flame spread, increasing the oxygen concentration raises the flame temperature. As flame temperature increases, the convective and radiative heat flux to the solid fuel increase resulting in an increased solid decomposition and faster flame spread rates. Increasing the oxygen concentration decreased the value of $\dot{q}''_{MIN}$ in all materials tested. Beyond a critical oxygen concentration, flames are able to spread without an external radiant flux, see Table 2.1.

2. Oxidizer flow velocity, u_∞, has a small effect in $\dot{q}''_{MIN}$. As u_∞, increases the thickness of the boundary layer decreases resulting a higher convective heat transfer coefficient that increases the convective heat flux $\dot{q}''_{conv}$ from the flame to the sample. In charring and/or intumescent materials such as Nomex, the contribution of $\dot{q}''_{conv}$ to the total heat flux for sustained pyrolysis may be small in comparison to the radiative heat flux, $\dot{q}''_{fr}$, given the high oxygen concentrations required for flame spread. As the Nomex content of a material reduces, it is possible to sustain flame spread at lower oxygen concentrations and the contribution of $\dot{q}''_{conv}$ becomes more significant. At this point changes in $\dot{q}''_{conv}$ will results in more noticeable changes in $\dot{q}''_{MIN}$.

3. Reducing the amount of Nomex in a fabric blend allows flame spread to occur at lower oxygen concentrations. As FR material is substituted by NFR material it is possible to sustain flame spread at lower oxygen concentrations due to changes in the pyrolysis of the fabric blend.

The combination of $\dot{q}''_{MIN}$ as a function of $[O_2]$ can be used to develop flammability diagrams of both, FR and NFR materials. Such flammability diagrams can be used to gain a better understanding of the material flammability and the role environmental variables play in the flammability of materials. There is a possibility that exact results presented in this chapter are specific to the experimental configuration used. However, the relationships between the minimum external radiant flux for flame spread and other environmental variables are valid for any kind of fabric.

2.7 References

[1] T.L. Bergman et al. *Fundamentals of Heat and Mass Transfer*. Seventh Edition. Wiley, 2011. ISBN: 9780470501979.

[2] John R. Howell, Robert Siegel, and M. Pinar Menguc. *Thermal Radiation Heat Transfer*. Fifth Edition. Taylor & Francis, 2011. ISBN: 9781439805336.

[3] Phil Cheney and Andrew Sullivan. *Grassfires: Fuel, Weather and Fire Behaviour*. Second Edition. CSIRO Publishing, 2008. ISBN: 9780643093836.

[4] ASTM Standard E1321-13, (2013). *Standard Test Method for Determining Material Ignition and Flame Spread Properties*. West Conshohocken, PA: ASTM International, 2013. DOI: 10.1520/E1321-13. URL: http://www.astm.org.

[5] ASTM Standard E970-14, (2014). *Standard Test Method for Critical Radiant Flux of Exposed Attic Floor Insulation Using a Radiant Heat Energy Source*. West Conshohocken, PA: ASTM International, 2014. DOI: 10.1520/E0970-14. URL: http://www.astm.org.

[6] ASTM Standard E648-10, (2010). *Standard Test Method for Critical Radiant Flux of Floor-Covering Systems Using a Radiant Heat Energy Source*. West Conshohocken, PA: ASTM International, 2010. DOI: 10.1520/E0648-10E01. URL: http://www.astm.org.

[7] ASTM Standard D2863-13, (2013). *Standard Test Method for Measuring the Minimum Oxygen Concentration to Support Candle-Like Combustion of Plastics (Oxygen Index)*. West Conshohocken, PA: ASTM International, 2013. DOI: 10.1520/D2863-13. URL: http://www.astm.org.

[8] Julie Kleinhenz and James S. T'ien. "Combustion of Nomex III Fabric in Potential Space Habitat Atmospheres: Cyclic Flame Spread Phenomenon". In: *Combustion Science and Technology* 179.10 (2007), pp. 2153–2169. DOI: 10.1080/00102200701386172.

[9] *Flammability, Odor, Offgassing, and Compatibility Requirements and Test Procedures for Materials in Environments that Support Combustion, NASA STD 6001*. 1998. URL: http://www.nasa.gov/centers/johnson/pdf/485934main_NASA-STD-(I)-6001A%20Released.pdf.

[10] David B. Hirsch et al. "Oxygen Concentration Flammability Thresholds of Selected Aerospace Materials Considered for the Constellation Program". In: (2007). URL: http://ntrs.nasa.gov/archive/nasa/casi.ntrs.nasa.gov/20070018178_2007017304.pdf.

[11] Sandra L. Olson, Gary A. Ruff, and Fletcher J. Miller. "Microgravity Flame Spread in Exploration Atmospheres: Pressure, Oxygen, and Velocity Effects on Opposed and Concurrent Flame Spread". In: *38th International Conference on Environmental Systems*. San Francisco, CA: SAE International, June 2008. DOI: 10.4271/2008-01-2055.

[12] DuPont. *Technical Guide for Nomex Brand Fiber*. Tech. rep. H-52720. E.I. du Pont de Nemours and Company, 2001.

[13] David Rich et al. "Mass Flux of Combustible Solids at Piloted Ignition". In: *Proceedings of the Combustion Institute* 31.2 (2007), pp. 2653–2660. DOI: 10.1016/j.proci.2006.08.055.

[14] *16 CFR Volume 2 Chapter II Subchapter D - Flammable Fabrics Act Regulations*. 2012. URL: http://www.gpo.gov/fdsys/pkg/CFR-2012-title16-vol2/pdf/CFR-2012-title16-vol2-chapII-subchapD.pdf.

[15] S. Villar-Rodil, A. Martinez-Alonso, and J.M.D. Tascon. "Studies on Pyrolysis of Nomex Polyaramid Fibers". In: *Journal of Analytical and Applied Pyrolysis* 58-59 (2001), pp. 105–115. DOI: 10.1016/S0165-2370(00)00124-8.

[16] C. Fernandez-Pello, in: G. Cox (Ed.) *Combustion Fundamentals of Fire*. San Diego, CA: Academic Press, 1995. ISBN: 0121942309.

[17] K. Saito, J.G. Quintiere, and F.A. Williams. "Upward Turbulent Flame Spread". In: *Fire Safety Science* 1 (1986), pp. 75–86. DOI: 10.3801/IAFSS.FSS.1-75.

[18] James G. Quintiere, Margaret Harkleroad, and Yuji Hasemi. "Wall Flames and Implications for Upward Flame Spread". In: *Combustion Science and Technology* 48.3-4 (1985), pp. 191–222. DOI: 10.1080/00102208608923893.

[19] Y. Hasemi. "Thermal Modeling of Upward Flame Spread". In: *Fire Safety Science* 1 (1986), pp. 87–96. DOI: 10.3801/IAFSS.FSS.1-87.

[20] T. Hirata, T. Kashiwagi, and J.E. Brown. "Thermal Oxidative Degradation of Poly(methyl methacrylate): Weight Loss". In: *Macromolecules* 18 (1985), pp. 1410–1418. DOI: 10.1021/ma00149a010.

CHAPTER 3

AMBIENT PRESSURE

3.1 Introduction

At sea level the atmospheric pressure is 101.3 kPa, and the average surface temperature can be assumed to be 15^oC. However, as the elevation above sea level increases, atmospheric pressure decreases. The highest point on the earth surface is Mount Everest at an elevation of 8,850 m above sea level, which corresponds to an atmospheric pressure of 35.5 kPa, or about 35% of the value at sea level. Although nobody resides at this elevation, there are cities with populations above one million that are located at high elevations. Examples include: El Alto, Bolivia (4,150 m), Quito, Ecuador (2,850 m), Bogota, Colombia (2,620 m), and Addis Ababa, Ethiopia (2,500 m) to name a few[1]. Fires still occur at high elevations and they may or may not behave similarly to fires at sea level, and therefore it is important to study fire behavior in reduced ambient pressures.

There are other situations in which ambient pressure may depart from sea level conditions. Commercial airplane cabins are typically pressurized to an equivalent elevation ranging from 1,680 m (5,500 $ft.$) to 2,440 m (8,000 $ft.$)[2]. This allows passenger to breathe normally while at the same time reducing stress in the airplane's fuselage. Newer aircraft like the Boeing 787 use a cabin pressure equivalent to 1,830 m (6,000 $ft.$) compared to the 2,440 m equivalent used by older airplanes. Recently, there has been an increased interest in fires inside airplanes, particularly those that may be caused by batteries, providing an added motivation for studying material flammability in reduced ambient pressures. Reduced ambient pressures are also found inside spacecraft environments. Development of a next generation of space exploration vehicles resulting in cabin conditions with elevated oxygen concentrations and reduced ambient pressures[Ref.] has brought attention to the flammability behavior of materials that may be used in future spacecraft[3–7]. Prior to a extra vehicular activities, more commonly known as space walks, the spacecraft ambient pressure is reduced from 101.3 kPa to 70.3 kPa in order to reduce the risk of decompression sickness in the astronauts. The reduction in ambient pressure is often accompanied by an increase in the oxygen

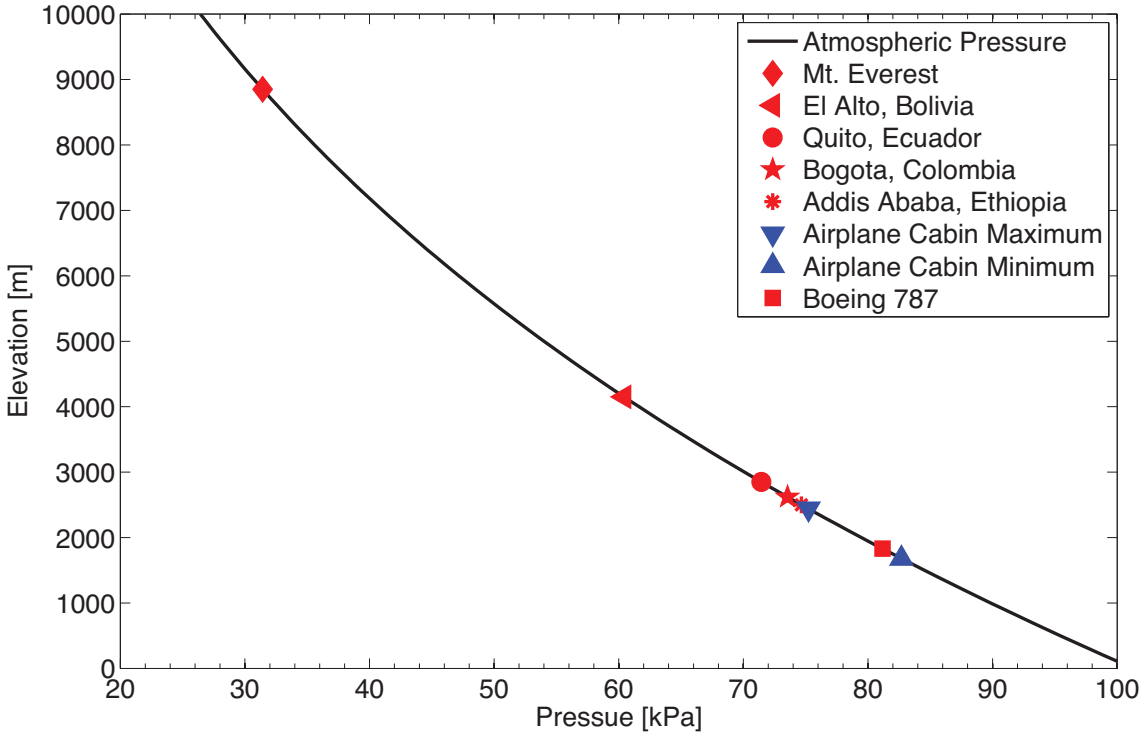

Figure 3.1: Atmospheric pressure as function of elevation.

concentration, which may increase the risk of a fire onboard.

At this time the combined effect of reduced ambient pressure, increased oxygen concentration and microgravity on the flammability of materials has not been extensively studied and constitutes an active area of fire safety research. Piloted ignition studies using PMMA have shown that in low pressure environments with high oxygen concentrations the ignition delay time and fuel mass flux at ignition decrease resulting in enhanced flammability at low ambient pressures[8, 9]. Hirsch *et al.*[6] conducted flammability experiments that determined the flammability behavior of materials used in space applications in ambient pressures of 48.2kPa and 85.3 kPa. Their results showed that the maximum oxygen concentration resulting in consistent self-extinguishment increased with decreasing ambient pressure. They also noted a reduction in the partial pressure of oxygen that resulted in self-extinguishment of the material.

Exploring the effect of ambient pressure in the flammability behavior of materials is an important step towards a better understating of the effect of environmental variables in the flammability of materials. This chapter will present experiments focused on studying the effect of ambient pressure on the flammability limits for flame spread over two fire-resistant

fabrics, Nomex HT90-40 and a Nomex/Nylon/Cotton fabric blend. The experiments were conducted over a wide range of low ambient pressures and different flame spread orientations. The objective of this work is to develop flame spread boundaries for two fire-resistant fabrics in terms of ambient pressure and the Limiting Oxygen Concentration (LOC) for flame spread. Such flame spread boundaries can be used to provide a more accurate representation of the expected flammability behavior of materials in reduced ambient pressure environments.

3.2 Experiment Description

Limiting Oxygen Concentration (LOC) flammability experiments were conducted in a small-scale combustion wind tunnel housed inside a sealed chamber. The small-scale combustion wind tunnel is based on the original Forced Ignition and Flame Spread Test (FIST) apparatus and has been previously used to study ignition delay[8] and critical mass flux at ignition[9] in reduced ambient pressures. The tunnel shown schematically in Figure 3.2, is 400 mm long with a rectangular cross-section of 150 mm wide by 120 mm tall. The original bottom section of the tunnel was replaced in order to accommodate testing of fabric samples and is made up of a 12.5 mm aluminum plate covered by a 1.6 mm ceramic insulation sheet with a 50.8 mm by 152.4 mm rectangular cutout section located 130 mm from the tunnel inlet. Fabric samples are secured to an aluminum sample holder that is attached to the tunnel allowing the samples to sit flushed to the bottom surface of the tunnel. A 1.6 mm aluminum plate placed 10 mm below the test sample is used to prevent air entrainment once the sample ignites. Side walls of the tunnel are made of 12.5 mm thick aluminum plates with quartz windows for optical access and the top surface of the tunnel is made of a 1.6 mm aluminum plate.

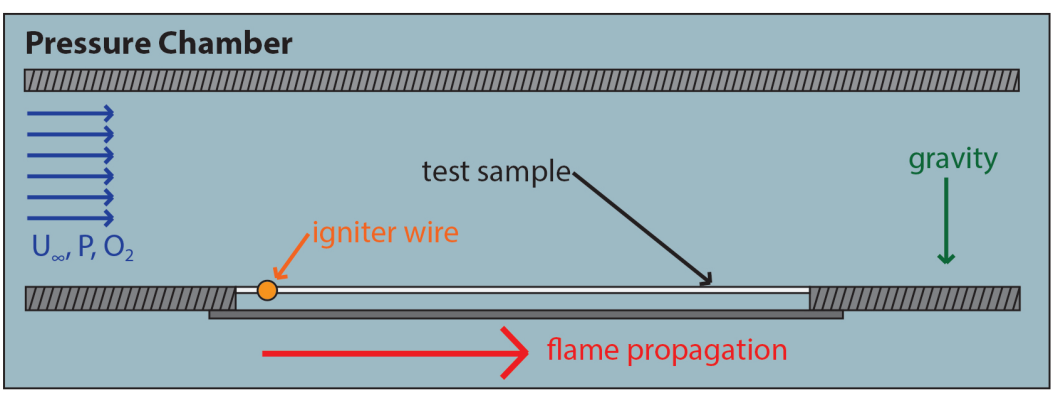

Figure 3.2: Reduced ambient pressure experiment diagram. Depending on pressure chamber orientation and igniter wire position four different flame spread configurations can be tested.

The tunnel slides inside a 105 L sealed chamber that allows adjusting the ambient pressure

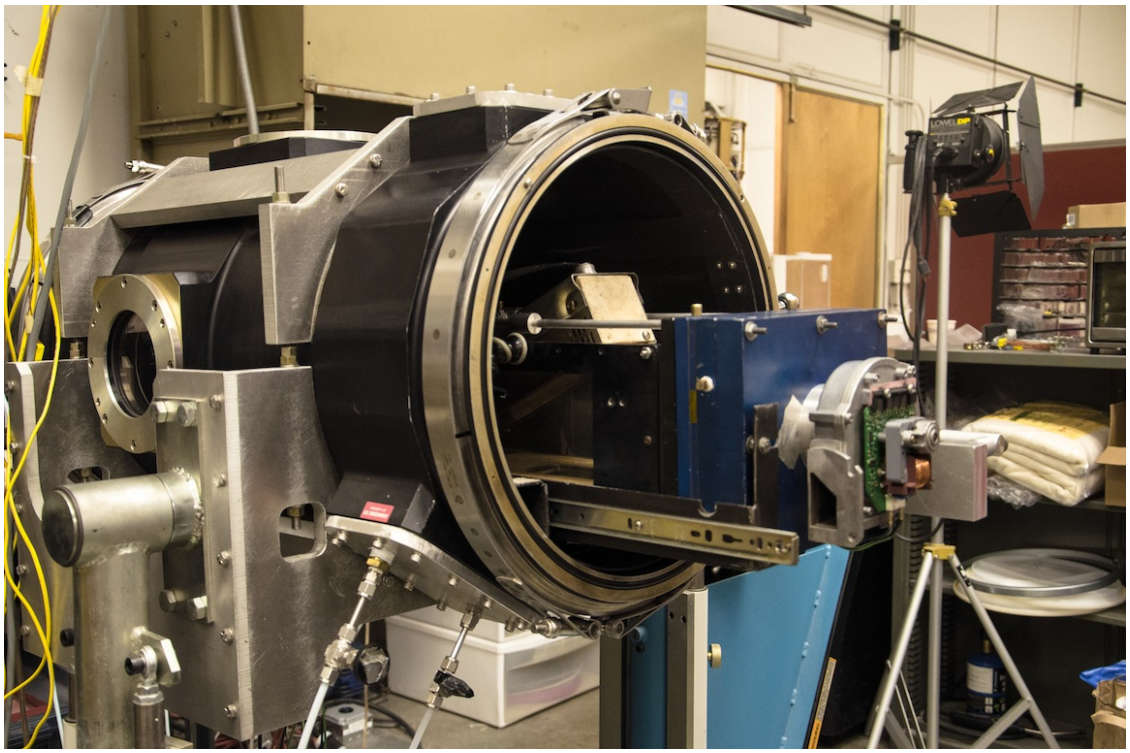

Figure 3.3: Pressure chamber and tunnel in horizontal position.

and oxygen concentration. Experiments were conducted in ambient pressures ranging from 20 to 100 kPa with oxygen concentrations ranging from 24% to 70%. The sealed chamber is mounted in an external base that allows positioning the chamber and the small-scale combustion wind tunnel horizontally or vertically, as shown in and respectively. Ignition of the fabric samples is accomplished using a 29 AWG Kanthal wire woven across the sample that are connected to an external power supply. Depending on chamber orientation, i.e. horizontal or vertical, and sample holder position, i.e. upstream or downstream, the tunnel can be used to study flame spread limits in four different configurations: concurrent-vertical, opposed-vertical, concurrent-horizontal, and opposed-horizontal. For example, Figure 3.2 shows the configuration that was used for concurrent-horizontal flame spread experiments. Tests were conducted with a single layer of Nomex HT90-40 (Stern and Stern Industries Inc., Hornell, NY, USA), and a 29% Cotton/ 31% Nylon/ 40% Nomex fabric blend (Magnafabrics, Denton, NC, USA). Sample size dimensions were 50.8 mm by 152.4 mm, similarly to the external radiant flux LOC experiments discussed in Chapter 2.

At the beginning of an experiment the test samples are loaded into the experimental apparatus and the pressure chamber is closed. Following chamber closure, a vacuum pump is used to vacuum air until the partial pressure of nitrogen reaches the value of the desired

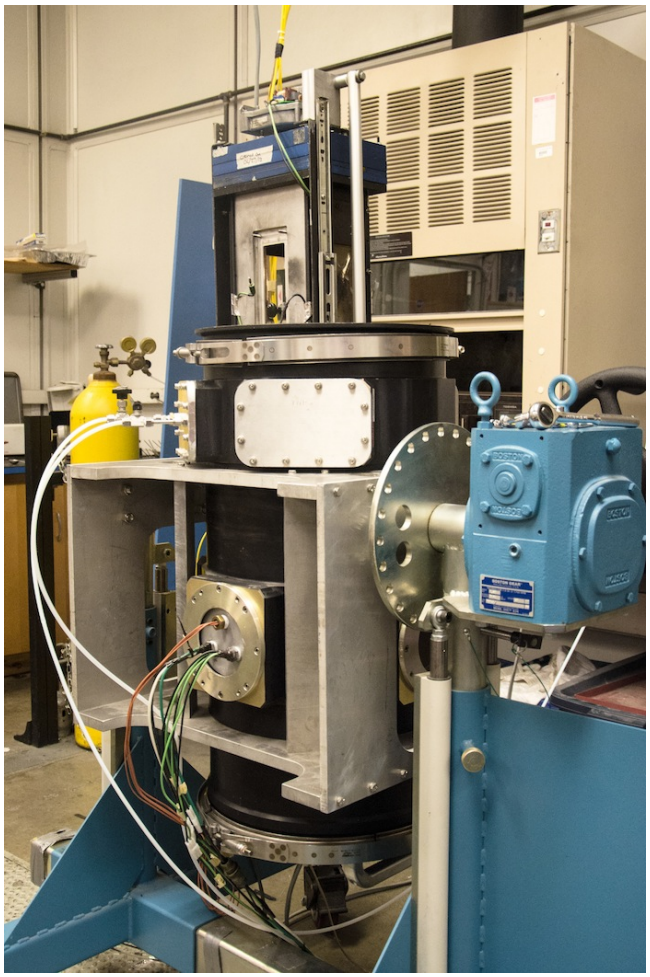

Figure 3.4: Pressure chamber and tunnel in vertical position.

mixture. At this point, pure oxygen from a tank is injected into the sealed chamber until the desired ambient pressure is reached. Pressure inside the chamber is monitored using a pressure transducer (Omega Engineering, Inc., Stamford, CT, USA). Oxygen concentrations are set using partial pressures and verified with an oxygen sensor (Apogee Instruments, Logan, UT, USA). After the desired ambient pressure and oxygen concentration conditions inside the chamber are attained, a suction fan located at the downstream section of the tunnel is turned on and allowed to run up to three minutes in order to create a homogeneous gas mixture.

The suction fan is supplied with a constant voltage in all experiments, which results in a measured oxidized flow velocity of 0.3 m/s in atmospheric conditions. Once the gas mixture is deemed homogeneous, the igniter wire is energized and if the conditions are appropriate

a flame propagates over the test sample. In the experiments, the LOC for flame spread is defined as the maximum oxygen concentration for which the flame does not propagate beyond the influence of the igniter. The igniter influence region is defined as a 10 mm region centered around the point where the igniter wire is woven. Measurements of the LOC as a function of ambient pressure are used to generate Flame/No-Flame spread boundaries for different types of flames spread configurations. Video recording and flame behavior are also used to determine flame spread boundaries.

3.3 Results

3.3.1 Nomex HT90-40

Flame spread experiments using Nomex HT90-40 were conducted in ambient pressures ranging from 20 to 100 kPa and oxygen concentrations ranging from 21% to 75%. A constant oxidizer flow velocity of 0.3 m/s was used in all experiments. Four flame spread configurations were used in the experiments, concurrent-horizontal, opposed horizontal, concurrent-vertical, and opposed vertical. Based on the flame spread distance two possible experiment outcomes were considered, *Propagation* or *No Propagation*. Flame spread distances longer than 10 mm were considered to be *Propagation*. *No Propagation* points typically exhibited flame spread distances not greater than 10 mm, justifying the selection of 10 mm as an adequate propagation criterion. For a particular ambient pressure, the LOC was defined as the oxygen concentration at which three consecutive experiments resulted in *No Propagation*. Figure 3.5 shows an example of the experimental data obtained for horizontal-concurrent experiments. The green line in the plot represents an approximation of the flame spread boundary for this particular configuration.

Starting with oxygen concentrations greater than the LOC, flames propagated over the entire sample leaving behind a charred residue. When the oxygen concentration reached values closer to the LOC the flame spread distance decreased and in some instances no propagation occurred. Of those experiments near the LOC that resulted in propagation, some resulted in a cyclic flame spread behavior. An example of the cyclic flame spread behavior is presented in Figure 3.6. In (a) the burning front is consuming the char residue, and once the smoldering front merges with the char front a visible flame appears as seen in (b). The visible flame propagates a short distance ahead of the smoldering front and eventually extinguishes. At the same time the smoldering front continues to consume the char residue (c) allowing the cyclic flame spread to continue (d). Cyclic flame spread was often observed in experiments at low ambient pressures, i.e. 20 to 40 kPa, and as the ambient pressure increased cyclic flame spread became more sporadic. Finally, oxygen concentrations below the LOC resulted in short propagation distances that did not exceed 10 mm.

Similar flame spread boundaries for the other configurations were obtained using the experimental data found in Appendix A. Figure 3.7 presents the flammability boundaries

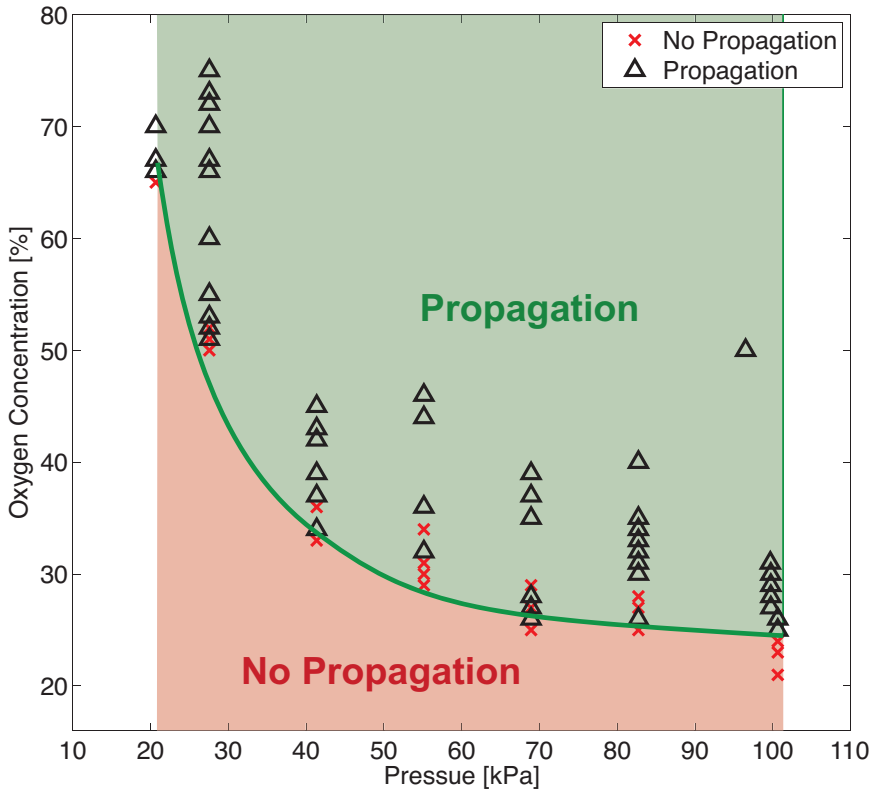

Figure 3.5: Concurrent-Horizontal flame spread boundary plot for Nomex HT90-40.

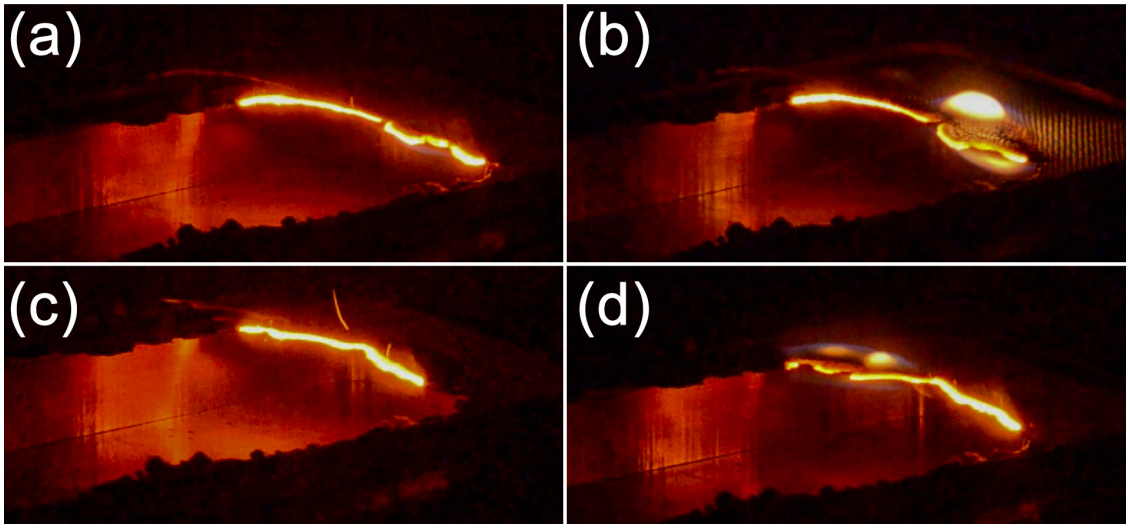

Figure 3.6: Cyclic flame spread in Nomex HT90-40. $p = 27.6\ kPa,\ [O_2] = 68\%$.

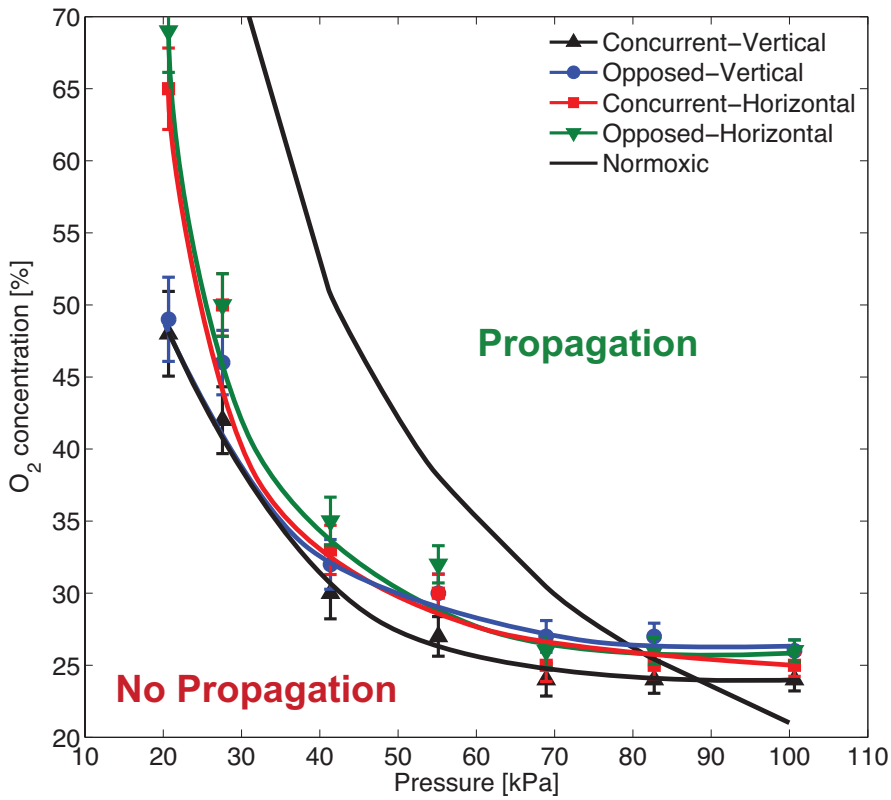

Figure 3.7: Flame spread boundaries for Nomex HT90-40 (p $vs.$ $[O_2]$).

for all four configurations tested. The black line labeled "Normoxic" represents an ambient pressure in which the oxygen partial pressure is the same as in atmospheric conditions, i.e. $p_{O2} = 21\ kPa$, is included in the figure for reference purposes. From this figure it can be seen that concurrent configurations had a slightly higher LOC than those for opposed flame spread, on average 1% to 2%. Comparing horizontal and vertical orientations showed that in ambient pressures greater than 41.4 kPa horizontal and vertical orientations resulted in approximately the same LOC. Once the ambient pressure reduced below 41.4 kPa the LOC for the horizontal orientation increased faster than the one for vertical orientation. Independent of the flame spread configuration the results showed that decreasing the ambient pressure resulted in an increase in the LOC. In ambient pressures between 70 and a 100 kPa, the increase in the oxygen concentration required for flame spread was minimal. Below 70 kPa, reductions in ambient pressure resulted in an increase in the LOC.

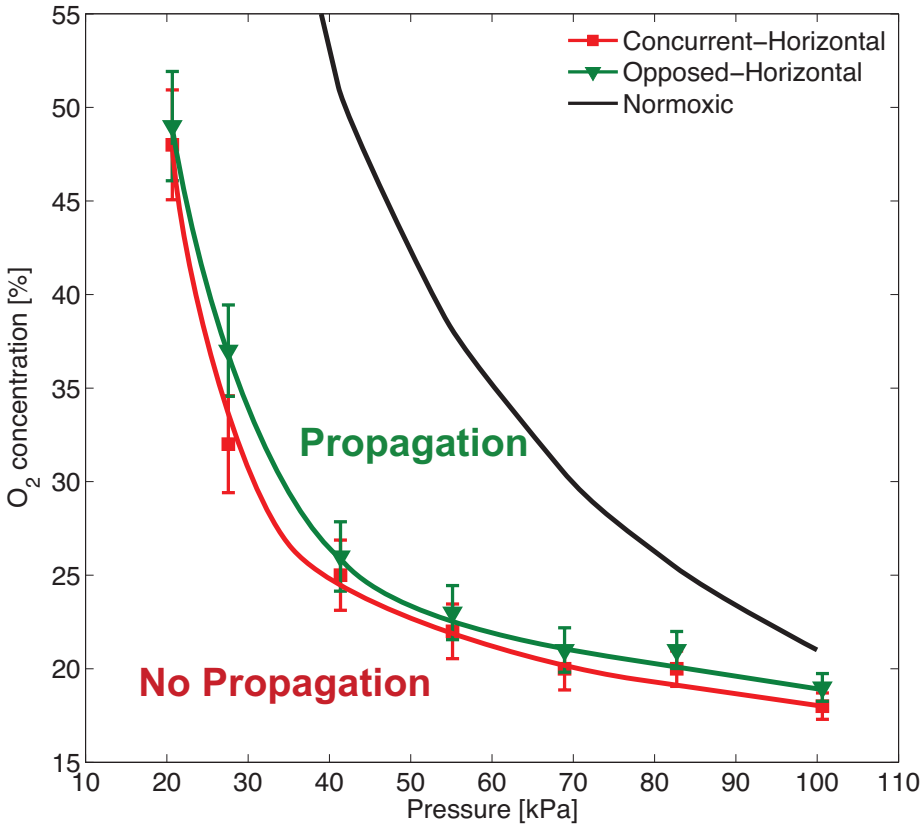

Figure 3.8: Flame spread boundaries for Cotton/Nomex/Nylon fabric blend (p $vs.$ $[O_2]$).

3.3.2 Cotton/Nomex/Nylon Fabric Blend

Flame spread experiments with a 29% Cotton/31% Nylon/40% Nomex fabric blend were conducted in ambient pressures ranging from 20 to 100 kPa and oxygen concentrations ranging from 18% to 56%. A constant oxidizer flow velocity of 0.3 m/s was used in all experiments. Experiments were conducted using two configurations: concurrent-horizontal and opposed-horizontal. Experimental data obtained from the concurrent-horizontal and opposed-horizontal configurations is presented in Appendix A and was used to obtain the flammability boundaries shown in Figure 3.8. Similar to Nomex HT90-40, the fabric blend results showed an increase in the LOC with a decrease in ambient press, and a difference of about 1% between concurrent-horizontal and the opposed-horizontal flammability limits.

3.3.3 Nomex HT90-40 vs. Cotton/Nomex/Nylon Fabric Blend

The results obtained with Nomex HT90-40 and the Cotton/Nylon/Nomex fabric blend allowed studying the combined effect of fabric composition and ambient pressure on the LOC.

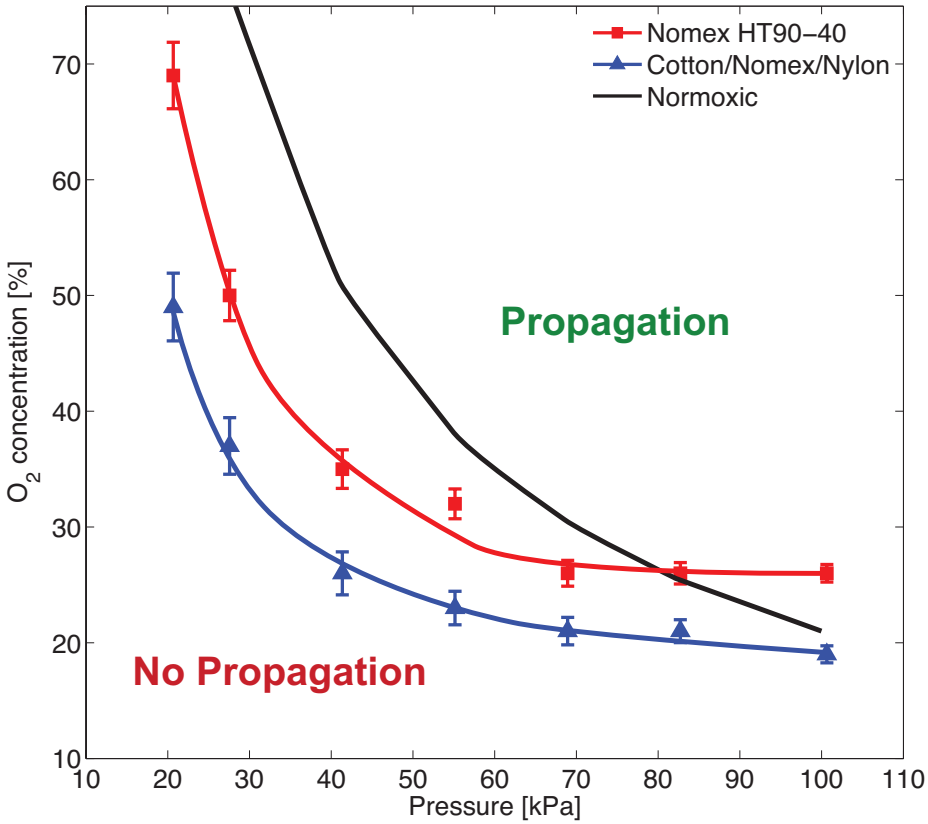

Figure 3.9: Nomex HT90-40 and Cotton/Nylon/Nomex fabric blend Concurrent-Horizontal flame spread boundary (p $vs.$ $[O_2]$).

Plotting the flame spread boundaries of Nomex HT90-40 and the fabric blend revealed that the lower Nomex content of the fabric blend results in a downward shift of the flammability boundary as shown in Figure 3.9. The downward shift was approximately the same in both concurrent-horizontal and opposed-horizontal flame spread configurations. The data showed that the difference between the Nomex HT90-40 and the Cotton/Nylon/Nomex fabric blend is a function of ambient pressure. For ambient pressures greater than 41.4 kPa the difference in LOC remains approximately constant. However, for pressures below 41.4 kPa there is a sharp increased in LOC difference. The differences between Nomex HT90-40 and the Cotton/Nylon/Nomex fabric blend LOC for both, concurrent-horizontal and opposed-horizontal flame spread, are presented in Table 3.1.

Ambient Pressure [kPa]	Concurrent-Horizontal LOC change [%]	Opposed-Horizontal LOC change [%]	Average LOC change [%]
99.7	7.0	7.0	7.0
82.7	5.0	5.0	5.0
68.9	5.0	5.0	5.0
55.1	7.0	9.0	8.0
41.4	8.0	9.0	8.5
27.6	18.0	13.0	15.5
20.7	17.0	20.0	18.5

Table 3.1: Combined effect of fabric composition and ambient pressure in LOC. LOC change is defined as the difference between the Nomex HT90-40 and the Cotton/Nylon/Nomex fabric blend LOC.

3.3.4 Oxygen Partial Pressure

The results presented in Figures 3.7, 3.8 and 3.9 can be alternatively presented in terms of the oxygen partial pressure, p_{O2}, required for flame spread. Flammability boundaries in terms of p_{O2} for Nomex HT90-40 and the Cotton/Nomex/Nylon fabric blend are respectively shown in Figures 3.10 and 3.11. In these figures the normoxic equivalent corresponds to the horizontal black line at 21 kPa. The results for both fabrics showed a nearly linear relationship between p and p_{O2} that was independent of configuration tested. A linear least squares fit of the data shows good agreement with the results and is included in the plots as the dotted lines. The regression coefficients for both fabrics are summarized in Tables 3.2 and 3.3.

Slope and y-intercept values can be used to analyze differences between concurrent and opposed flame spread, and vertical versus horizontal orientations. The positive slope of the flame spread boundaries follows the same behavior observed by Hirsch *et al.*[6] when looking at flammability limits in terms of partial pressure of oxygen. Values in Tables 3.2 and 3.3 show that differences between opposed and concurrent are small, while differences between horizontal and vertical orientations are more significant. For the case of concurrent-horizontal and opposed-horizontal, the slope and y-intercept values of Nomex HT90-40 are greater than those of the fabric blend. This shows that although Nomex HT90-40 has a higher LOC in atmospheric conditions, the flammability boundary of the fabric blend is less sensible to ambient pressure.

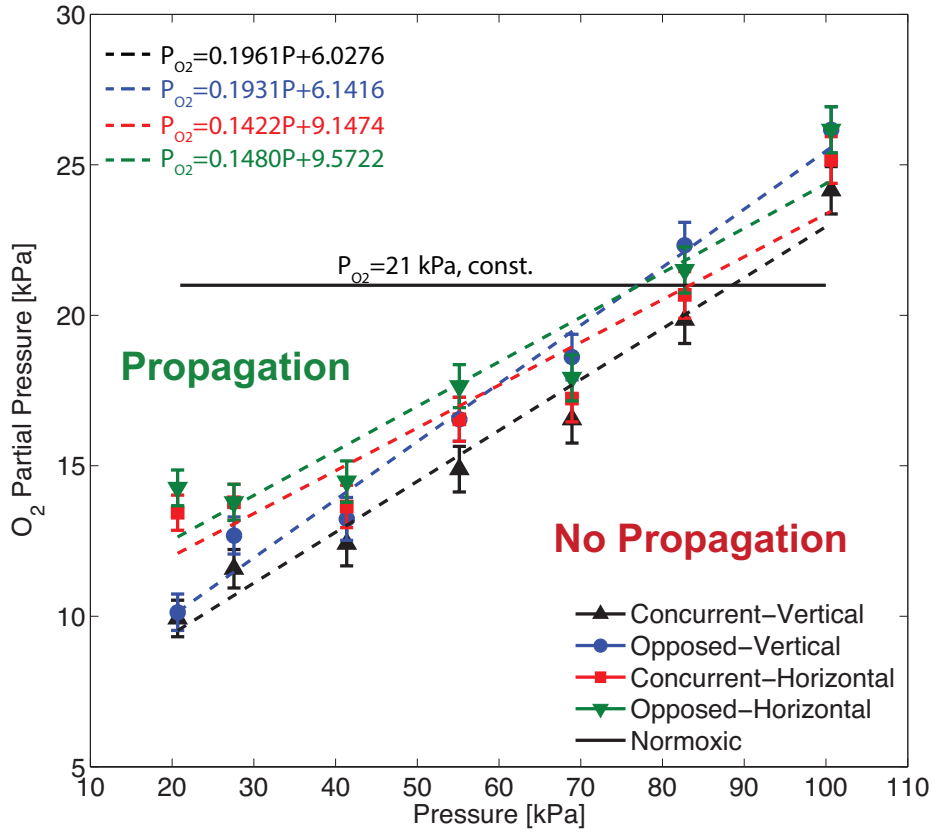

Figure 3.10: Flame spread boundaries for Nomex HT90-40 (p *vs.* p_{O_2}).

Configuration	Slope	y-Intercept	R^2
Concurrent-Vertical	0.1961	6.0276	0.9729
Opposed-Vertical	0.1931	6.1416	0.9823
Concurrent-Horizontal	0.1422	9.1474	0.9095
Opposed-Horizontal	0.1480	9.5722	0.9140

Table 3.2: Linear regression coefficients for Nomex HT90-40.

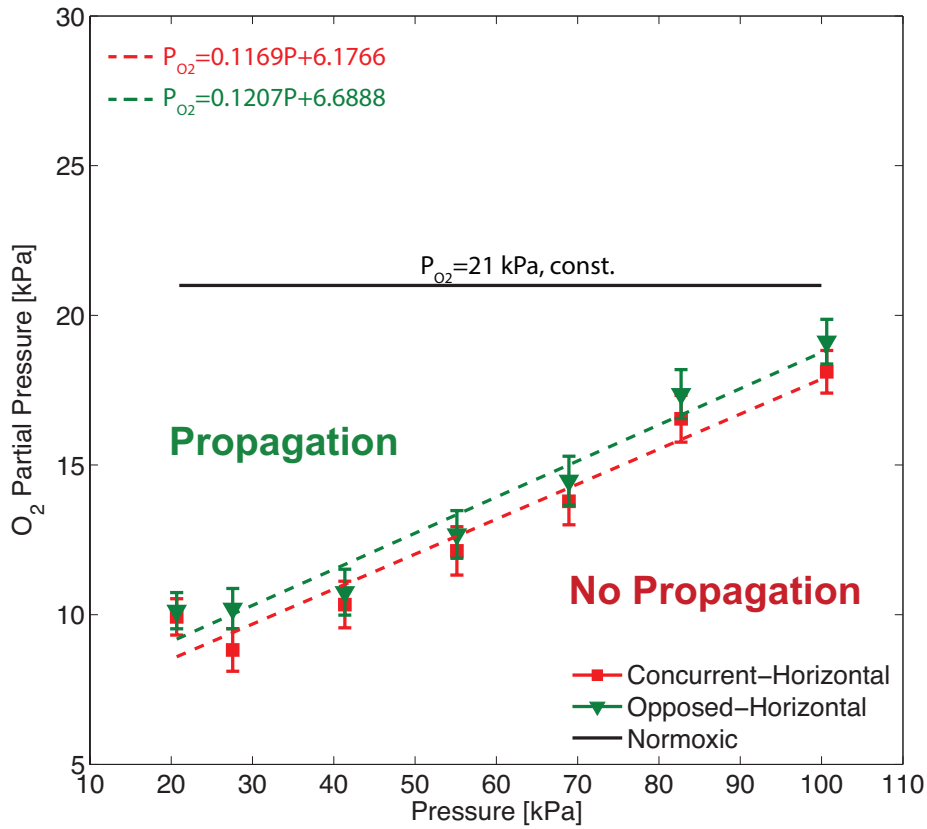

Figure 3.11: Flame spread boundaries for Cotton/Nomex/Nylon fabric blend (p $vs.$ p_{O_2}).

Configuration	Slope	y-Intercept	R^2
Concurrent-Horizontal	0.1169	6.1766	0.9524
Opposed-Horizontal	0.1207	6.6888	0.9604

Table 3.3: Linear regression coefficients for Cotton/Nomex/Nylon fabric blend.

Looking at flammability boundaries in terms of p_{O2} can be useful in determining if materials are flammable in normoxic equivalent atmospheres, or similar fixed partial pressure conditions. Materials that are not flammable will have flammability boundaries that sit above the normoxic lines, whereas materials that are always flammable will have boundaries sitting below the normoxic line. Not all materials will sit completely above or below the normoxic line, but instead will intersect the normoxic line as Nomex HT90-40 does. Figure 3.12 shows the concurrent-horizontal flame spread boundary of Nomex HT90-40 and the

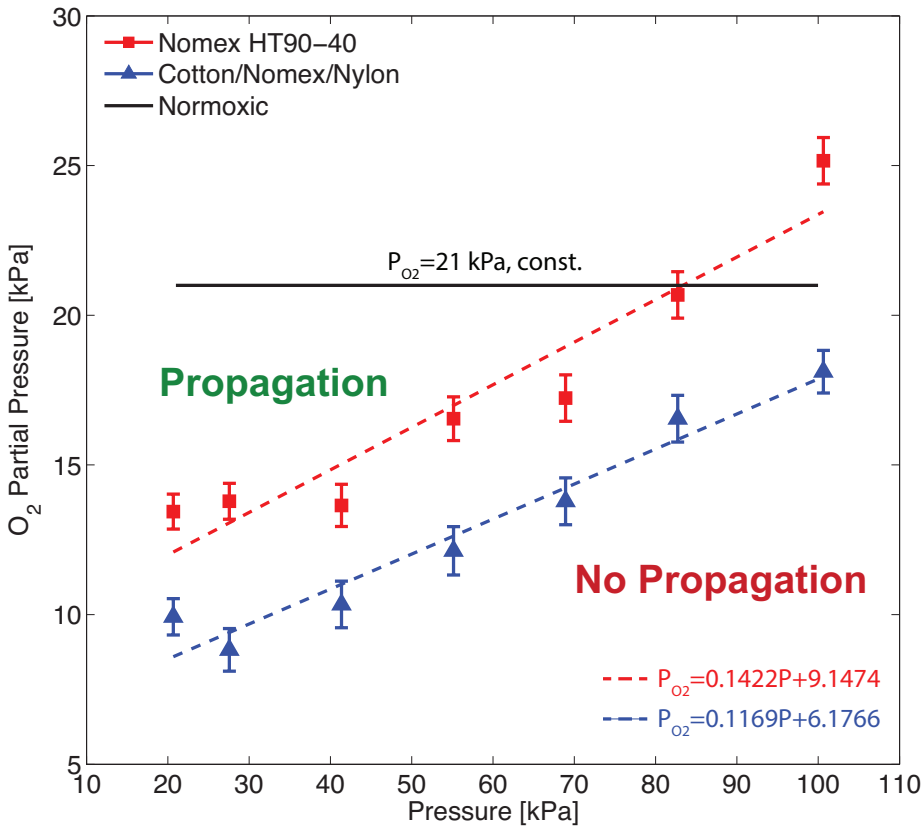

Figure 3.12: Nomex HT90-40 and Cotton/Nylon/Nomex fabric blend Concurrent-Horizontal flame spread boundary (p $vs.$ p_{O_2}).

Cotton/Nomex/Nylon fabric blend. From this figure it can be seen that the fabric blend boundary sits below the normoxic line, meaning that this fabric is flammable over the entire range of normoxic equivalent atmospheres. On the other hand, the Nomex HT90-40 boundary crosses the normoxic line at $p = 83.4$ kPa based on the data fit. The point at which the flammability boundary intersects the normoxic line is important because it shows that bellow this pressure limit, fire-resistant (FR) materials such as Nomex HT90-40 become flammable. The pressure at which the flammability boundary intersects the normoxic line has been suggested as an alternative flammability test method to NASA Standard 6001Test 1[10]. In this proposed method the oxygen partial pressure is maintained at 21 kPa and the ambient pressure is increased until the material passes NASA Standard 6001 Test 1. Thus, this test would report the ambient pressure above which materials are not be flammable.

3.4 Analysis

The response of the Flame/No-Flame spread boundaries to environmental variables can be analyzed in terms of the combined effects of ambient pressure and flame spread configuration. Ambient pressure is a very important variable that affects several phenomena such as heat transfer from the flame to the fabric, buoyancy induced flows and transport and chemical timescales. Heat transfer from the flame to the fabric is a key component in flame spread given that the flame acts as both, the heat source for the solid decomposition and the pilot for the flammable vapors[11]. Hence it can be expected that changes in the heat transfer from the flame to the solid will affect the flame spread and flammability limits.

For a flame to propagate, the flame has to heat the solid above its pyrolysis temperature resulting in the production of gaseous fuel. The gaseous fuel then combines with the oxidizer creating a flammable mixture. Finally, the flame will ignite the flammable mixture allowing the flame spread process to continue. Ambient pressure will affect each of these processes simultaneously resulting in a complex interaction responsible for the observed flammability behavior. The discussion regarding the effect of ambient pressure is centered around the role played by ambient pressure in each of the processes required for flame spread, solid fuel pyrolysis, mixing of flammable vapors, and gas-phase chemical reaction.

The results with Nomex HT90-40 and the Cotton/Nylon/Nomex fabric blend followed a similar behavior independent of the flame spread configuration. For ambient pressures ranging between 70 and 100 kPa, reductions in the ambient pressure resulted in minimal changes to the LOC. Once the ambient pressure dropped below 70 kPa, reducing ambient pressure resulted in an increase in LOC. The observation that the LOC behaves differently in these two ambient pressure regimes could be explained in terms heat transfer from the flame to the solid, heat losses from the fuel, and gas phase kinetics.

Gas phase heat conduction is the dominant form of heat transfer in flame spread over thin fuels[12]. Thus, it follows that the heat transfer to the thin fuel is proportional to the difference between the flame and solid temperatures divided by a representative length scale, that is $q \propto (T_f - T_s)/l$, where the representative length scale if often assumed to the boundary layer thickness, δ[11]. In flow over a flat plate the thermal boundary layer thickness, δ_t, is proportional to $x/(Re^{1/2}Pr^{1/3})$. From the respective definitions of the Reynolds(Re) and Prandtl (Pr) numbers only the Re number is a function of ambient pressure, $Re = \rho U x/\mu$. Assuming that the oxidizer behaves as an ideal gas, $Re \propto p$, resulting in $\delta_t \propto 1/p^{1/2}$.

Phenomenologically this means that as ambient pressure is reduced the thermal boundary layer thickness and flame stand off distance increase. In concurrent flame spread the gas phase conduction heat flux from the flame to the unburned solid can be estimated as $q \approx -k_g(T_s - T_f)/\delta_t$. Hence, as ambient pressure is reduced, the thermal boundary layer thickens and the heat transfer from the flame to the solid reduces. In opposed flame spread, the flame

is located at a small distance above the solid fuel and as the boundary layer grows the flame moves away from the surface and the heat transfer ahead of the flame also decreases.

Reducing ambient pressure not only affects the heat transfer from the flame to the solid, but also the heat losses of the solid. The hot gases from the flame induce a buoyant flow that results in convective heat losses over the surface. In a completely buoyant flow, the heat transfer coefficient, h, is proportional to $Gr^{1/4}Pr^{1/4}$, where Gr is the Grashof number defined as

$$Gr = \frac{g\beta l^3(T_s - T_\infty)}{\nu^2} \tag{3.4.1}$$

where β is the volumetric thermal expansion coefficient and l is a representative length scale that is proportional to the boundary layer thickness δ.

Based on the above expression $Gr \propto p^2$, but most importantly, $h \propto p^{1/2}$. Therefore, as ambient pressure is reduced the convective heat losses will decrease, especially in opposed flame spread. In reduced ambient pressure ignition delay experiments with thick PMMA samples researchers noted that the reduction in heat losses resulted in shorter ignition delay times, and lower sample surface temperatures at the moment of ignition. McAllister[8] went on to propose that the reduction in heat losses combined with a lower oxidizer mass flow rate would require a lower fuel mass flux to reach a flammable mixture. Fereres[9] measured the fuel mass flux at ignition and found that it decreased as ambient pressure was reduced. Although these conclusions were reached in ignition delay studies, it is possible that a similar behavior occurs in reduced ambient pressure flame spread.

In addition to the heat transfer to and from the fabric sample, ambient pressure also affects the gas phase chemical reaction. In its most basic form, the gas phase combustion reaction rate can be expressed as a single-step Arrhenius type reaction of the form where n is the reaction order. Typically n is a positive number ranging greater or equal to 1.0[13].

$$\dot{\omega} = A_g p^n Y_F Y_O \exp(-Ea/RT) \tag{3.4.2}$$

Using Equation 3.4.2 it is possible to estimate the chemical time, t_{chem}, as

$$t_{chem} = \frac{[\text{Fuel}]}{\dot{\omega}} \propto \frac{p}{Y_O p^n} \tag{3.4.3}$$

The effect of ambient pressure on the gas phase reaction can be analyzed in terms of the Damkohler number, Da, defined as the ratio of the flow characteristic time to the chemical

time, i.e. $Da = t_{mix}/t_{chem}$. When $t_{chem} << t_{mix}$ or $Da >> 1$, the gas phase reaction proceeds very fast and the flame spread is controlled by the heat transfer to the unburned material. From Equation 3.4.2 it can be seen that decreasing ambient pressure results in a reduced reaction rate and increased chemical time, which in turn lead to a decrease in Da. Once Da starts decreasing the gas phase reaction becomes more important, and if Da drops below a critical number the flame does not propagate[12]. At the same time the increased oxygen concentration raises the flame temperature and makes possible to compensate the decreased net heat transfer from the flame to the solid fuel.

One additional factor that may be responsible for the sharp increase of the LOC in reduced ambient pressures is radiation. Surface radiation losses can considerably affect flame shape and the flame spread process[14]. Limited oxygen transport to the flame can reduce the flame temperature in addition to radiation heat losses from the flame resulting in a lower net heat flux to the unburned fuel. Such reduction combined with reradiation from the solid fuel will result in a decrease in both the heating and the pyrolysis rate.

From the experimental results it is possible to identify two regions in the flammability maps. The first region consists of ambient pressures ranging from 70 to 100 kPa, and the second region is for ambient pressures less than 70 kPa. The first region is characterized by a near constant LOC, which suggests that the combined effects of decreased heat transfer, heat losses and increase in chemical time counteract each other and result in a flammability behavior similar to that of ambient conditions. In the second region, a decrease in ambient pressure is accompanied by larger increases in the oxygen concentration required to observe flame spread. This increase in the LOC below 70 kPa for both fabrics tested shows that the balance among different phenomena, i.e. gas phase heat conduction, chemical kinetics, and radiation losses is disrupted and that ambient pressure affects some processes more than others. At this moment is not clear which of these phenomena is more dominant, or how they counteract each other. However, it is likely that chemical kinetics and radiation play a role in low ambient pressures as a result of changes in Da[14, 15].

The effect of buoyancy on the fuel samples depends on sample orientation. In the case of a horizontally oriented samples, the buoyant flow that arises due to the presence of the flame moves perpendicular and away from the fuel, resulting in heat losses to the surrounding gases. In vertically oriented samples, the buoyant flow induced by the flame is parallel to the fuel sample, which results in heat losses that are smaller than those of horizontally oriented fuel samples. Therefore, in order to overcome the larger heat losses present in horizontally oriented fuel samples, it is necessary to increase the flame temperature by increasing the oxygen concentration.

In the experiments it was observed that the LOC for flame spread in the direction of the oxidizer flow was lower than that for flame spread opposite to the oxidizer flow. The reason for this behavior is that in concurrent and upward flame spread, there is an additional convective heat transfer from the flame to the solid fuel as a result of the mixed flow conditions

in the tunnel. In the other hand, for opposed-vertical and opposed flame spread, gas phase conduction is the main mechanism of heat transfer, and therefore in order to maintain a heat transfer capable of sustaining the pyrolysis process it is necessary to increase the flame temperature by increasing the oxygen concentration. Comparing horizontal versus vertical flame spread boundaries showed a divergence of the boundaries in low ambient pressures. This divergence is unexpected and could be a result of the mixed flow conditions present in the experiment. In a quiescent and low ambient pressure environment it would be expected that the horizontal and vertical LOC values would converge since buoyant flow is nearly eliminated. Additional experiments in quiescent environment would be required to test this hypothesis.

Flame/No-Flame spread boundaries in terms of the oxygen partial pressure revealed a nearly linear relationship between ambient pressure and oxygen partial pressure. A linear least squares fit of the data showed that differences was in good agreement with the results and showed that concurrent and opposed flame spread have similar slop and y-intercept values. The linear relationship between p and p_{O2} had also been observed by Hirsch et al.[6] and Nakamura and Aoki[16] in experiments with fire resistant materials and thin cellulosic papers. A subset of the results obtained by Hirsch et al.[6] and the results with Nomex HT90-40 and the Cotton/Nomex/Nylon fabric blend in Concurrent-Horizontal configuration are presented in Figure 3.13. In this figure, it can be seen that in some materials the flammability boundary is completely above the normoxic equivalent. In others it is completely below and in some others, it crosses the normoxic line.

The observation that some materials cross the normoxic equivalent is an important issue for spacecraft safety. Normoxic equivalent atmospheres have been suggested as possible environmental conditions in future spacecraft designs[17]. Materials crossing the normoxic line can exhibit different flammability behavior depending on ambient pressure and this could increase the risk of fires in reduced ambient pressures. The linear relationship between p and p_{O_2} allows the possibility of developing LOC correlations in terms of p_{O_2}. Additional studies and analyses are required to gain a better understanding the nature of this relationship. Numerical modeling, in particular, could be the key to understanding how the competing effects of ambient pressure, heat losses and chemical kinetics result in the observed p vs. p_{O_2} relationship.

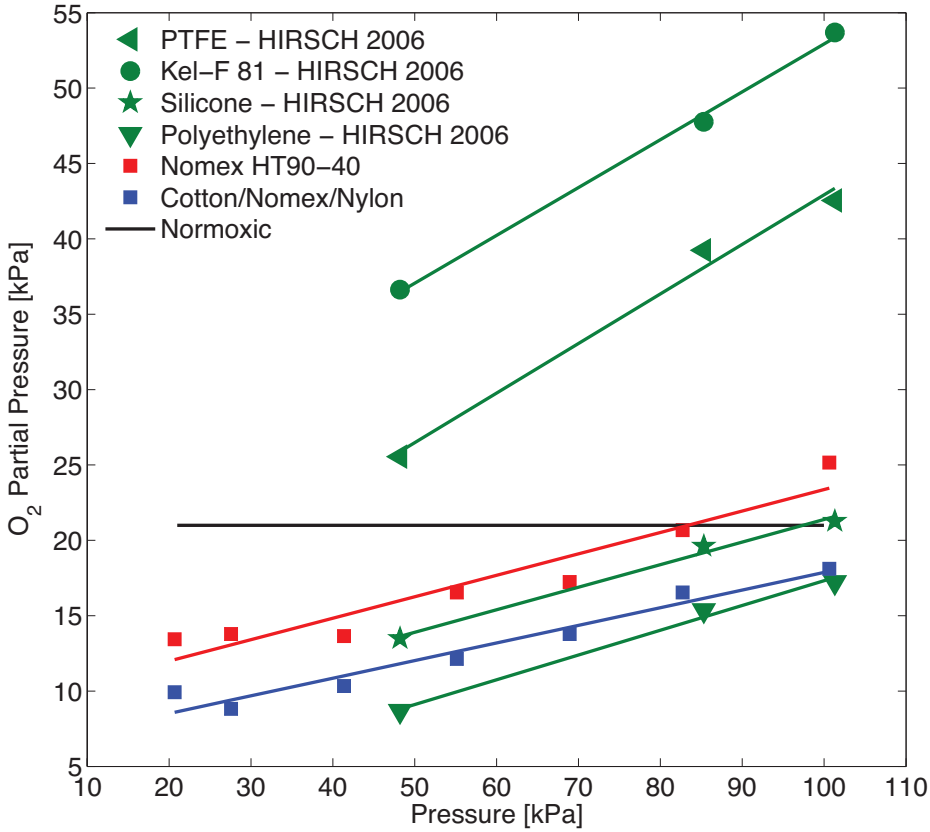

Figure 3.13: Flammability boundary for selected materials (p $vs.$ p_{O_2}).

3.5 Conclusions

There are several factors that affect the flammability of a material. This work has focused on developing Flame/No-Flame spread boundaries in terms of the ambient pressure and oxygen concentration. Additional parameters considered were the effect of sample orientation, flame spread configuration and material composition. The Flame/No-Flame spread boundary corresponds to the Limiting Oxygen Concentration (LOC), the maximum oxygen concentration at which a flame does not propagate over the sample surface. Overall, the results showed that as ambient pressure is reduced the LOC increases. This behavior can be phenomenologically explained in terms of factors such as heat transfer between the flame and the unburned solid, buoyancy induced flows, and chemical kinetics. Reducing ambient pressure can increase or decrease the effect of each of these factors, which can be summarized as follows:

1. As ambient pressure is reduced the gas phase heat conduction from the flame to the

solid fuel is reduced. Conduction heat transfer is proportional to $\dot{q}'' \propto (T_f - T_p)/\delta_t$. The thermal boundary layer thickness, δ_t, is proportional to $Re^{-1/2}$, which results in $\delta_t \propto p^{-1/2}$. Thus, as ambient pressure is reduced, the boundary layer thickness and flame stand off distance increase. This increase reduces the conduction heat transfer from the flame to the solid unless $(T_f - T_p)$ increases. An increase in the oxygen concentration raises the flame temperature, T_f, and compensates for the increase in δ_t. Near atmospheric conditions, the increase in δ_t is small, but as ambient pressure is reduced the increase is more significant resulting in larger increases in the LOC.

2. Reducing ambient pressure reduces buoyancy induced flows and with it the associated convective heat losses from the fuel and the flame. Convective heat losses in forced flow, purely buoyant or a combination of both are proportional to $p^{1/2}$. Therefore, low ambient pressures reduce heat losses, which result in an increase in the net heat flux to the fuel surface. Reduction of buoyancy induced flows results in limited transport of oxygen to the flame, which may reduce T_f.

3. Decreasing ambient pressure increases the chemical time. In its most simple case, the gas phase combustion reaction can be assumed to follow an Arrhenius type behavior. For this reaction type, the characteristic chemical reaction time increases with decreasing ambient pressure, resulting in a decrease in the Damkohler number, Da, and once Da decreases below a critical value the flame extinguishes[12]. Increasing the oxygen concentration not only raises the flame temperature but also allows maintaining a short chemical time despite the decrease in ambient pressure.

For both fabrics tested opposed flame spread had LOC values 1% to 2% greater than those of concurrent flame spread. This difference can be attributed the presence of convective heat transfer in concurrent flame spread. In opposed flame spread conduction is the main heat transfer mechanism, and in order to transfer the same heat to the fabric it is necessary to raise T_f through an increase in oxygen concentration. Except at an ambient pressure of 20 kPa, vertical and horizontal orientation flame spread boundaries are comparable. At 20 kPa, the vertically oriented samples have a significantly lower LOC. This difference could be a result of mixed flow conditions inside the experiments. In a purely quiescent environment, low ambient pressures would greatly reduce buoyant flows making diffusion the main mechanism transport. In this limit it would be expected that concurrent or opposed flame spread configurations, and horizontal or vertical orientations, result in the same LOC.

Plotting the Flame/No-Flame spread boundaries in terms of p_{O2} showed a nearly linear relationship between p and p_{O2}. This linear relationship can be used to determine the pressure at which materials become flammable in normoxic equivalent atmospheres. Normoxic equivalent atmospheres refer to ambient pressures in which the oxygen concentration changes in order to maintain a fixed oxygen partial pressure of 21 kPa, that is $p_{O2} = 21\ kPa$ independent of p. Flame spread boundaries in terms of p_{O2} could sit: (1) completely below

the normoxic line, (2) completely above the normoxic line, or (3) intersect the normoxic line. Case 1 refers materials that are flammable over the entire range of ambient pressures such as the Cotton/Nomex/Nylon fabric blend. Case 2 refers to materials such as PTFE, which are not flammable in any normoxic atmosphere. Finally, Case 3 refers to materials that are flammable or non-flammable depending on ambient pressure. Nomex HT90-40 is an example of the materials that cross the Normoxic line. Normoxic atmospheres have been suggested for future spacecraft designs[17], and the observation that FR materials could become flammable in a low pressure normoxic conditions is an important result. The linear relationship between p and p_{O2} could be exploited to develop alternative flammability tests that measure the pressure at which the flammability boundary intersects the normoxic line as proposed by Olson et al.[10].

3.6 References

[1] Wikipedia. *List of highest large cities in the world — Wikipedia, The Free Encyclopedia*. [Online; accessed 04/02/2014]. 2014. URL: http://en.wikipedia.org/wiki/List_of_highest_large_cities_in_the_world.

[2] Pasquale Sforza. *Commercial Airplane Design Principles*. Boston: Butterworth-Heinemann, 2014. ISBN: 978-0-12-419953-8.

[3] Julie Kleinhenz and James S. T'ien. "Combustion of Nomex III Fabric in Potential Space Habitat Atmospheres: Cyclic Flame Spread Phenomenon". In: *Combustion Science and Technology* 179.10 (2007), pp. 2153–2169. DOI: 10.1080/00102200701386172.

[4] Sandra L. Olson, Gary A. Ruff, and Fletcher J. Miller. "Microgravity Flame Spread in Exploration Atmospheres: Pressure, Oxygen, and Velocity Effects on Opposed and Concurrent Flame Spread". In: *38th International Conference on Environmental Systems*. San Francisco, CA: SAE International, June 2008. DOI: 10.4271/2008-01-2055.

[5] David B. Hirsch et al. "Oxygen Concentration Flammability Thresholds of Selected Aerospace Materials Considered for the Constellation Program". In: (2007). URL: http://ntrs.nasa.gov/archive/nasa/casi.ntrs.nasa.gov/20070018178_2007017304.pdf.

[6] David Hirsch, Jim Williams, and Harold Beeson. "Pressure Effects on Oxygen Concentration Flammability Thresholds of Polymeric Materials for Aerospace Applications". In: *Journal of Testing and Evaluation* 36.1 (2008), p. 100975. DOI: 10.1520/jte100975.

[7] David B. Hirsch et al. "Pressure Effects on the Self-Extinguishment Limits of Aerospace Materials". In: *39th International Conference on Environmental Systems*. Savannah, GA: SAE International, July 2009.

[8] Sara McAllister et al. "Piloted Ignition Delay of PMMA in Space Exploration Atmospheres". In: *Proceedings of the Combustion Institute* 32.2 (2009), pp. 2453–2459. ISSN: 1540-7489. DOI: 10.1016/j.proci.2008.05.076.

[9] Sonia Fereres et al. "Mass Flux at Ignition in Reduced Pressure Environments". In: *Combustion and Flame* 158.7 (2011), pp. 1301–1306. DOI: 10.1016/j.combustflame.2010.11.013.

[10] Sandra L. Olson, Harold Beeson, and Carlos Fernandez-Pello. "Applying Flammability Limit Probabilities and the Normoxic Upward Limiting Pressure Concept to NASA STD-6001 Test 1". In: *Submitted to 44th International Conference on Environmental Systems*. Tucson, AZ: AIAA, July 2014.

[11] C. Fernandez-Pello, in: G. Cox (Ed.) *Combustion Fundamentals of Fire*. San Diego, CA: Academic Press, 1995. ISBN: 0121942309.

[12] A.C. Fernandez-Pello and T. Hirano. "Controlling Mechanisms of Flame Spread". In: *Combustion Science and Technology* 32.1 – 4 (1983), pp. 1–31. DOI: 10.1080/00102208308923650.

[13] S. McAllister, J.Y. Chen, and A.C. Fernandez-Pello. *Fundamentals of Combustion Processes*. Mechanical Engineering Series. Springer, 2011. ISBN: 9781441979438.

[14] S. Bhattacharjee and R.A. Altenkirch. "The Effect of Surface Radiation on Flame Spread in a Quiescent, Microgravity Environment". In: *Combustion and Flame* 84.1 – 2 (1991), pp. 160–169. DOI: 10.1016/0010-2180(91)90045-D.

[15] S. Bhattacharjee et al. "A Theoretical Description of Flame Spreading over Solid Combustibles in a Quiescent Environment at Zero Gravity". In: *Combustion Science and Technology* 69.1 – 3 (1990), pp. 1–15. DOI: 10.1080/00102209008951599.

[16] Y. Nakamura and A. Aoki. "Irradiated Ignition of Solid Materials in Reduced Pressure Atmosphere with Various Oxygen Concentrations for Fire Safety in Space Habitats". In: *Advances in Space Research* 41.5 (2008), pp. 777–782. DOI: 10.1016/j.asr.2007.03.027.

[17] Kevin E. Lange et al. *Bounding the Spacecraft Atmosphere Design Space for Future Exploration Missions NASA/CR-2005-213689*. 2005. URL: http://spaceflightsystems.grc.nasa.gov/repository/NRA/cr-2005-213689.pdf.

CHAPTER 4

MICROGRAVITY

4.1 Introduction

The risk of a fire during a space mission has motivated ample research in space fire safety, particularly in flame spread in microgravity. Over the years researchers have studied the differences and similitudes between flame spread in normal ($1g$) and microgravity (μg) conditions using thermally-thin fuels such as thin plastics, paper sheets and electrical cables. The findings from these studies have shown that μg results higher flame spread rates, lower flammability limits, and different flame extinction mechanisms when compared to $1g$[1–9]. Independent of the geometry of fuel used, i.e. flat versus round, the increased flammability behavior observed in microgravity environments has been explained in terms of the elimination of buoyancy induced flows and associated heat losses, changes in flame shape, and increases in residence time of the flammable mixture.

Electrical cables and harnesses have been identified as a possible source of fires in a spacecraft and their combustion in microgravity has received much attention. Kikuchi et al.[5] studied the effects of oxygen concentration, wire temperature and size, ambient pressure and carrier gas in the flame spread over ETFE insulated wires. In their experiments it was found that the combination of μg and preheating of the wire core resulted in a 2 mm/s average increase of the flame spread rate, while μg alone increased the spread rate by an average of 1.2 mm/s. The same authors also found that smaller wire sizes resulted in higher spread rates in microgravity, and that as wire size increased the difference between microgravity and normal gravity flame spread rates decreased. Similar experiments conducted by Fujita et al.[10] studied the effect of oxidizer flow speed in flame spread over polyethylene (PE) insulated wires. One key finding was that in μg, flame spread rate is the maximum for flow conditions approximately equal to 0.10 m/s, which are similar to those of air ventilation velocities found inside a spacecraft. This result matched observations by Olson et al.[1] and Olson[2], who also found that flow velocities ranging from 0.06 to 0.10 m/s resulted in the highest flame spread rate over thin cellulosic fuels.

More recent research has focused on studying ignition and extinction limits. Fujita et al.[7] studied the ignition delay and ignition limits of PE insulated Nichrome wires subject to short-term excess current. The results showed that the minimum current required for ignition and ignition delay times decreased in microgravity. Expanding on the ignition of short-term overloaded wires, Takano et al.[8] investigated the Limiting Oxygen Concentration (LOC) for the ignition of PE insulated Nichrome wires. The numerical results agreed with the trends observed in microgravity experiments and showed a reduction in the LOC in μg. The decrease in the LOC was explained in terms of the increase of the fuel layer thickness with increasing supply of energy. As the fuel layer thickens the ignition delay time increases resulting in lower oxygen concentrations for ignition. Takahashi et al.[9] also observed that microgravity results in lower LOC for flame spread over PE insulated Copper and Nichrome wires and related the decrease in LOC to the elimination of natural convection and increased heat input to the unburned insulation.

As microgravity fire safety research has shifted to the study of ignition and extinction limits, the types of fuels have also changed. Except a few studies, the majority of microgravity flame spread research has been conducted using materials that are not used in space applications, like for example thin cellulosic paper, PMMA sheets or PE insulated wires. Nonetheless, these materials posses a unique advantages, their combustion behavior is well understood, and the materials have high burning rates that allow conducting experiments in short microgravity periods such the ones provided by drop towers and parabolic flights. Still, microgravity flame spread experiments with materials used in space applications are less common. Material selection for a next generation of space exploration vehicles has brought attention to the flammability behavior of materials likely to be used in future spacecraft[11–16]. These studies have focused on studying materials that exhibit fire-resistant (FR) characteristics such self-extinction, high Limiting Oxygen Index (LOI) values, charring, intumescence, etc. The major research objective with candidate materials has been quantifying differences in flammability behavior due to changes in gravity and other environmental variables.

In 2013, the Japanese Aerospace Exploration Agency (JAXA) approved a series of microgravity combustion experiments as part of third stage usage of the Japanese Experiment Module (JEM) onboard the International Space Station (ISS). The microgravity combustion experiments aim is to evaluate the effect of gravity on the combustion of solid fuels and develop methods for predicting the effect of gravity in flammability indices like for example LOC, LOI, etc. The first step towards conducting experiment onboard the ISS is the development and validation of an experiment prototype, from which a final version can be flown into space.

This chapter will describe the development of an experiment prototype and introduce $1g$ and μg flammability limit experiments of ETFE insulated copper wires exposed to an external radiant flux. The experiment prototype was developed in collaboration between Hokkaido University and UC Berkeley and it is modeled after the minimum external radiant

flux for flame spread in Nomex HT90-40 presented in Chapter 2. Studies using electrical cables with fire-resistant insulations have been limited and have not considered the effect of an external radiant flux on the flammability limits for flame spread in $1g$ or μg. In the present work, experiments with different levels of external radiation subject to varied oxygen concentrations are used to determine flammability boundaries in terms of external radiation, oxygen concentration, and gravity conditions. In addition, the results obtained with ETFE insulated wires are compared to similar results with PE insulated wires. This comparison is an important step towards understanding how microgravity affects the flammability of materials used in space exploration, and whether or not changes these changes can be predicted using non fire-resistant materials such as PMMA, PE, etc.

4.2 Experiment Description

4.2.1 Conceptual Design

The experiment apparatus was designed to test the flammability limits of electrical cables subject to an external radiant source and based on a cylindrical adaptation of the modified FIST apparatus previously developed at UC Berkeley. In this adaptation, shown in Figure 4.1, cylindrical samples are mounted at the center of a Pyrex tube that is used to create a flow duct and doubles as an attachment point for a set of external radiant heaters. The external radiant heaters are mounted along the duct length and create a uniform radiant heat flux distribution over the sample surface.

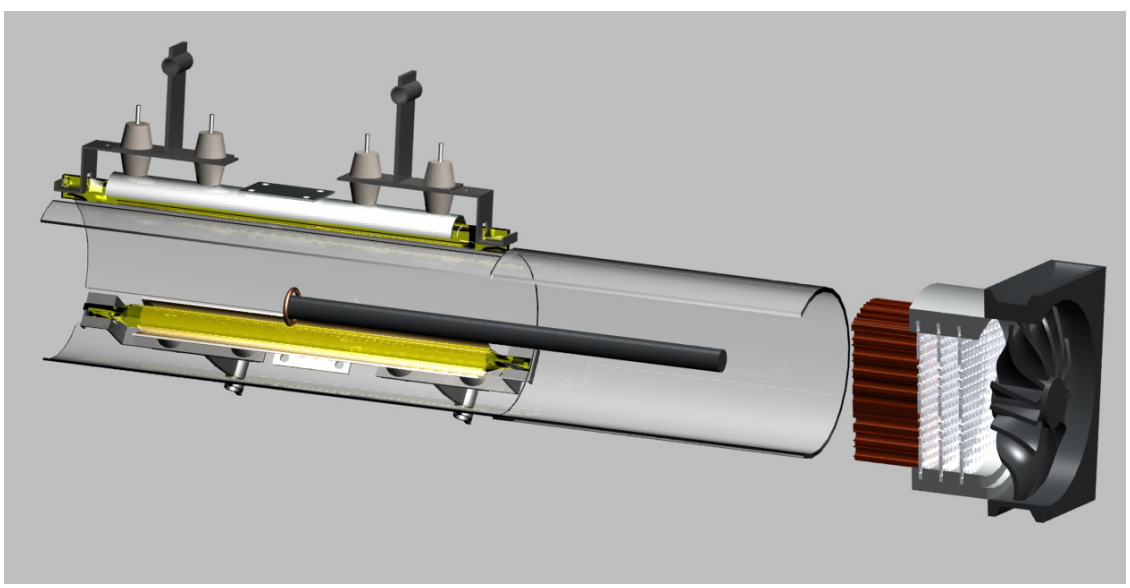

Figure 4.1: Cylindrical adaptation of the modified FIST apparatus.

Selection of ETFE and polytetrafluoroethylene (PTFE) insulated cables as fuel samples resulted in substantial modifications to the early conceptual design, most notably the adoption of a two-compartment experiment enclosure, which is discussed in detail in subsection 4.2.2. In addition, the anticipated usage in parabolic flight experiments placed restrictions on the size, mass, and power consumption of the experiment apparatus. The experiment apparatus and supporting equipment were required to fit within a experimental rack 900 mm tall, 700 mm long, and 450 mm wide not exceeding a total mass of 100 kg. Maximum power consumption was limited to 1,5000 W.

4.2.2 ETFE and PTFE Combustion

ETFE and PTFE are polymers that have been used as electrical cable insulations and wire harnesses in space applications. In normal atmospheric conditions both materials are fire-resistant, with PTFE exhibiting a higher degree of fire resistance than ETFE. PTFE has a LOI of 96% and a melting temperature ranging from 330 to 340 ^oC[17], whereas ETFE has a LOI value of 30% and melting temperature ranging from 255 to 285 ^oC[18]. PTFE and ETFE belong to the family of fluoropolymers, meaning they consist of fluorine atoms attached to a carbon backbone[19]. The carbon-fluorine bond is responsible for the high stability of fluoropolymers. However, when exposed to high temperatures, like in the case of a fire, decomposition of fluoropolymers can result in the production of toxic gases including CO and HF. When combined with water HF can form hydrofluoric acid, a highly corrosive and toxic acid. Unpublished PTFE and ETFE combustion data provided by JAXA is presented in Tables 4.1 and 4.2[20].

Product	Production Rate ($wt.$ %)	Amount (g)
CO	19	0.19
CO_2	80	0.80
CH_4	0.3	0.003
C_2- hydrocarbon	0.5	0.005
HF	27	0.27
PFIB	0.002	0.00002
Others	34.54	0.3454

Table 4.1: Combustion products for 1g of PTFE[20].

As a result of the corrosive and toxic nature of HF it was necessary to design a sealed experiment enclosure that contains the combustion products and limits exposure to individuals. At the same time it was necessary to incorporate an air filtering system that maintained HF and CO_2 concentrations at a level that would not affect results. The air filtering system also allowed running consecutive experiments without opening the experiment enclosure.

Product	Production Rate ($wt.$ %)	Amount (g)
CO	13	0.13
CO_2	141	1.41
CH_4	0.3	0.003
C_2- hydrocarbon	0.5	0.005
HF	24	0.24
PFIB	0.002	0.00002

Table 4.2: Combustion products for $1g$ of ETFE[20].

The approach taken was to divide the experiment enclosure into two sections, a bottom section that included the flow duct and air filtering system, and a top section that isolated the external radiant heaters from the HF emissions.

The bottom section is 410 mm long, 310 mm wide and 195 mm tall. Sidewalls feature vacuum-type electrical connectors that are used to connect a type-T thermocouple, an oxygen sensor, a suction fan, and an auxiliary mixing fan. In addition, three Rc1/4 fittings attached to the left side wall are used as ports for Oxygen/Nitrogen supply, chamber pressure monitoring, and a vacuum line. A 20 mm thick middle plate covers the bottom section and serves as the mounting surface for the manifolds that hold the flow duct in place. The flow duct and bottom section create a close air flow path, shielding the top section from HF emissions. The size and shape of the manifolds are dictated by the external radiant heaters (See subsection 4.2.3). The flow duct is made of Pyrex and it has a 60 mm inside diameter and a total length of 250 mm. Two 3 mm surface holes located 20 mm and 50 mm from one of the tube edges serve as mounting points for the igniter wire of the fuel samples. The Pyrex glass tube is treated as disposable component of the experiment, since production of HF turns the inside surface of the tube opaque to the point that it makes experiment observations difficult. A suction fan (San Ace 60 - 9GV0612P1H031) and an air filter located downstream of the test sample are used to achieve a low-velocity air flow over the sample wires. A constant airflow speed of 0.12 m/s through the flow duct is used for all experiments. Two 18mm thick honeycomb flow straighteners placed at both ends of the Pyrex glass tube are used to ensure flow uniformity. The flow duct manifolds and the flow duct are shown in Figure 4.2, and the effect of HF on the Pyrex glass tube is shown in Figure 4.3.

The air filter system is made of a combination of HF filtering material, mainly consisting of activated charcoal, and *zeolite* used for removal of CO_2 and H_2O. As air containing HF and CO_2 leaves the flow duct it passes through the air filtering material, which absorbs a portion of the undesired combustion products. Although the air filtering system does not completely absorb all of the HF, its effectiveness can be observed when comparing the upstream and downstream flow duct manifolds shown in Figure 4.4. In the upstream (left)

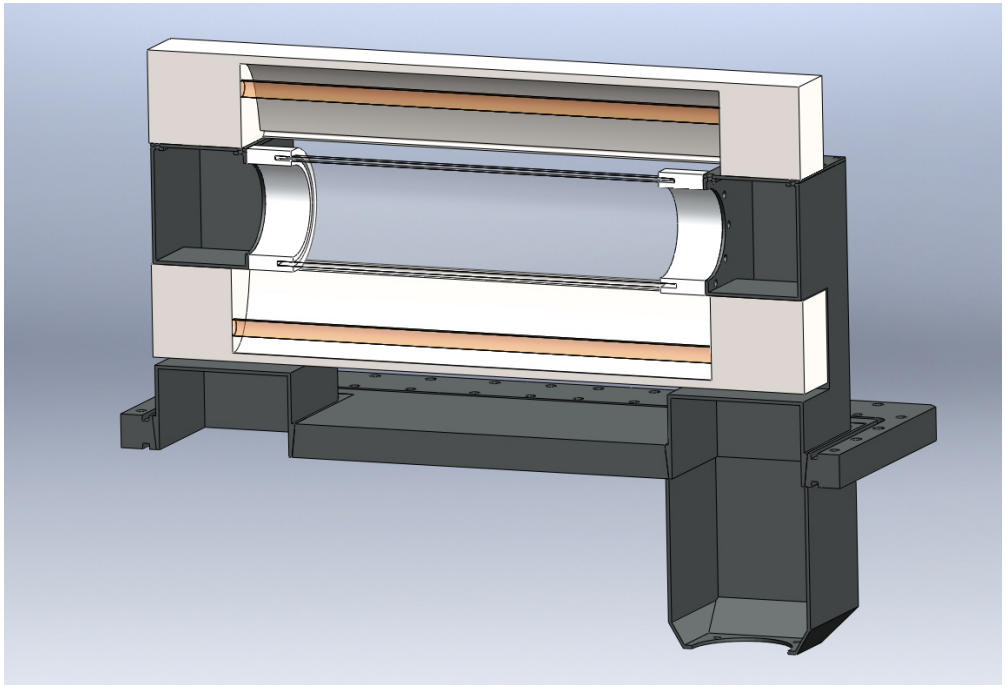

Figure 4.2: Manifolds and flow duct detail.

manifold no noticeable corrosion is observed since the air flowing through this manifold first has to pass through the air filter. The downstream (right) manifold is directly after the flow duct, meaning the air flowing through the manifold contains HF resulting in corrosion.

4.2.3 External Radiant Heaters

The top section is 410 mm long, 211 mm wide and 250 mm tall with two 90mm diameter glass windows for optical access. When bolted to the bottom section, the top and bottom sections create a 46L sealed chamber. Inside the top section there are two halogen external radiant heaters (Ushio UH-USC-CL300) 406 mm long, 70 mm wide and 55.2 mm tall, each one has a maximum power consumption of 900 W. The heaters have a peak wavelength emission of 1.2 microns and provide a maximum external radiant flux of 25 kW/m^2 as measured using a heat flux sensor with an accuracy of 5% (International Thermal Instrument Company ITI-HT-50). The reason for selecting halogen heaters is that they have a fast response time, which is desirable given the short duration of parabolic flight experiments. The heaters have a 300 mm lighted length, but during the experiments an actual lighted length of 230 mm is used in order to achieve a nearly uniform heat flux distribution along the wire sample length. Radiant flux measurements at different power settings showed the normalized radiant flux along the sample length had an average value of 0.923, a standard deviation of 0.042, and a minimum value of 0.838. Additional radiant heat flux measurements along the flow

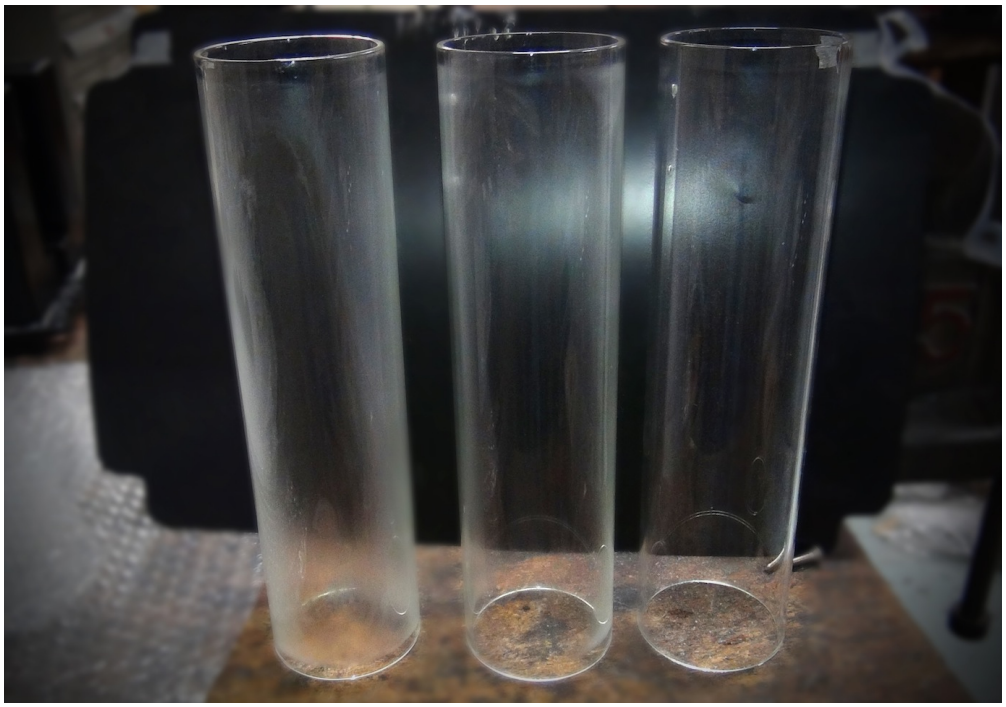

Figure 4.3: Effect of HF in Pyrex tube.

duct radial direction showed that in a region within a 3 mm from the tube centerline the normalized radiant flux had an average value of 0.920 and a standard deviation of 0.071.

Power to the heaters is controlled via a $120VAC$, $20A$ transformer. The lamps are connected in parallel in order to guarantee equal radiant fluxes from the top and bottom heater. Current to each lamp is monitored using a digital panel current meter. Voltage across the lamps is measured using a voltage panel meter, the panel meter also has an analog output that is connected to a data acquisition system. Calibration curves for the external radiant heaters can be found in Appendix B. During a test the external radiant heaters are turned on and allowed to irradiate the sample wire for about $30s$ prior to sample wire ignition. Experiments with different preheating times showed no significant influence on the results, and therefore a $30s$ preheating time was used in both $1g$ and μg experiments.

The heaters are mounted above and below the Pyrex glass tube at a distance of 35.8 mm, which is the focal length of the heaters. The Pyrex tube has an inside diameter of 60 mm, and a thickness of 2.5 mm resulting in a 3.3 mm clearance between the external heaters and the flow duct. Hence, the glass tube centerline coincides with the focal length of both, the top and bottom halogen heaters. The unique shape of the flow duct manifolds is a consequence of the need to accommodate the bottom heaters within the top section and preserve optical access to the flow duct. Similar to the bottom section, vacuum-type

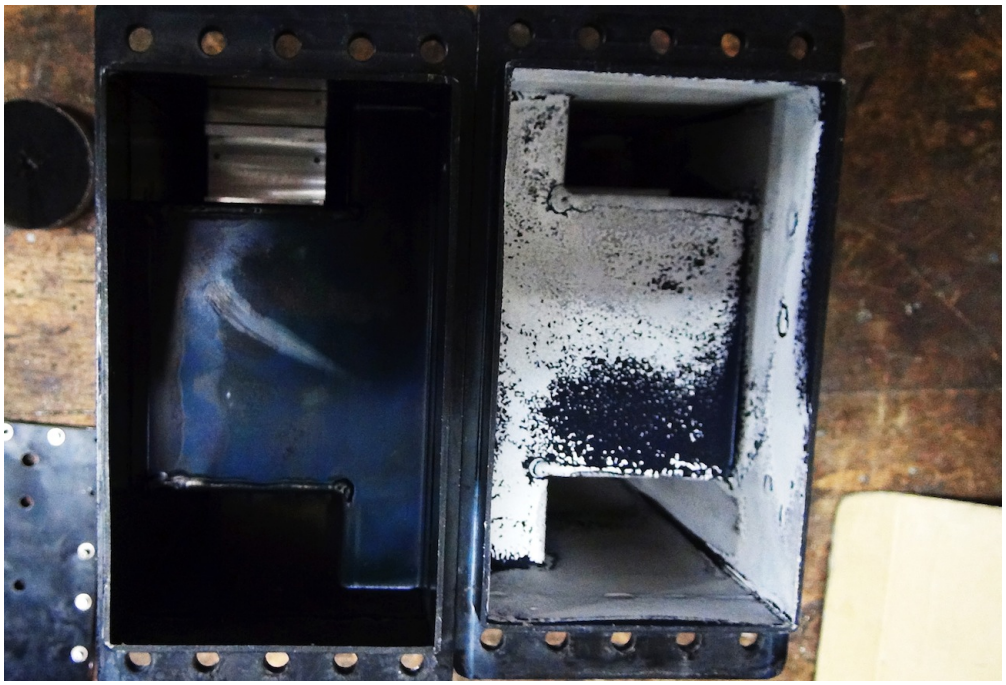

Figure 4.4: Upstream (left) and downstream (right) flow duct manifolds. Note the corrosion effect HF in the downstream manifold.

electrical connectors are for supplying electricity to the external radiant heaters, igniter wire and motor of the automatic sample feed system.

4.2.4 Automatic Sample Feed System

An automatic sample feed system is used to supply an ETFE insulated copper wire (Sugita Densen Co., Ltd.) with a core diameter of $0.50mm$ and an insulation thickness of 0.30mm for all experiments. The system consists of two assemblies that are housed inside the upstream and downstream flow duct manifolds. The upstream assembly shown in Figure 4.5 contains a 3-3.5 m spool of unburned, electrical cable. The spool is pinned to the walls of the manifold. A friction block at the shaft of the spool is used to create tension in the spool and prevents the spool from unwinding. After leaving the spool the cable wraps around two pulleys that help align the electrical cable with the flow duct centerline.

The downstream assembly contains an empty spool for winding the burnt, electrical cable. The bottom shaft of this spool is fitted with a ratchet gear, which locks the electrical cable in place during an experiment. The top shaft of the spool has a driver gear that is in contact with a shaft driven by a $7.2VDC$ electrical motor. The ratio of the drive gear to the shaft is 6:1, which helps reduce the speed of the electrical motor. The electrical motor is

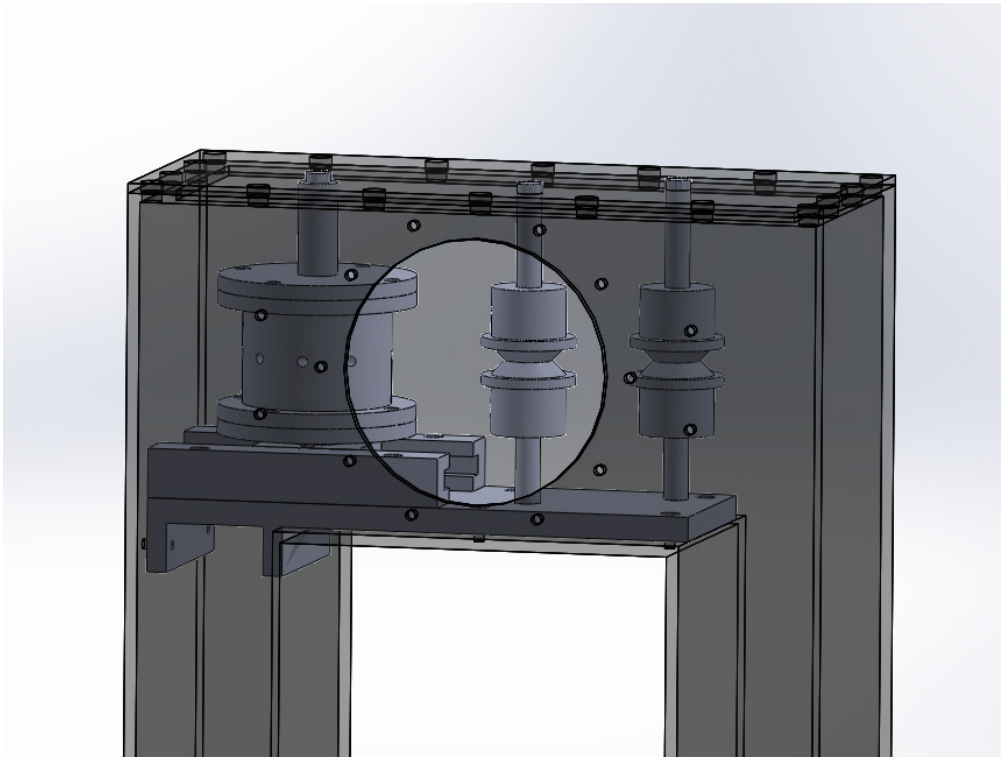

Figure 4.5: Upstream assembly of the automatic sample feed system.

mounted on top of the downstream flow duct manifold, and is operated in $0.2s$ pulses with the help of a programmable logic controller (PLC). Usually, two to three pulses are required to advance the full length of the flow duct. The automatic sample feed system holds enough electrical cable to conduct at least 10 experiments assuming a burn length of 250 mm for each experiment. Ignition of the wire samples is accomplished using a 0.5 mm thick Kanthal wire coil with a diameter of 8 mm. The downstream assembly of the automatic sample feed system is shown in Figure 4.6.

4.2.5 Additional Considerations

Microgravity experiments are conducted in parabolic flights operated by Diamond Air Service (DAS) in Nagoya, Japan. Each parabolic flight consists of approximately 10 parabolas, with each parabola providing about $20s$ of $10^{-2}g$. The elevated gravity experienced in the moments before or after microgravity conditions make difficult to perform tasks such as the operation of switches or monitoring of conditions. Moreover, the short duration of microgravity conditions, require a simple and streamlined experimental procedure that reduces human input to the minimum. In the current experiment this is partly accomplished using a programmable logic controller (PLC) (Mitsubishi MELSEC FX2N-16MR) for the

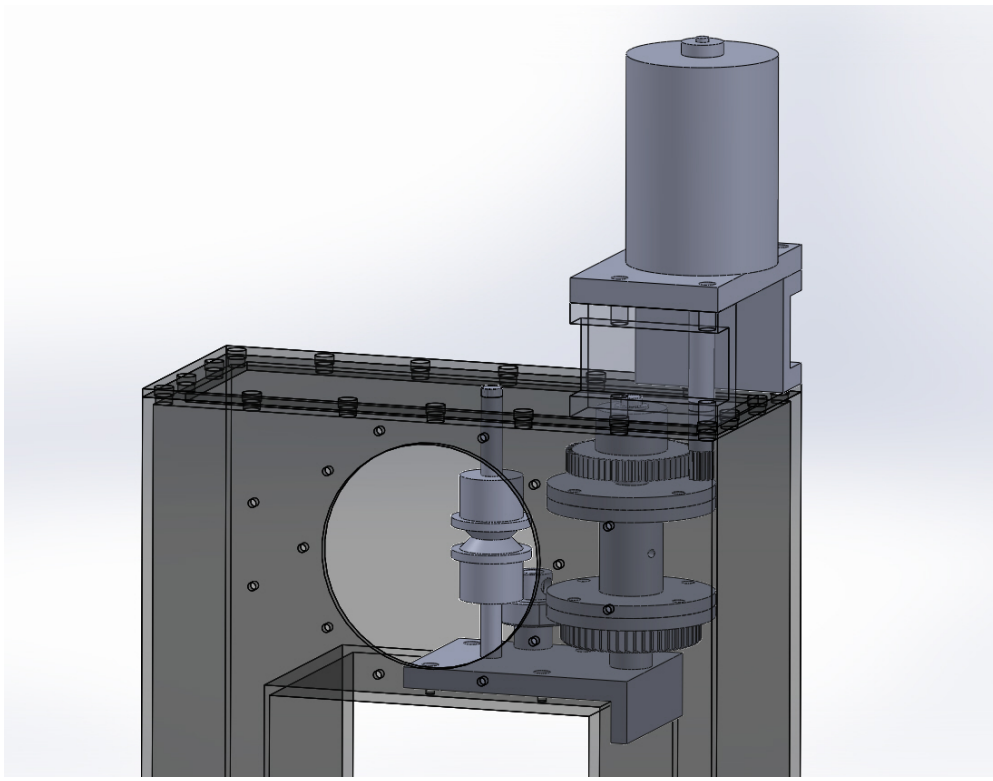

Figure 4.6: Downstream assembly of the automatic sample feed system.

following:

1. $12s$ ON/OFF pulse of the power supply that supplies the sample wire igniter coil with a maximum power of $92W(14.7VDC, 6.3A)$.
2. $0.2s$ ON/OFF pulse to drive the electrical motor of the automatic sample feed system.
3. ON/OFF status of pressure transducer, flow duct suction fan, auxiliary mixing fan, and master experiment master switch.

One type-T thermocouple is used to measure air temperature in the bottom section. Although the thermocouple is in contact only with air, the temperature represents an approximation of the temperature of air inside the sealed chamber, and in all experiments did not exceed 25^oC. A pressure sensor (Nagano Keiki KP15-17G) and oxygen sensor (Jikco JKO-25LII) are used to monitor pressure and oxygen concentration. The oxygen concentration inside the chamber is set using the oxygen partial pressures for a total chamber pressure of 100kPa and the observed maximum oxygen concentration variation during experiment is

less than 1.0% of the initial oxygen concentration. Chamber pressure, oxygen concentration, air temperature, and acceleration in the case of microgravity experiments, are recorded using data recorder (Graphtec GL220 midi LOGGER dual) with a 2 Hz sampling frequency.

Pure Oxygen and Nitrogen gas supply lines are fitted with pressure regulators and quick release connectors. The gas supply lines are connected to pressurized cylinders stored in the laboratory or the airplane cargo bay. During the parabolic flight experiments, a LED located in the back window of the top section is used to provide a visual cue when microgravity conditions are achieved. The LED signal is simultaneously recorded in the data acquisition system and used to synchronize experiment video recordings with acceleration data from the airplane. During post processing acceleration data with a 100 Hz sampling rate is overlaid onto the original video resulting in a video recording that also displays the instantaneous acceleration.

4.2.6 Normal Gravity ($1g$) Test Protocol

The following test protocol is used in all $1g$ experiments:

Before experiment:

1. ADJUST oxygen concentration and PRESET external radiant flux.
2. RECORD experiment conditions in logbook.

Experiment is ready for new experiment:

3. t_{on}-120s: Turn OFF auxiliary mixing fan. Turn ON flow duct suction fan.
4. t_{on}-60s: START video recording.
5. t_{on}-30s: Turn ON external radiant heaters.
6. t_{on}-10s: Turn ON igniter.
7. t_{on}: OBSERVE experiment outcome.

After Experiment:

8. Turn OFF external radiant heaters.
9. STOP video recording.
10. Turn OFF flow suction fan. Turn ON auxiliary mixing fan.

11. ADVANCE wire sample.

Return to top.

4.2.7 Microgravity (μg) Test Protocol

The following test protocol is used in all μg experiments:

New parabola begins:

1. RECORD experiment conditions in logbook.
2. START video recording.
3. t_{on}-60s: Turn OFF auxiliary mixing fan. Turn ON flow duct suction fan.
4. t_{on}-30s: Turn ON external radiant heaters.
5. t_{on}-10s: Turn ON igniter.
6. t_{on}-2s: μg conditions START, i.e. $g \approx \mu g$.
7. t_{on}: OBSERVE experiment outcome.
8. t_{on}+18s: μg conditions STOP, i.e. $g \neq \mu g$.

After μg period is over:

9. Turn OFF external radiant heaters.
10. STOP video recording.
11. Turn OFF flow suction fan. Turn ON auxiliary mixing fan.
12. Advance wire sample.
13. ADJUST oxygen concentration and PRESET external radiant flux.

Wait for next parabola.

An schematic of the complete experimental apparatus is shown in Figure 4.7. The fully assembled experiment apparatus, including the experiment rack and supporting equipment is shown in Figure 4.8.

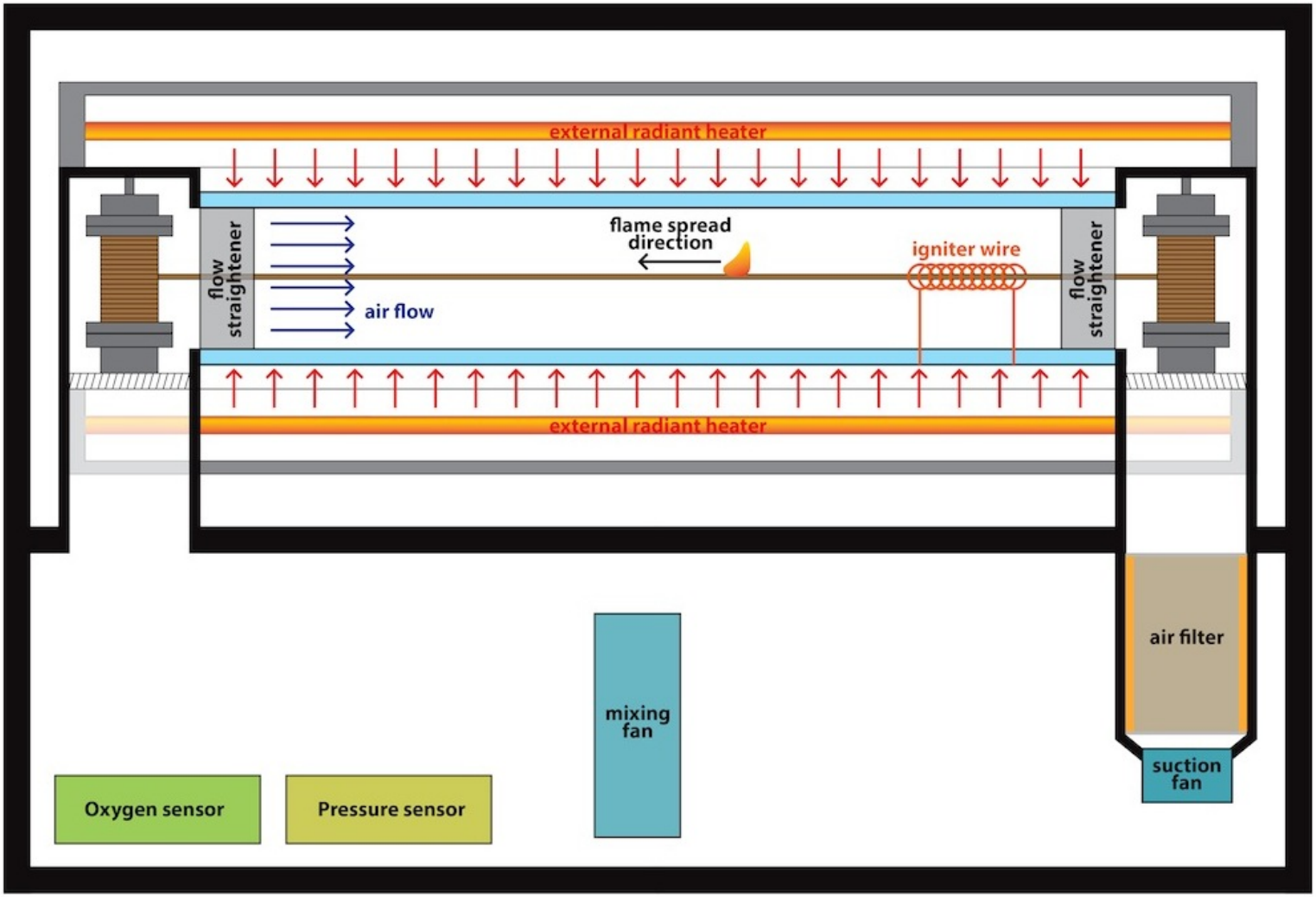

Figure 4.7: Experiment schematic.

Figure 4.8: Experiment rack used during the parabolic flight experiments.

4.3 Results

All of the experiments reported in this chapter were conducted with a ETFE insulated copper wire (Sugita Densen Co., Ltd.) with a core diameter of $0.50mm$ and an insulation thickness of 0.30 mm. In both, normal gravity ($1g$) and microgravity (μg) experiments, the LOC was defined as the lowest oxygen concentration resulting in opposed flame spread over the sample wire for a given external radiant flux, $\dot{q}''_{ext}$. Depending on experiment conditions two possible outcomes were considered, *Propagation* and *No Propagation*. In $1g$ the experiment result was defined in terms of the flame spread distance. Conditions resulting in flame spread distances longer than half the length of the sample wire, i. e. 100 mm, were considered to be *Propagation*. Although it was possible to select a shorter propagation distance as the criteria, experiments with flame spread distances greater than 100 mm routinely resulted in flame spread over the entire length of the sample. Therefore, the $1g$ *Propagation* points represent conditions for which a steady-state flame spread occurs.

Adoption of the $1g$ propagation criteria in μg experiments would have resulted in *No Propagation* for all conditions considered. The reason is that the short microgravity time obtained during parabolic flights is not long enough for any of the flames to reach a spread distance equal or greater than 100 mm. Therefore, it was decided that conditions resulting in the presence of a flame at the end of the microgravity period would be defined as *Propagation*. Similar considerations are common in microgravity experiments and do not significantly affect the behavior of flammability limits[9].

4.3.1 Normal Gravity (1g)

Experiments resulting in *Propagation* exhibited flame spread rates of around 2 mm/s in agreement with results obtained by Kikuchi[5]. Typically, flames wrapped around the cable insulation and exhibited elongated shapes as a result of buoyant flow. In addition, the flame was slightly titled in the direction of the forced flow, away from the unburned insulation and onto the burned electrical wire. As the flames propagated, the unburned ETFE insulation at the leading edge of the flame softened and started to accumulate. When the accumulation was large enough it created a droplet that eventually dripped onto the Pryex glass tube. Once the oxygen concentration reached values closer to the LOC at a particular external radiant flux, the flame was characterized by alternating periods of growing and shrinking and increased dripping of molten ETFE. Figure 4.9 presents a typical ETFE flame during experiments in normal gravity.

In the absence of $\dot{q}''_{ext}$ the LOC was determined to be 31.5% and it provides reasonable agreement with ETFE LOI data[18]. For oxygen concentrations below 31.5% no propagation was observed unless an external radiant flux was applied. The addition of $\dot{q}''_{ext}$ extended the flammability of the sample wire, and allowed flame spread to continue at oxygen concentrations below the LOI. The lowest oxygen concentration at which flame spread was

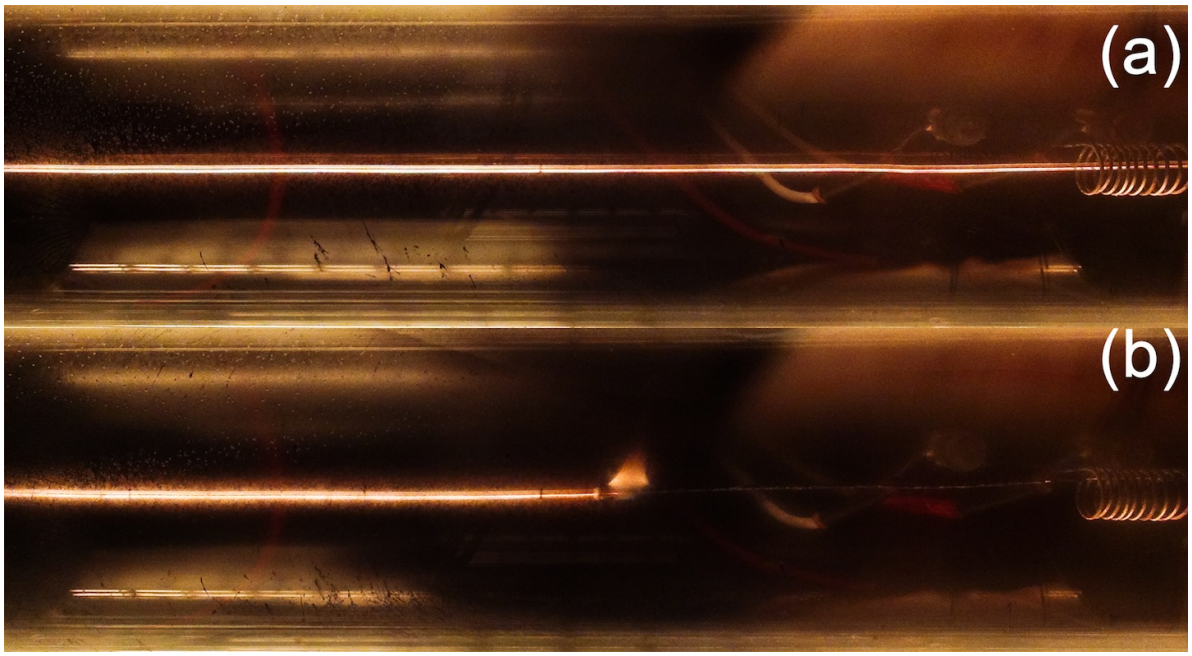

Figure 4.9: ETFE opposed flame spread in normal gravity. Inset (a): Sample wire exposed to external radiant flux prior to ignition. Inset (b): A flame propagating along the sample wire. Test conditions were 26.3% O_2 with an external radiant flux ($\dot{q}''_{ext}$) of 24.3 kW/m^2.

observed corresponded to 26.3% with a $\dot{q}''_{ext}$ of 24.3 kW/m^2. It may be possible for flames to propagate in oxygen concentrations below 26.3%; however, this was not explored because experiments with large $\dot{q}"_{ext}$ values increased the production of soot and HF gas that rapidly deteriorated the visibility through the Pyrex glass tube. The approximated flammability boundary in Figure 4.10 shows that a 1% reduction in oxygen concentration can result in significantly different changes in the value of $\dot{q}''_{MIN}$. As oxygen concentration is reduced, increasing amounts of external radiant flux are required to maintain *Propagation*. This behavior suggests the existence of an asymptotic limit for the LOC as a function of $\dot{q}"_{ext}$, but due to experiment limitations the existence of this asymptotic limit could not be confirmed.

4.3.2 Microgravity (μg)

Microgravity resulted in very different flames in comparison to normal gravity. Ignition of the sample wire was characterized by the appearance of a smoke cloud that completely surrounded the sample. Short flashes followed the smoke cloud and eventually resulted in a steady propagating flame that wrapped around the electrical cable, see Figure 4.11. Flames in microgravity had a cylindrical appearance, they were long along the sample wire direction and had a short height. Figure 4.11 is an example of an ETFE flame propagating

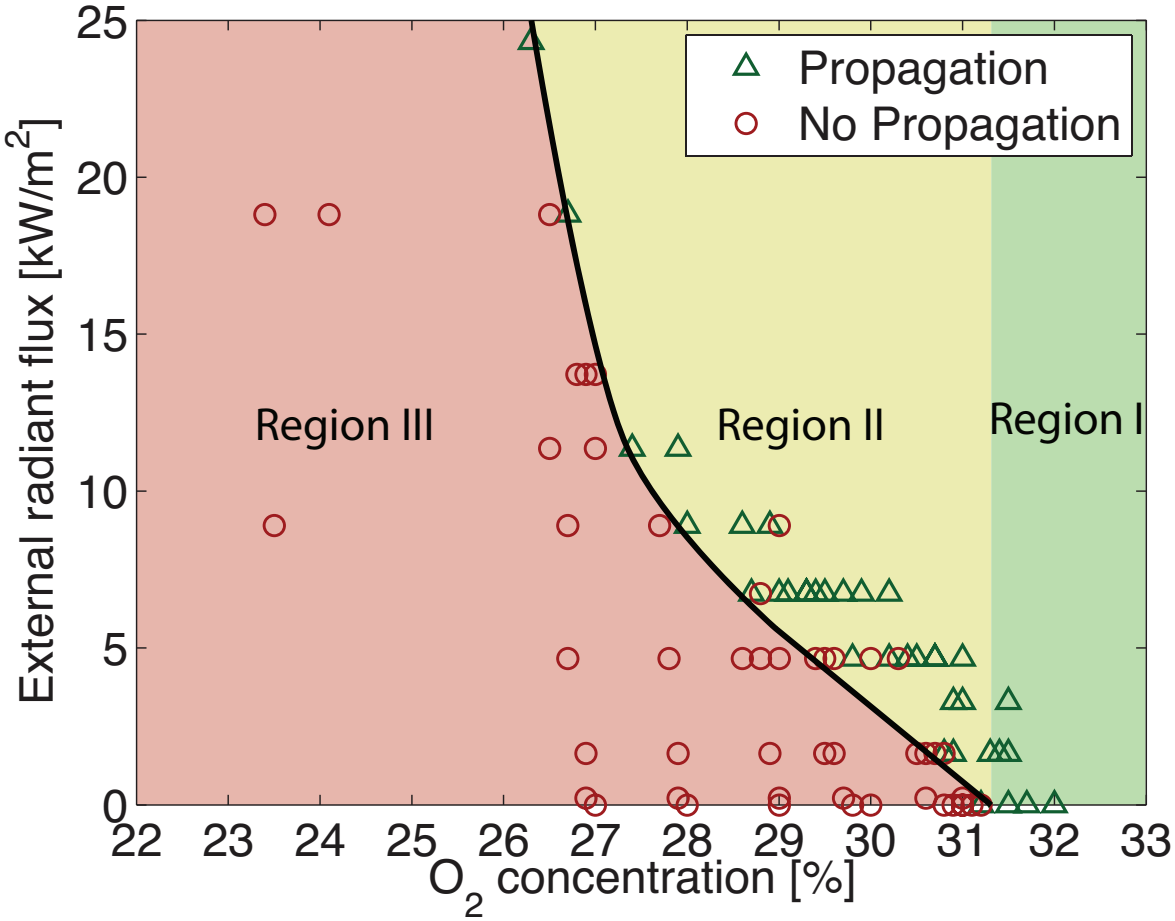

Figure 4.10: Normal gravity flammability limits of a 0.50 mm core diameter and 0.30 mm insulation thickness ETFE insulated Copper wire.

in microgravity conditions and its subsequent extinction once gravity increased. The sudden increase in gravity at the end of the parabola resulted in extinction of the flame and shows the effect of gravity in the LOC of materials.

In addition, flames in microgravity were less bright than flames in normal gravity. At $t = 13.78s$ $g \approx 0$, and the flame had a cylindrical shape with a dim orange color. When gravity increased to $1.4g$ at $t = 22.02s$, the flame lost the cylindrical shape, became stretched in a direction perpendicular to the fuel sample, and had a bright yellow appearance. The changes in flame brightness can be attributed to the production of soot, meaning that microgravity conditions result in more complete combustion of ETFE and lower production of soot. Examination of samples revealed that unlike experiments in normal gravity, in microgravity experiments there was no insulation residue on the surface of the conductor, which can also

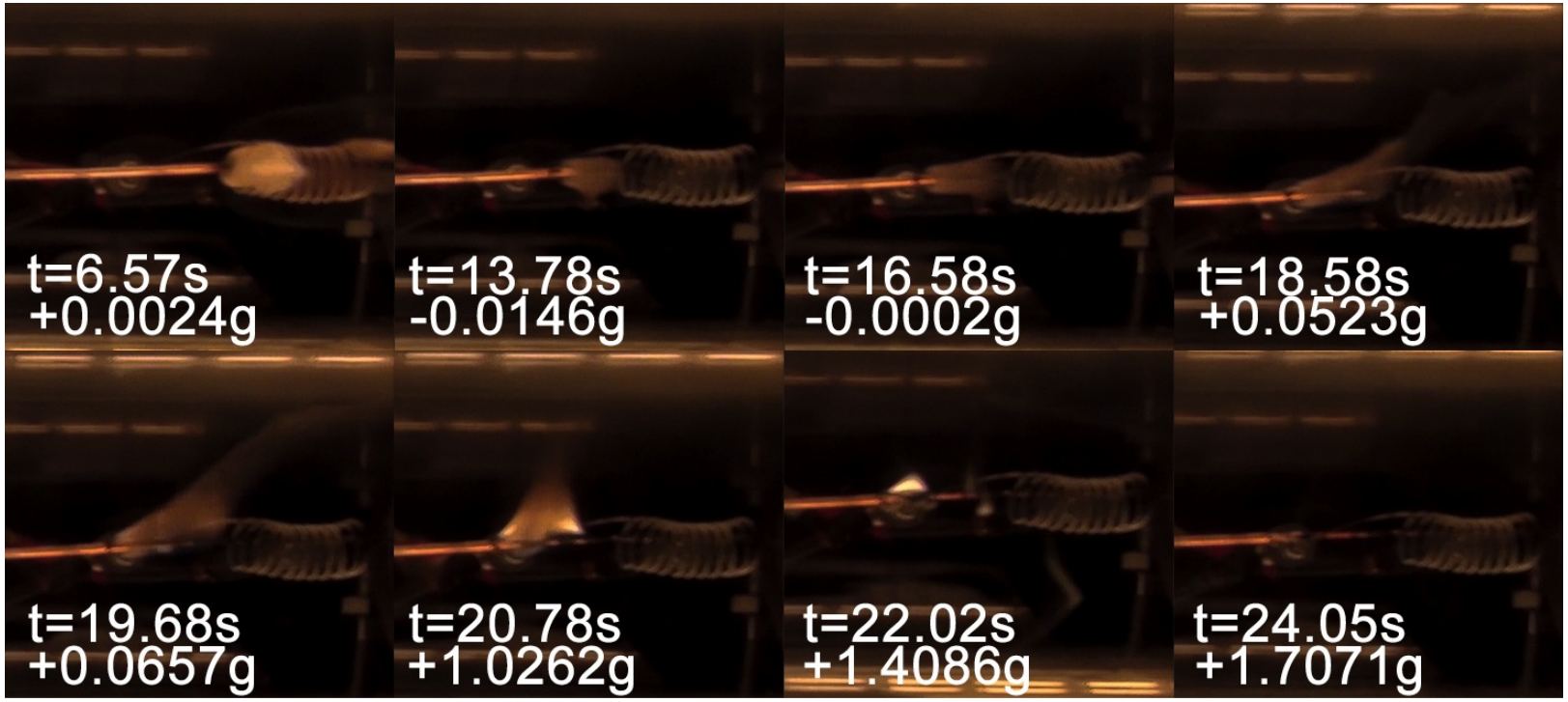

Figure 4.11: ETFE opposed flame spread in microgravity conditions and subsequent extinction due to gravity. Test conditions were 21.2% Oxygen and external radiant flux ($\dot{q}''_{ext}$) of 19 kW/m^2.

be interpreted as an indicator of the more complete combustion of ETFE in microgravity.

Experiments showed that microgravity has a pronounced effect in the flammability characteristics of ETFE insulated cables. In the absence of an external radiant flux the LOC had a value of 26.4%, which is lower than the corresponding $1g$ value. Despite the limited number of experiments conducted in μg, the results showed that similar to $1g$, the addition of an external radiant flux allowed flame spread to continue in oxygen concentrations less than the μg LOC with no external radiant flux. The lowest oxygen concentration at which opposed flame spread was observed was 20.3% and corresponded to a $\dot{q}''_{ext}$ of 18.8 kW/m^2. Figure 4.12 shows a plot of the LOC as a function of $\dot{q}''_{ext}$, where the black line represents an approximation of the flammability boundary in microgravity. From this plot it can be seen that microgravity and the addition of an external radiant flux can turn ETFE flammable in oxygen concentrations similar to those found in the ISS, i.e. 21% O_2 and 100 kPa, which constitutes a novel and important finding in space fire safety.

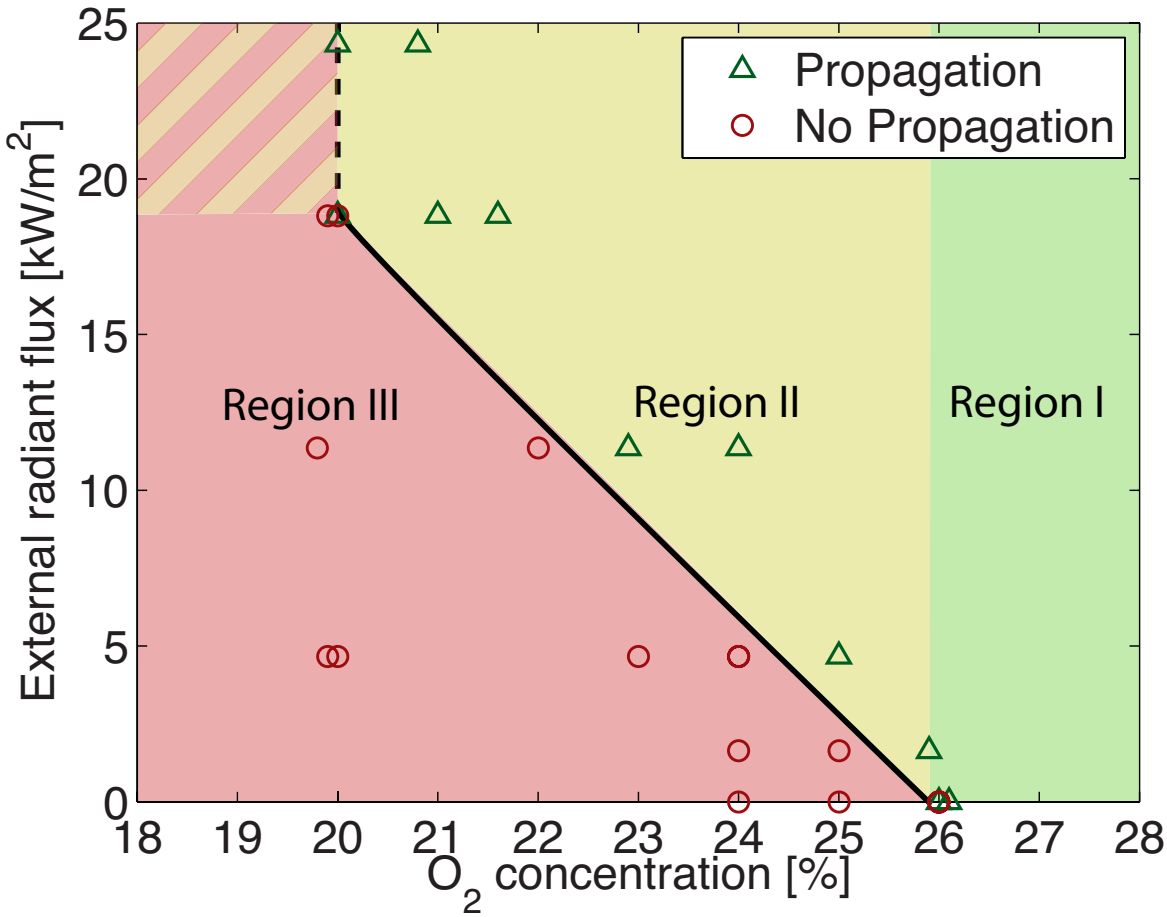

Figure 4.12: Microgravity flammability limits for a 0.50 mm core diameter and 0.30 mm insulation thickness ETFE insulated Copper wire.

4.4 Analysis

4.4.1 Normal Gravity and Microgravity

There are two oxygen concentrations that are important for understanding the flammability boundaries shown in Figures 4.10 and 4.12. The first one is the LOC for the case of no external radiant flux, and the second one is the LOC for the maximum external radiant flux, $\dot{q}''_{ext} \approx 25\ kW/m^2$. These two oxygen concentrations can be used to divide the flammability map into three distinct regions that facilitate interpretation of the results in $1g$ and μg conditions.

Region I, shown in green in Figures 4.10 and 4.12, corresponds to oxygen concentrations

at or above the no external radiation LOC. In this region, flame spread occurs without the aid of an external radiant flux, $\dot{q}''_{ext}$, similar to the ASTM D 2863[21]. In this high oxygen concentration region, the heat released by the combustion reaction is large enough to overcome any heat losses, and maintain a minimum solid decomposition rate that supports a sustained flame. As the oxygen concentration increases beyond the no external radiation LOC, both the flame temperature, T_f, and the total heat transfer to the solid, $\dot{q}''_{tot}$, will increase. For purposes of this discussion $\dot{q}''_{tot}$ can be defined as

$$\dot{q}''_{tot} = \dot{q}''_{cond} - \dot{q}''_{conv} + \dot{q}''_{core} \tag{4.4.1}$$

where $\dot{q}''_{cond}$ is the gas-phase conduction heat flux from the flame, $\dot{q}''_{conv}$ is the $1g$ natural convection heat losses, and $\dot{q}''_{core}$ is the heat flux from/to the wire core.

As the oxygen concentration increases the chemical reaction time, t_{chem}, decreases, resulting in smaller heat losses. Starting with oxygen concentrations within *Region I* and moving towards the *Region I / Region II* boundary, decreasing the oxygen concentration will decrease T_f, and $\dot{q}''_{tot}$; while increasing t_{chem} and the heat losses. The reduction in $\dot{q}''_{tot}$, and the increase in the heat losses will decrease the solid decomposition rate to the point that the flame becomes unable to generate the amount of fuel required for sustained combustion.

The effect of gravity will appear through the heat losses of the sample. The smaller heat losses in μg require lower total heat fluxes that can be achieved by flames at lower oxygen concentrations. In $1g$, natural convection heat losses require an additional heat transfer that for the purpose of *Region I* require raising the $\dot{q}_{tot}$ through the increase in $\dot{q}''_{cond}$, i.e. oxygen concentration and flame temperature. Depending on the gravity conditions $\dot{q}''_{core}$ can increase or decrease $\dot{q}"_{tot}$. In $1g$, $\dot{q}''_{core}$ is negative because natural convection losses cool the regions adjacent to the flame resulting in heat flowing out from the core. However, in μg the core is not subject to convective heat losses and remains at a high temperature, acting as a heat source to the unburned insulation.

Region II, shown in yellow in Figures 4.10 and 4.12, is a region in which flame spread is contingent on two variables, the oxygen concentration and external radiant flux. In this region, oxygen concentrations less than the no external radiation LOC result in flame temperatures that are lower than those of *Region I*. The reduced T_f in *Region II*, decreases $\dot{q}"_{tot}$, but most importantly reduces the solid decomposition rate, $\dot{m}$. When $\dot{m}$ drops below a critical rate, $\dot{m}_{cr}$, the gas phase reaction consumes the fuel faster than it can produce and a flame cannot be sustained. In order to circumvent the heat transfer deficit incurred by the reduction of T_f it becomes necessary to increase the heat flux to the solid. The addition of $\dot{q}''_{ext}$ can compensate the decrease in $\dot{q}''_{net}$ and maintain $\dot{m}$ above its critical value. As the oxygen concentration deceases and the reduction in flame temperature becomes more significant a larger $\dot{q}''_{ext}$ is required, explaining the trend observed in the flammability boundaries.

When the oxygen concentration reaches a value closer to the $\dot{q}''_{ext}$= 25 kW/m^2 LOC, $\dot{q}''_{ext}$ cannot keep up with the reduction in oxygen concentration allowing $\dot{m}''$ to drop below its critical value and resulting in extinction of the flame.

In $1g$ the total heat input to the wire is less than in μg due to natural convection heat losses, differences in flame shape, and core effects. Natural convection induces buoyant flows that result in cooling of the sample surface and reduce $\dot{q}''_{tot}$. Changes in the flame shape also affect the total heat input to the wire. Whereas in $1g$ flames are short and stretched upwards, in μg flames are long and completely surround the sample wire. These differences can affect the area of the insulation over which heat transfer can take place, as well as reinforce core effects. Though in $1g$ the core is subject to convective heat losses and effectively acts as a heat sink, in μg it provides an additional heat input to the unburned insulation.

Once the oxygen concentration reaches values below the $\dot{q}''_{ext} = 25kW/m^2$ LOC, the transition from *Region II* to *Region III* occurs. In *Region III*, shown as the red region in Figure 4.10 and Figure 4.12, no flame spread is observed despite the addition of an external radiant flux. This suggests that although the external radiant flux may be enough to reach the $\dot{m} = \dot{m}_{cr}$ condition, the rate at which heat is released by the combustion reaction is not enough to overcome heat losses. Low oxygen concentrations reduce T_f and $\dot{q}''_{tot}$ and increase the chemical reaction time, t_{chem}, allowing flame heat losses to occur over a longer period of time. Thus, the reduced net heat transfer combined with increased heat losses leads to quenching of the flame. Microgravity conditions eliminate convective heat losses, allowing to maintain the same $\dot{q}''_{tot}$ despite a lower T_f.

4.4.2 Comparison between ETFE and PE

Given the limited number of studies that have considered fire-resistant materials, it is not known whether microgravity changes the flammability of fire-resistant (FR) and non fire-resistant (NFR) materials equally, or, if instead microgravity affects one more than the other. In addition to the flammability boundaries developed in $1g$ and μg, the results obtained with ETFE can also be compared to similar ones obtained using polyethylene (PE) insulted wires. PE insulated wires have been a common choice for studying flammability limits of electrical wires[7–9]. Despite inherent differences in experiment apparatus and the methodology, the $1g$ and μg flammability limits of ETFE and PE can be used to gain a better insight on the effect of gravity in the flammability of FR and NFR materials.

The effect of gravity in the flammability limits of materials can be analyzed in terms of ΔLOC, which is defended as the difference between the $1g$ and μg in the LOC, i.e $\Delta\text{LOC} = \text{LOC}_{1g} - \text{LOC}_{\mu g}$. If microgravity acts equally on both, FR and NFR materials, their ΔLOC would be expected to be approximately the same. However, if the effect of microgravity is more pronounced in either type of material, different ΔLOC values would be expected. In the present analysis, the PE flammability limits data taken from Takahashi et al.[9] show

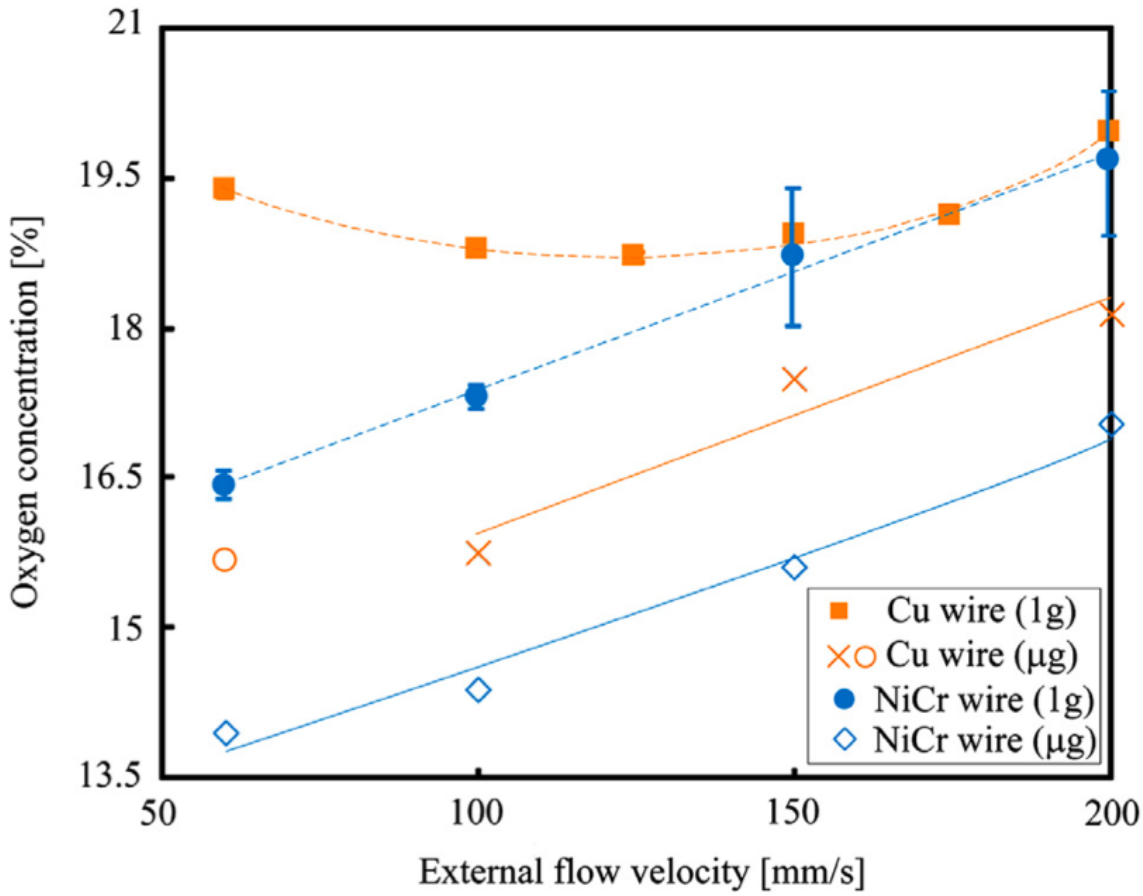

Figure 4.13: Flammability limits of PE in normal and microgravity conditions (Takahashi et al.[9]).

that PE ΔLOC has a value of around 3%. In contrast, ETFE insulated copper wires under no external radiant flux had a ΔLOC of 5.5%. The observation that ΔLOC for ETFE is larger than ΔLOC for PE is an interesting results that suggests microgravity has a more pronounced effect on the flammability limits of FR materials. A possible explanation for this observation is proposed in terms of differences in thermal ignition parameters and the solid mass loss rate is presented below.

Lyon and Quintiere[22] proposed that a critical Heat Release Rate, HRR_{cr} can be used as a material-independent criterion for ignition of solid fuels and can be interpreted as the minimum rate of heat production required to overcome heat losses and maintain a critical mass flux. The critical heat release rate is calculated according to Equation 4.4.2, where ΔH_c is the heat of combustion and $\dot{m}''_{cr}$ is the critical mass flux at ignition. For the case of flashing

ignition, $\text{HRR}_{cr} \approx 22\ kW/m^2$, and for the case of sustained ignition $\text{HRR}_{cr} \approx 66\ kW/m^2$. The difference between the flashing and sustained ignition value of HRR_{cr} is expected due to the transition from lower flammability limit combustion during flashing to stoichiometric combustion at sustained ignition resulting in an increase in $\dot{m}''_{cr}$.

$$\text{HRR}_{cr} \propto \dot{m}''_{cr} \Delta H_c \tag{4.4.2}$$

The heat of pyrolysis, ΔH_p and the heat release parameter (HRP) listed in Table 4.3 can be used to show that ΔH_c, calculated as the product of ΔH_p and HRP, is larger for PE than ETFE. The higher ΔH_c of PE implies that at ignition, the mass flux of PE is smaller than that of ETFE. Moreover, since ETFE has a higher $\dot{m}''_{cr}$, it requires a greater total heat transfer from the flame to the unburned solid, resulting in higher oxygen concentrations and thus fast gas-phase reaction rates, $\dot{\omega}$.

Polymer	ΔH_p (MJ/kg)	Cp_s (kJ/kg K)	HRP	$T_{ig,meas}$ (^{o}C)
PE	2.2	1.5	18	380
ETFE	1.1	1.0	6	540

Table 4.3: Thermal ignition parameters for PE and ETFE[22].

Oxygen concentrations above the $1g$ LOC result in fast $\dot{\omega}$ and high Heat Release Rate (HRR) values that can easily overcome natural convection and core effect heat losses. As oxygen concentration is reduced, the longer t_{chem} required to maintain the critical HRR leads to larger heat losses, and once t_{chem} becomes long enough heat losses take over and the flame extinguishes. For the case of PE, the lower $\dot{m}$" allows reducing the oxygen concentration to the point that the increased t_{chem} not only leads to larger heat losses but may also start affecting the rate at which fuel is consumed. Microgravity conditions eliminate convective heat losses and result in heat feedback from the core, which is similar to the addition of an external radiant flux increases $\dot{q}''_{tot}$. However, because the gas phase reaction rate may already be limited, an increase in $\dot{q}''_{tot}$ follows the behavior explained in *Region III* resulting in a small change to the μg LOC and explaining the small ΔLOC observed in PE.

On the other hand, the larger $\dot{m}''$ needed to sustain combustion of ETFE requires a high $\dot{\omega}$ and consequently leads to higher $1g$ and μg LOC values. For the case of no external radiation, the $1g$ and μg extinction arises due to the lack of heat transfer to the unburned solid fuel and not the inability to consume the decomposed fuel. If the gas phase reaction rate was a factor, the addition of external radiation would not extend the flammability limits of ETFE; but as seen in Figures 4.10 and 4.12, the addition of external radiation lowered the LOC in both, $1g$ and μg. Since gas phase reaction is not the limiting factor, increasing

$\dot{q}''_{tot}$ through the addition of $\dot{q}_{ext}$ or elimination of $\dot{q}''_{conv}$ becomes effective in extending the range of oxygen concentrations over which ETFE is flammable. Therefore, it could be said that the low HRP of ETFE resulting in high LOC values is also responsible for the larger ΔLOC.

4.5 Conclusions

The present chapter examines the flammability boundaries of ETFE insulated wires exposed to external radiation in $1g$ and μg. From the results it was found that external radiation is able to extend the flammability limits of ETFE in both, $1g$ and μg. In the experiments, two critical LOC values were identified, the LOC for no external radiation, and the LOC for the maximum external radiation possible with the current experimental setup. Oxygen concentrations above the no external radiation LOC result in flame spread whether or not external radiation is present. For oxygen concentrations between the two LOC values, it is possible for flames to propagate as long as an external radiant flux is present. The magnitude of this external radiation increases with decreasing oxygen concentration. For oxygen concentrations below the maximum external radiation LOC flames extinguish as a result of heat losses, and possibly chemical kinetics. The relationship between oxygen concentration and external radiation can be explained in terms of the attainment of a critical solid mass loss rate. When the oxygen concentration is reduced, flame temperature and the total heat transferred to the solid fuel reduce. The addition of an external radiant flux is able to compensate for such decrease up to a certain point, resulting in an extension of the flammability limits of the material. Microgravity reduces heat losses and has a similar effect to the addition of an external radiant flux. The combination of an external radiant flux and μg are able to further extend the flammability limits of FR materials. Experiments with ETFE showed that the addition of external radiation and μg resulted in flame spread in oxygen concentrations as low as 20.3%.

Comparing the results obtained with ETFE to those available with PE shows that μg has a more pronounced effect on the flammability of ETFE. Examining the thermal properties suggests that due to its lower heat of combustion, ETFE requires a larger fuel mass flux than PE. The larger $\dot{m}''$ associated with ETFE requires higher oxygen concentrations that lead to fast reaction rates and short chemical times. Elimination of natural convection has a similar effect to the addition of $\dot{q}''_{ext}$, an increase in $\dot{q}''_{tot}$. The $1g$ and μg extinction limits of PE are close to each other because the larger t_{chem} not only increases heat losses, but may also affect the gas-phase reaction rate, at which point addition of external heating makes no major difference in the LOC. For the case of ETFE, $1g$ extinction is the result of insufficient mass loss as a result of limited heat transfer to the unburned fuel. Therefore, the elimination of heat losses in μg becomes an effective way of extending the range of oxygen concentrations over which ETFE becomes flammable as evidenced by the larger ΔLOC.

4.6 References

[1] Sandra L. Olson, Paul V. Ferkul, and James S. T'ien. "Near-Limit Flame Spread Over a Thin Solid Fuel in Microgravity". In: *Symposium (International) on Combustion* 22.1 (1989), pp. 1213–1222. DOI: 10.1016/S0082-0784(89)80132-8.

[2] S. L. Olson. "Mechanisms of Microgravity Flame Spread Over a Thin Solid Fuel: Oxygen and Opposed Flow Effects". In: *Combustion Science and Technology* 76.4 – 6 (1991), pp. 233–249. DOI: 10.1080/00102209108951711.

[3] S. Bhattacharjee and R.A. Altenkirch. "The Effect of Surface Radiation on Flame Spread in a Quiescent, Microgravity Environment". In: *Combustion and Flame* 84.1 – 2 (1991), pp. 160–169. DOI: 10.1016/0010-2180(91)90045-D.

[4] S.L. Olson and F.J. Miller. "Experimental Comparison of Opposed and Concurrent Flame Spread in a Forced Convective Microgravity Environment". In: *Proceedings of the Combustion Institute* 32.2 (2009), pp. 2445–2452. DOI: 10.1016/j.proci.2008.05.081.

[5] Masao Kikuchi et al. "Experimental Study on Flame Spread over Wire Insulation in Microgravity". In: *Symposium (International) on Combustion* 27.2 (1998), pp. 2507–2514. DOI: 10.1016/S0082-0784(98)80102-1.

[6] Akira Umemura et al. "Physical Model Analysis of Flame Spreading along an Electrical Wire in Microgravity". In: *Proceedings of the Combustion Institute* 29.2 (2002), pp. 2535–2543. DOI: 10.1016/S1540-7489(02)80309-1.

[7] Osamu Fujita et al. "Ignition of Electrical Wire Insulation with Short-term Excess Electric Current in Microgravity". In: *Proceedings of the Combustion Institute* 33.2 (2011), pp. 2617–2623. DOI: 10.1016/j.proci.2010.06.123.

[8] Yoshitomo Takano et al. "Ignition Limits of Short-term Overloaded Electric Wires in Microgravity". In: *Proceedings of the Combustion Institute* 34.2 (2013), pp. 2665–2673. DOI: 10.1016/j.proci.2012.06.064.

[9] Shuhei Takahashi et al. "Extinction Limits of Spreading Flames over Wires in Microgravity". In: *Combustion and Flame* 160.9 (2013), pp. 1900–1902. DOI: 10.1016/j.combustflame.2013.03.029.

[10] Osamu Fujita, Katsuhiro Nishizawa, and Kenichi Ito. "Effect of Low External Flow on Flame Spread over Polyethylene-insulated Wire in Microgravity". In: *Proceedings of the Combustion Institute* 29.2 (2002), pp. 2545–2552. DOI: 10.1016/S1540-7489(02)80310-8.

[11] Julie Kleinhenz and James S. T'ien. "Combustion of Nomex III Fabric in Potential Space Habitat Atmospheres: Cyclic Flame Spread Phenomenon". In: *Combustion Science and Technology* 179.10 (2007), pp. 2153–2169. DOI: 10.1080/00102200701386172.

[12] Sandra L. Olson, Gary A. Ruff, and Fletcher J. Miller. "Microgravity Flame Spread in Exploration Atmospheres: Pressure, Oxygen, and Velocity Effects on Opposed and Concurrent Flame Spread". In: *38th International Conference on Environmental Systems*. San Francisco, CA: SAE International, June 2008. DOI: 10.4271/2008-01-2055.

[13] David B. Hirsch et al. "Oxygen Concentration Flammability Thresholds of Selected Aerospace Materials Considered for the Constellation Program". In: (2007). URL: http://ntrs.nasa.gov/archive/nasa/casi.ntrs.nasa.gov/20070018178_2007017304.pdf.

[14] David Hirsch, Jim Williams, and Harold Beeson. "Pressure Effects on Oxygen Concentration Flammability Thresholds of Polymeric Materials for Aerospace Applications". In: *Journal of Testing and Evaluation* 36.1 (2008), p. 100975. DOI: 10.1520/jte100975.

[15] David B. Hirsch et al. "Pressure Effects on the Self-Extinguishment Limits of Aerospace Materials". In: *39th International Conference on Environmental Systems*. Savannah, GA: SAE International, July 2009.

[16] Andres F. Osorio et al. "Limiting Conditions for Flame Spread in Fire Resistant Fabrics". In: *Proceedings of the Combustion Institute* 34.2 (2013), pp. 2691–2697. DOI: 10.1016/j.proci.2012.07.053.

[17] J. Drobny. *Fluoroplastics*. RAPRA Review Reports: RAPRA Technology Limited. Smithers Rapra Technology, 2006. ISBN: 9781847350077.

[18] DuPont. *DuPont Tefzel fluoropolymer resin Properties Handbook*. Tech. rep. RWJ223. DuPont Fluoroproducts, 2003. URL: http://www2.dupont.com/KIV/zh_CN/assets/downloads/h96518.pdf.

[19] David Bashford. *Thermoplastics: Directory and Databook*. Springer Netherlands, 1997. ISBN: 9780412733505. DOI: 10.1007/978-94-009-1531-2.

[20] Japanese Aerospace Exploration Agency (JAXA). Unpublished data. 2013.

[21] ASTM Standard D2863-13, (2013). *Standard Test Method for Measuring the Minimum Oxygen Concentration to Support Candle-Like Combustion of Plastics (Oxygen Index)*. West Conshohocken, PA: ASTM International, 2013. DOI: 10.1520/D2863-13. URL: http://www.astm.org.

[22] Richard E. Lyon and James G. Quintiere. "Criteria for Piloted Ignition of Combustible Solids". In: *Combustion and Flame* 151.4 (2007), pp. 551–559. DOI: 10.1016/j.combustflame.2007.07.020.

CHAPTER 5

CONCLUSIONS

At the present moment our understanding of the effects of environmental variables on the flammability of materials has been primarily derived through the investigation of non fire-resistant (NFR) materials, see Chapter 1. The relatively simple burning behavior of such materials has enabled researchers to conduct fundamental level research and understand how variables such as ambient pressure, oxygen concentrations, external radiant flux and microgravity affect piloted ignition and flame spread in solid fuels. However, it still remains unclear if the same behavior applies to fire-resistant (FR) materials, and whether changes in environmental conditions affect both kinds of materials equally. To this date only a limited number of studies have directly measured how ambient pressure[1–4] and microgravity conditions[5] affect the flammability limits of FR materials. Understanding the relationship between flammability limits and environmental conditions is important because there are situations in which actual ambient conditions differ from standard ones. For example, in preparation for a space walk the ambient pressure of a spacecraft is reduced while the oxygen concentration is increased. These conditions in addition to microgravity may increase the risk of fires onboard. Another example constitutes flashover conditions, during which the buildup of hot gases inside a room radiates heat to its surrounding resulting in a near simultaneous auto ignition of the objects inside a room.

This project uses the Limiting Oxygen Concentration (LOC) for flame spread over thin fuels to experimentally investigate the effects of ambient pressure, external radiant heat and microgravity in the flammability limits of FR materials. Results are reported in the form of Flame/No-Flame spread boundaries that have revealed the dependence of the flammability limits such as the LOC, LOI, MOC, etc. with respect to ambient conditions. The major findings of this project with respect to the environmental variables studied can be summarized as follows:

5.1 External Radiation

The addition of an external radiant flux enhances heat transfer to the unburned solid fuel and it is able to extend the flammability limits of NFR and FR materials. There exists a LOC above which flame spread occurs without the addition of an external radiant heat source. Below this limit, an external heat flux is needed for flame spread to occur. The greater the reduction in oxygen concentration, the greater the value of the external radiant flux required. When no external radiation is applied the oxygen concentration and consequently the flame temperature have to be high since the flame acts as the only source of heat. A reduction in the oxygen concentration brings about a reduction in the heat transfer from the flame to the unburned fuel that reduces the solid decomposition rate, and if the reduction is large enough the flame extinguishes. An external radiant flux is an additional source of heat transfer to the unburned fuel that up to a certain extent is able to compensate for the reduction in heat transfer to the unburned solid.

For a given oxygen concentration, oxidizer flow velocity, u_∞, has a small effect in the minimum heat flux for flame spread, $\dot{q}''_{MIN}$. As u_∞ increases the thickness of the boundary layer decreases resulting in a higher convective heat transfer coefficient that increases the convective heat flux, $\dot{q}''_{conv}$, from the flame to the sample. This would suggest a reduction in $\dot{q}''_{MIN}$ when u_∞ increases, however this was not observed in the experiments possibly due to the narrow range of flow velocities tested. In charring and/or intumescent materials such as Nomex, the contribution of $\dot{q}''_{conv}$ to the total heat flux for sustained pyrolysis may be small in comparison to the radiative heat flux, $\dot{q}''_{fr}$, given the high oxygen concentrations required for flame spread. As the FR material content of a material is reduced it becomes possible to sustain flame spread at lower oxygen concentrations and the contribution of $\dot{q}''_{conv}$ becomes more significant. At this point, changes in $\dot{q}''_{conv}$ will result in more noticeable changes in $\dot{q}''_{MIN}$. In Chapter 2 the combination of $\dot{q}''_{ext}$, u_∞ and $[O_2]$ were used to develop flammability boundaries in terms of external radiant flux and oxygen concentration. Although it is likely that the results are specific to the experimental configuration used, the relationships and qualitatively behavior of the flammability boundaries are expected to be valid for both FR and NFR materials.

5.2 Ambient Pressure

Ambient pressure affects the flammability limits of FR materials through the heat transfer from the flame to the unburned solid and flame heat losses to the surroundings. Results showed that as ambient pressure is reduced the LOC increases. For ambient pressures above 70 kPa the change is minimal. However, as ambient pressure drops below 70 kPa reducing ambient pressure results in ever increasing LOC values. The appearance of two regions in the flammability limits can be attributed to changes in the heat transfer form the flame to the solid and heat losses from the fuel sample to the surroundings.

As ambient pressure is reduced the gas phase heat conduction from the flame to the solid fuel is also reduced. Reductions in ambient pressure increase the thermal boundary layer thickness, $\delta_t \propto p^{-1/2}$ resulting in lower heat fluxes from the flame to the solid fuel, $\dot{q}'' \propto (T_f - T_s)/\delta_t$ or $\dot{q}'' \propto (T_f - T_s)p^{1/2}$. At high pressure the change in $\dot{q}''$ is small, but as p is reduced the drop in $\dot{q}''$ becomes larger. This would justify the small increase in LOC values for $p > 70\ kPa$, and the more dramatic change for pressures below 70 kPa observed in the experiment. Increasing the oxygen concentration raises the flame temperature and allows maintaining an adequate heat transfer from the flame to the solid despite the increased separation. At the same time reducing ambient pressure reduces buoyancy induced flows and with it the associated convective heat losses.

Convective heat losses either in force flow, purely buoyant or a combination of both are proportional to $h \propto p^{1/2}$. Therefore in low ambient pressures heat losses are reduced, which result in an increase in the net heat flux to the fuel surface. It is also possible that reduced ambient pressures affect the characteristic chemical time. Decreasing ambient pressure, results in a decrease in the Damkohler number, Da. Once Da decreases below a critical value the flame extinguishes[6]. Increasing the oxygen concentration not only raises the flame temperature but also allows maintaining a short chemical time despite the decrease in ambient pressure.

Examining the Flame/No-Flame spread boundaries in terms of the oxygen partial pressure, p_{O_2}, revealed an approximately linear reduction in p_{O_2} when ambient pressure is decreased. A similar relationship had been previously observed by Hirsch et al.[3] in experiments with different FR polymeric materials and Nakamura and Aoki[7] using thin cellulosic paper samples. The reduction in p_{O_2} as a function of p suggests that is possible for materials to exhibit significantly different flammability behavior when following a constant oxygen partial pressure curve, like for example in normoxic atmospheres similar to those suggested for future spacecraft[8]. Although the reason behind this behavior is not known and constitutes an interesting area of future research, the existence of this nearly linear relationship between p_{O_2} and p could be exploited to develop correlations for predicting the LOC in reduce ambient pressures, which constitutes an active area of fire safety research.

5.3 Microgravity

Limiting Oxygen Concentration (LOC) experiments with ETFE insulated wires subject to an external radiant flux were conducted in normal ($1g$) and microgravity (μg) conditions. Based on these results it was concluded that μg increases the total heat flux to the unburned sample by a eliminating buoyancy induced flows and the associated heat losses. Following the same approach used in Chapter 2, Flame/No-Flame spread boundaries were developed for $1g$ and μg conditions. In these boundaries three distinct regions were observed:

- *Region I*: A high oxygen concentration region in which no external radiation is needed to observe flame spread. The high oxygen concentration in this region results in a fast reaction rate with high flame temperatures that is able to sustain the solid pyrolysis without requiring additional heat input.

- *Region II*: An intermediate region in which the addition of an external radiant flux is able to extend the flammability limit. In this region a reduction in oxygen concentration reduces the flame temperature and decreases the amount of heat transfer from the flame to the solid. The heat transferred by the flame alone is not enough to maintain the pyrolysis process and without an additional heat source the flame stops propagating. As the oxygen concentration drops further away from the *Region I/Region II* boundary greater amounts of additional heat are required in order to observe a propagating flame. The non linear increase of $\dot{q}''_{ext}$ with a decrease in oxygen concentration stems from the importance of radiation heat transfer from the flame to the solid which is proportional to ${T_f}^4$.

- *Region III*: A low oxygen concentration region in which despite the addition of an external radiation a flame fails to propagate. In this region the addition of an external radiant flux is not able to make up the heat transfer deficit and the result is a flame that fails to propagate. The actual position of the *Region II/Region III* boundary is up for discussion since it will change depending on the power of the external radiant heaters used. In the current experiment the maximum external radiant flux used was 25 kW/m^2, therefore, the transition from *Region II* to *Region III* occurs at an oxygen concentration for which the addition of $\dot{q}''_{ext} = 25\ kW/m^2$ does not result in flame spread. It also possible that at the low oxygen concentrations within *Region III* the reduction in oxygen concentration affects the reaction rate and enhances heat losses, particularly in μg conditions as originally suggested by Olson et al.[9, 10].

Microgravity conditions eliminate buoyancy induced flows resulting in differences in flame shape, i.e. teardrop in $1g$ versus spherical flame in μg. Most importantly, μg conditions eliminate buoyancy induced flows eliminating natural convection heat losses and effectively increasing Da. The elimination of natural convection heat losses is analogous to the addition of an external radiant flux ultimately resulting in an increase of the neat heat flux at the fuel surface. The elimination of buoyancy induced flows increases the flow residence time and allows to maintain a Da number above its critical extinction value.

A comparison of the ETFE results under no external radiation to those obtained by Takahashi et al.[11] using PE insulated wires revealed that μg conditions may have a more pronounced effect in FR than in NFR materials. For PE insulated wires the difference between the $1g$ and μg LOC is about 3%, (19% versus 16%) whereas for ETFE insulated wires the differences is around 5.5% (31.5% versus 26%). Examining the thermal properties of both materials suggests ETFE requires a large amount of fuel than PE in order to release

the same amount of energy. The larger amount of fuel associated with ETFE requires higher oxygen concentrations that lead to fast reaction rates and short chemical times. In μg, elimination of natural convection has a similar effect to the addition of $\dot{q}''_{ext}$, an increase in $\dot{q}''_{tot}$. The $1g$ and μg extinction limits of PE are close to each other because the greater energy release per unit fuel of PE requires reducing the oxygen concentration to a point that the larger t_{chem} increases heat losses and possibly affects the gas phase reaction rate. At this point, an increase in $\dot{q}''_{tot}$ has a small effect in the LOC. On the other hand, $1g$ extinction of ETFE is a result of insufficient heat transfer to the unburned solid that results in a slow solid decomposition that is not capable to sustain a flame. Thus, elimination of heat losses in μg conditions becomes an effective way of extending the ranges over which ETFE becomes flammable as evidenced by the larger ΔLOC. To the knowledge of the author the comparison between the $1g$ and μg flammability limits of ETFE and PE is the first of its kind and highlights the need of investigating the flammability of FR materials under varied environmental conditions.

5.4 Future Work

This research has developed Flame/No-Flame spread boundaries for different FR materials under varied ambient conditions. From the obtained results it can be concluded that flammability limits of both, non fire-resistant and fire-resistant materials depend not only on the material characteristics but also on the surroundings. Flammability limits such as LOC, LOI, MOC, etc. are specific to a particular set of conditions and should not be interpreted as a constant material property, specially as ambient conditions depart from the reference conditions. The methodologies, results and discussions presented in Chapters 2, 3, 4 constitute an early approach towards the understanding of the effects of environmental variables on the flammability of FR fabrics, and more specifically the sensitivity of flammability limits to ambient conditions. In order to achieve this goal it would be advisable to concentrate future efforts on the following areas: experimental work, numerical modeling, and integration into standardized flammability testing.

Although the experimental apparatuses used during the experiments were comparable to each other, the fact remains that each of them is a different apparatuses. As already pointed out, flammability limits are dependent on many factors, including testing methodologies. Hence, developing a flexible testing apparatus that allows testing different kinds of materials under a varied number of conditions would facilitate future experimental work. The apparatus described in Chapter 4 is a step in that direction, however, it only allows testing of electrical cables and does not accommodate thin fuel samples such as fabrics, sheets, etc. A common testing apparatus would allow conducting direct comparisons between the effects of the different environmental variables and would facilitate testing of an increased number of materials. Increasing the number of materials tested is important because it will provide a larger set of data from which conclusions can be drawn. A larger set of data would also fa-

cilitate the development of correlations and/or simplified theories that could predict changes in flammability limits of materials.

Fire-resistant (FR) materials undergo complex pyrolysis processes when exposed to heat that cannot be accurately predicted using one-step solid decomposition reactions. Processes such as charring and intumescence require solving mass, energy and species conservation equations as described by Lautenberger[12]. However, in order to use such numerical models the first step should be the measurement of relevant condensed fuel and reaction parameters for FR materials. At the present moment many of these parameters are not known and constitute an important barrier in the development of numerical models. The ability to accurately simulate the pyrolysis process of FR materials would be a major step towards the prediction of material flammability behavior under different ambient conditions. Once a suitable pyrolysis model with proper parameters is developed it will be possible to replicate experimental results, or make predictions for conditions in which it is not possible to conduct experiments.

Applicability constitutes the ultimate goal of the research described in this work. Additional experimental work and development of numerical models constitute important steps in order to better understand the flammability of FR materials. Taking this newfound knowledge and using it to improve fire safety is the real contribution of this work. There are several possible ways in which this could be accomplished. One of them is the development of new complementary standardized flammability tests that are capable of capturing relevant flammability behavior over a range of ambient conditions. For example, NASA Standard 6001[13] Test 1 and Test 4 describe flammability testing of materials and electrical cables respectively. The Pass/Fail nature of this test does not yield any relevant flammability measurement that would allow ranking materials or adopting minimum threshold values for particular applications. Adoption of testing methodologies similar to those described in the present work can produce flammability maps that provide more information than Pass/Fail methods while presenting a clearer picture of the flammability of materials under different ambient conditions.

5.5 References

[1] David B. Hirsch et al. "Oxygen Concentration Flammability Thresholds of Selected Aerospace Materials Considered for the Constellation Program". In: (2007). URL: http://ntrs.nasa.gov/archive/nasa/casi.ntrs.nasa.gov/20070018178_2007017304.pdf.

[2] David Hirsch, Jim Williams, and Harold Beeson. "Pressure Effects on Oxygen Concentration Flammability Thresholds of Polymeric Materials for Aerospace Applications". In: *Journal of Testing and Evaluation* 36.1 (2008), p. 100975. DOI: 10.1520/jte100975.

[3] David B. Hirsch et al. "Pressure Effects on the Self-Extinguishment Limits of Aerospace Materials". In: *39th International Conference on Environmental Systems*. Savannah, GA: SAE International, July 2009.

[4] Julie Kleinhenz and James S. T'ien. "Combustion of Nomex III Fabric in Potential Space Habitat Atmospheres: Cyclic Flame Spread Phenomenon". In: *Combustion Science and Technology* 179.10 (2007), pp. 2153–2169. DOI: 10.1080/00102200701386172.

[5] Sandra L. Olson, Gary A. Ruff, and Fletcher J. Miller. "Microgravity Flame Spread in Exploration Atmospheres: Pressure, Oxygen, and Velocity Effects on Opposed and Concurrent Flame Spread". In: *38th International Conference on Environmental Systems*. San Francisco, CA: SAE International, June 2008. DOI: 10.4271/2008-01-2055.

[6] A.C. Fernandez-Pello and T. Hirano. "Controlling Mechanisms of Flame Spread". In: *Combustion Science and Technology* 32.1 – 4 (1983), pp. 1–31. DOI: 10.1080/00102208308923650.

[7] Y. Nakamura and A. Aoki. "Irradiated Ignition of Solid Materials in Reduced Pressure Atmosphere with Various Oxygen Concentrations for Fire Safety in Space Habitats". In: *Advances in Space Research* 41.5 (2008), pp. 777–782. DOI: 10.1016/j.asr.2007.03.027.

[8] Kevin E. Lange et al. *Bounding the Spacecraft Atmosphere Design Space for Future Exploration Missions NASA/CR-2005-213689*. 2005. URL: http://spaceflightsystems.grc.nasa.gov/repository/NRA/cr-2005-213689.pdf.

[9] Sandra L. Olson, Paul V. Ferkul, and James S. T'ien. "Near-Limit Flame Spread Over a Thin Solid Fuel in Microgravity". In: *Symposium (International) on Combustion* 22.1 (1989), pp. 1213–1222. DOI: 10.1016/S0082-0784(89)80132-8.

[10] S. L. Olson. "Mechanisms of Microgravity Flame Spread Over a Thin Solid Fuel: Oxygen and Opposed Flow Effects". In: *Combustion Science and Technology* 76.4 – 6 (1991), pp. 233–249. DOI: 10.1080/00102209108951711.

[11] Shuhei Takahashi et al. "Extinction Limits of Spreading Flames over Wires in Microgravity". In: *Combustion and Flame* 160.9 (2013), pp. 1900–1902. DOI: 10.1016/j.combustflame.2013.03.029.

[12] Chris Lautenberger and Carlos Fernandez-Pello. "Generalized pyrolysis model for combustible solids". In: *Fire Safety Journal* 44.6 (2009), pp. 819–839. DOI: 10.1016/j.firesaf.2009.03.011.

[13] *Flammability, Odor, Offgassing, and Compatibility Requirements and Test Procedures for Materials in Environments that Support Combustion, NASA STD 6001*. 1998. URL: http://www.nasa.gov/centers/johnson/pdf/485934main_NASA-STD-(I)-6001A%20Released.pdf.

Appendix A

Reduced Ambient Pressure Experimental Data

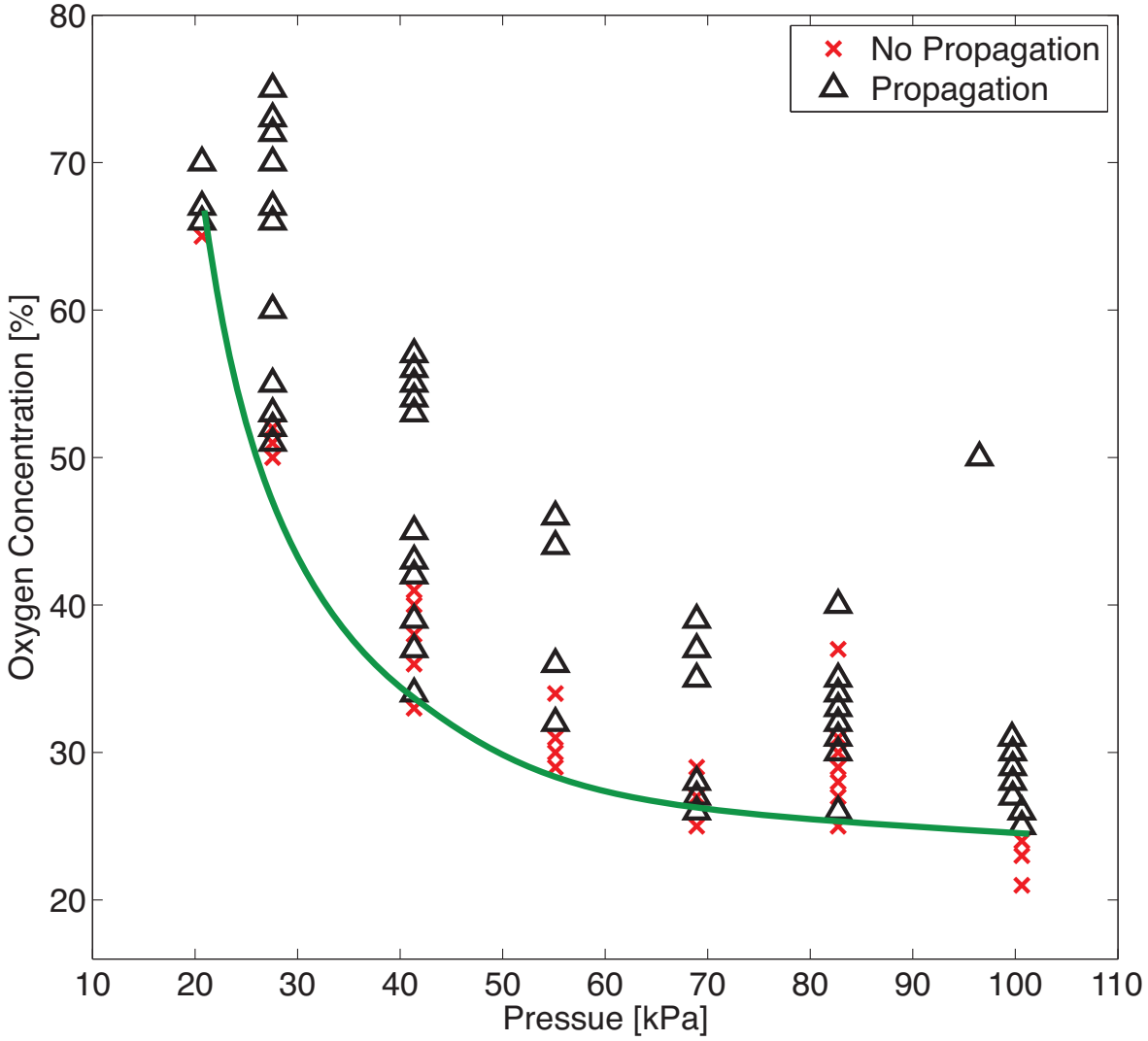

Figure A.1: Concurrent-Horizontal flame spread boundary plot for Nomex HT90-40.

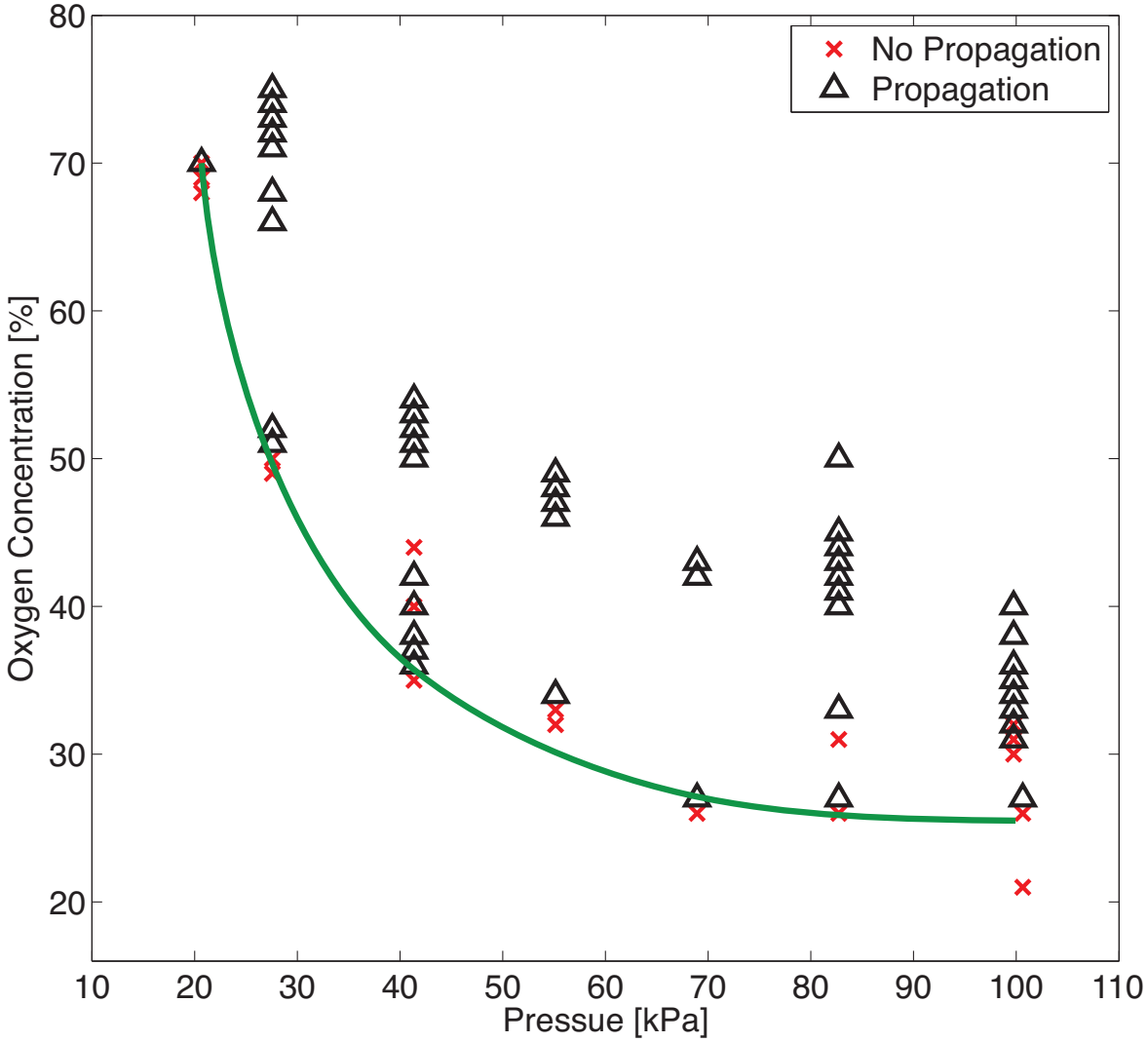

Figure A.2: Opposed-Horizontal flame spread boundary plot for Nomex HT90-40.

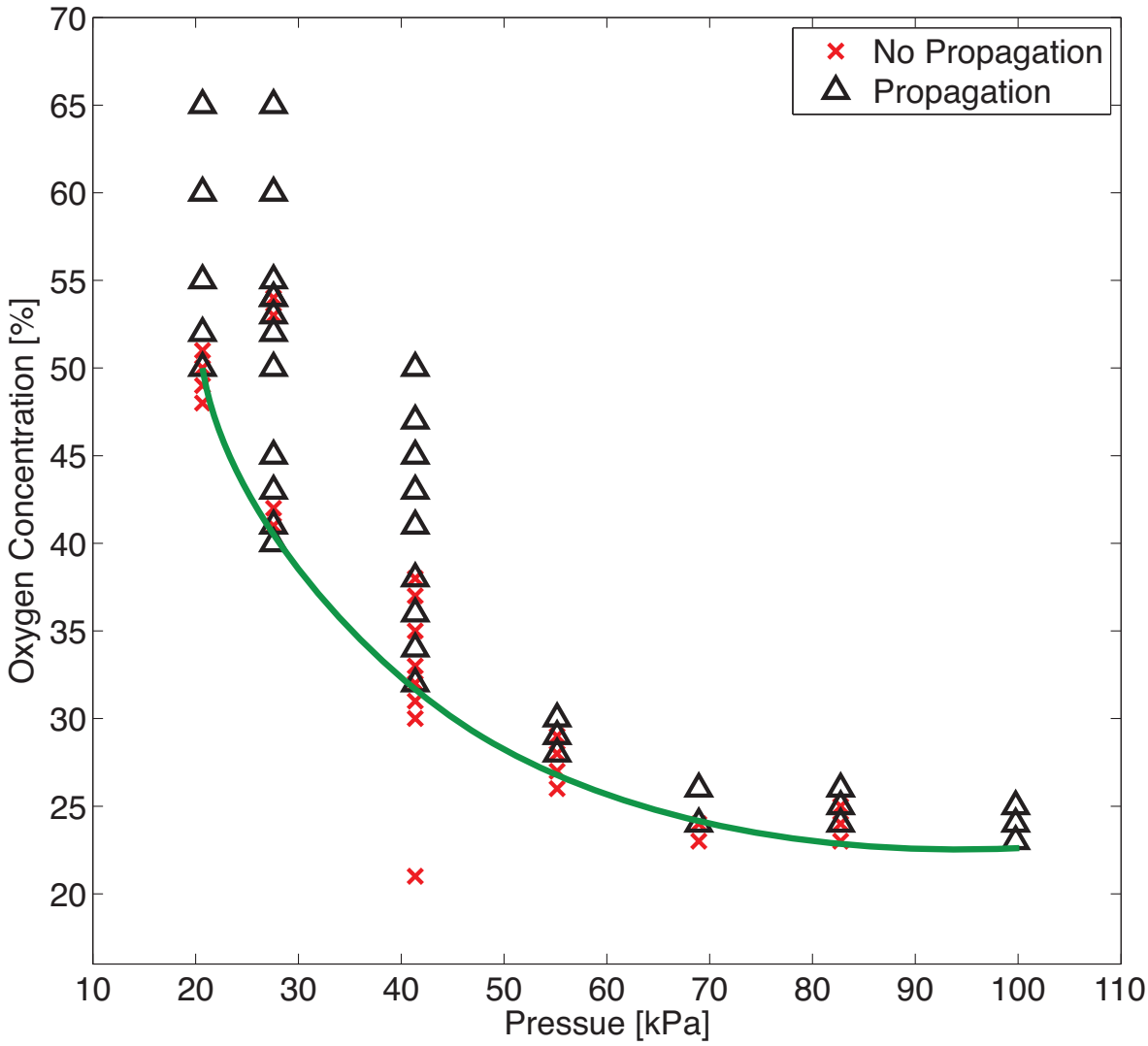

Figure A.3: Concurrent-Vertical flame spread boundary plot for Nomex HT90-40.

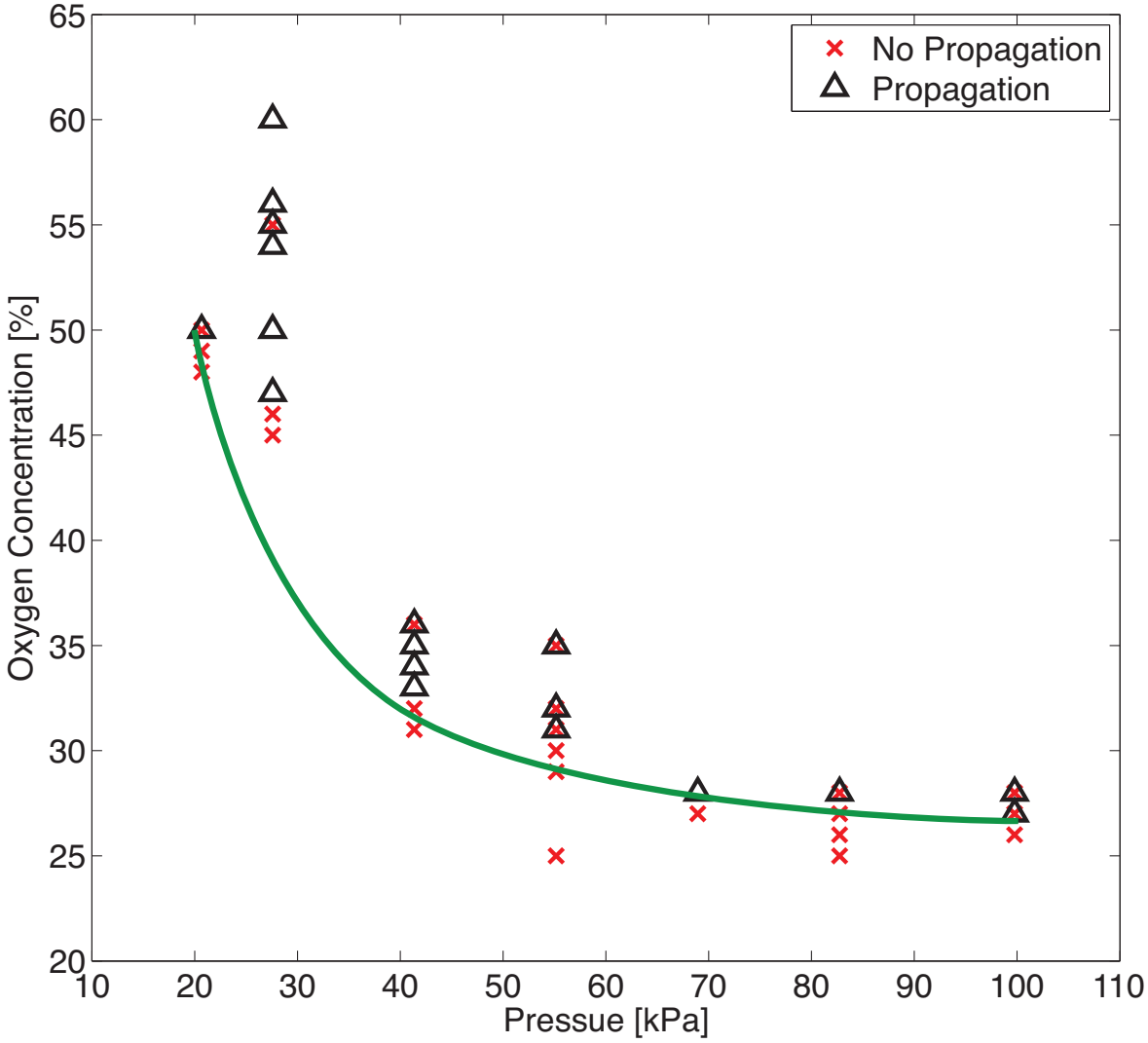

Figure A.4: Opposed-Vertical flame spread boundary plot for Nomex HT90-40.

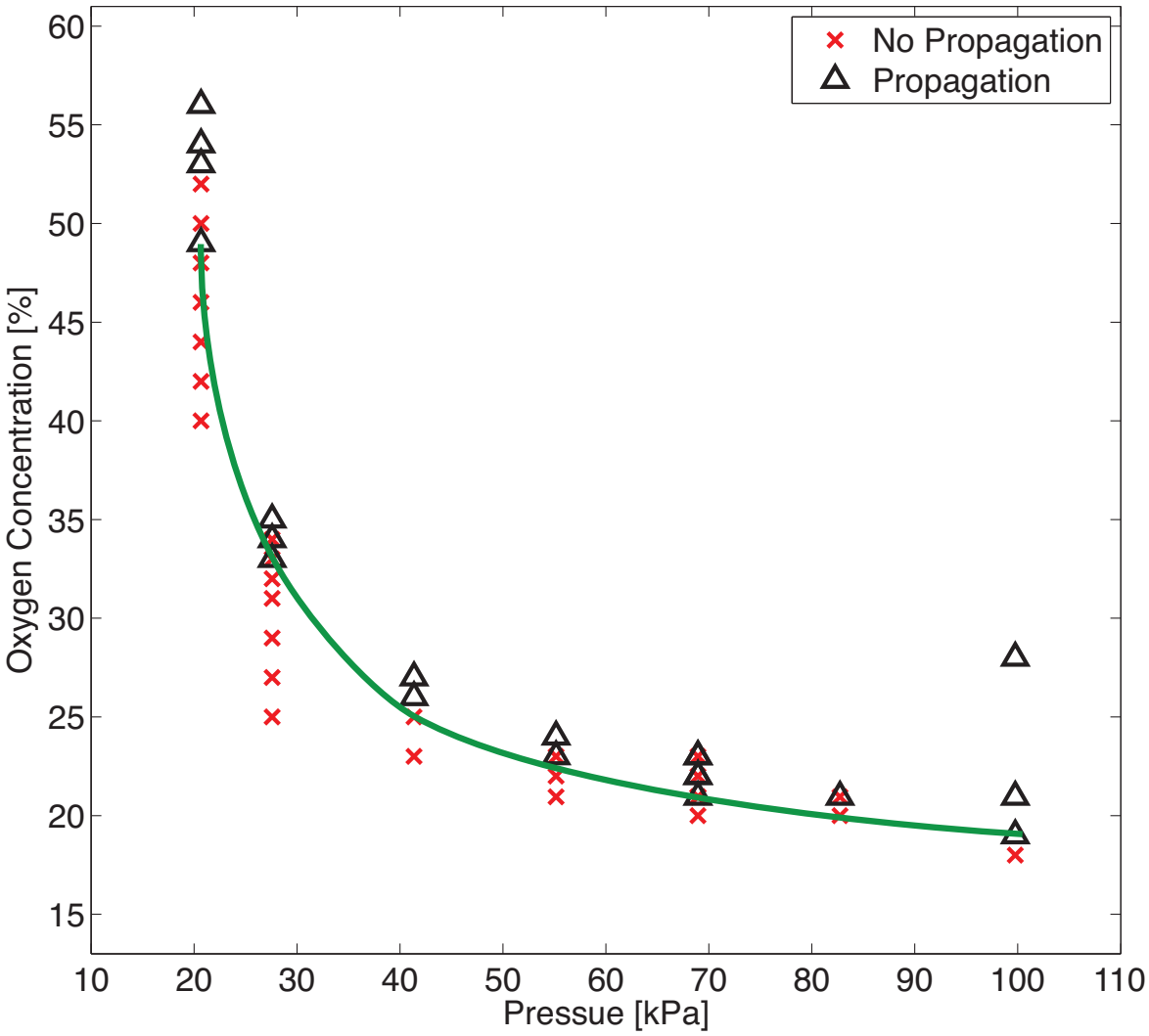

Figure A.5: Concurrent-Horizontal flame spread boundary plot for Cotton/Nylon/Nomex fabric blend.

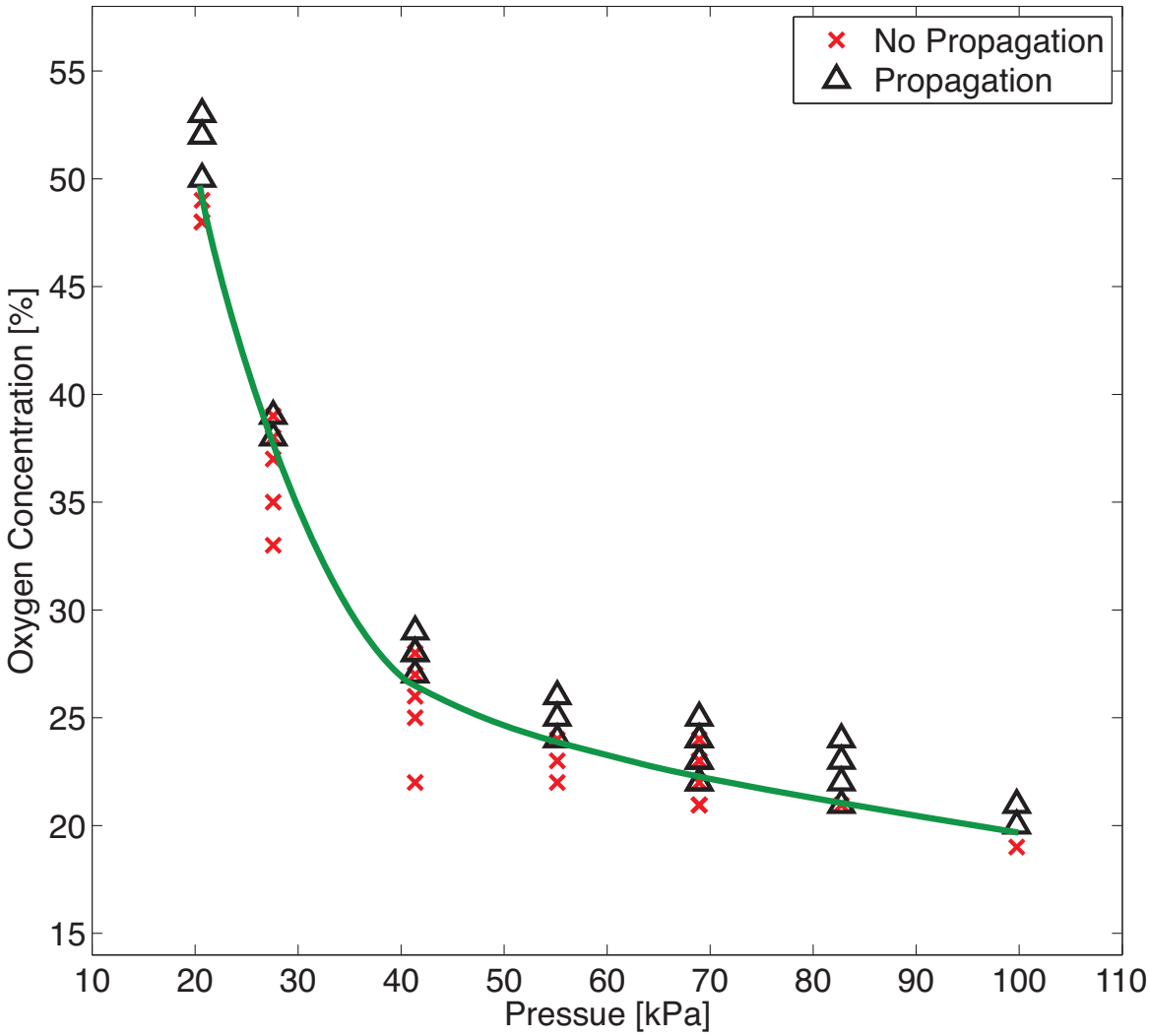

Figure A.6: Opposed-Horizontal flame spread boundary plot for Cotton/Nylon/Nomex fabric blend.

Appendix B

External Radiant Heaters Calibration

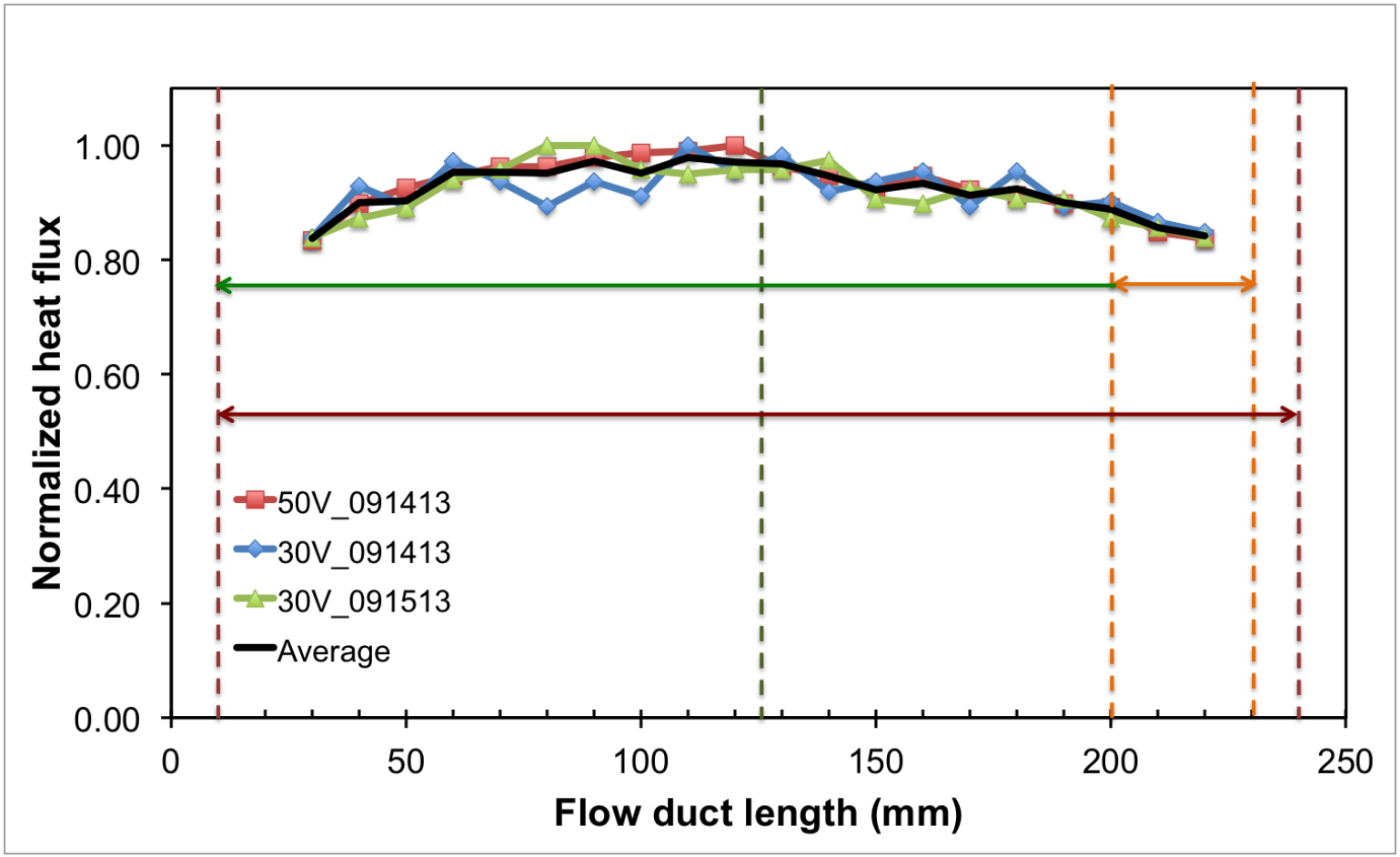

Figure B.1: Normalized heat flux distribution along flow duct. Red lines represent flow duct length. Orange lines represent igniter coil wire. Green line represent flow duct half-length.

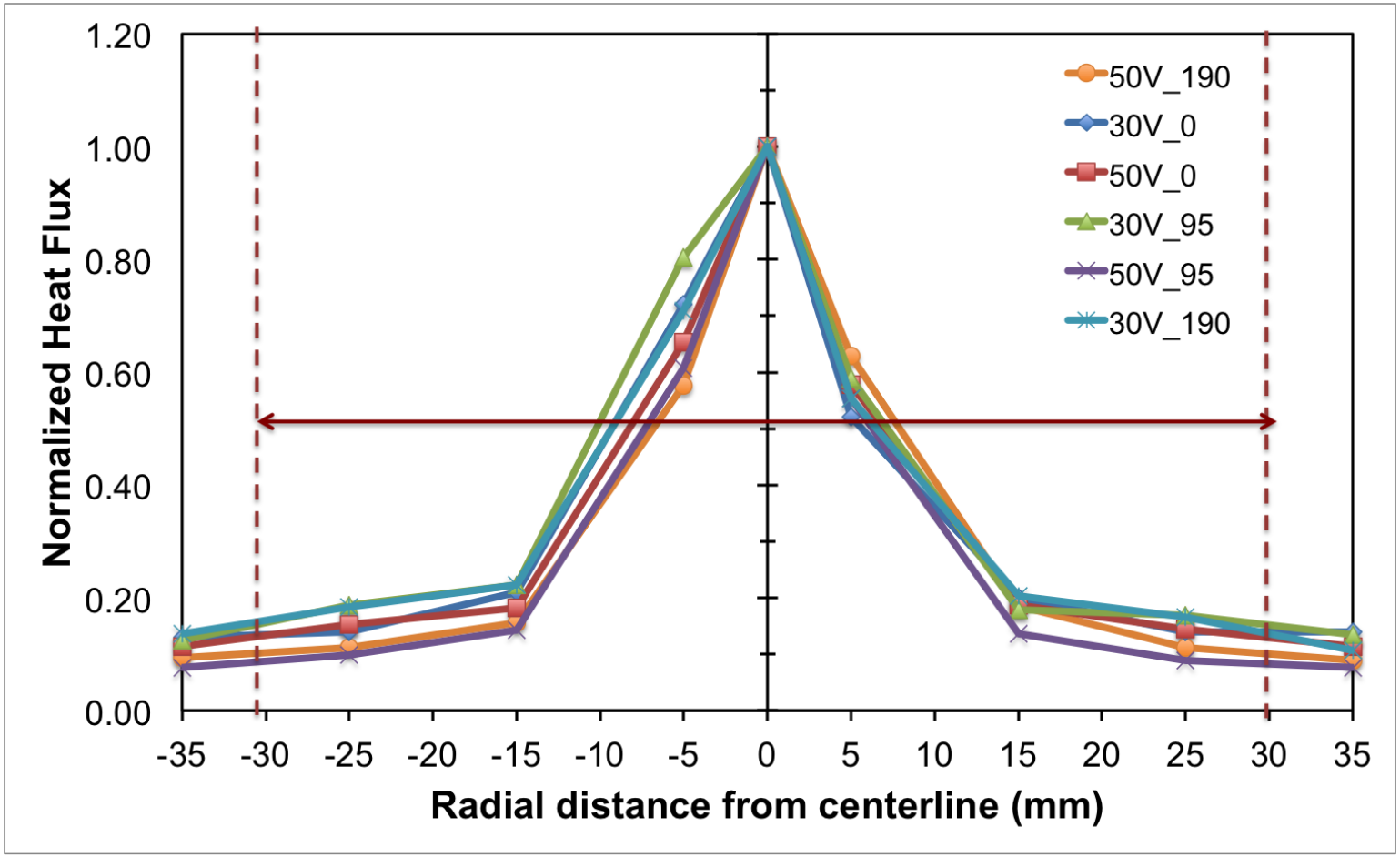

Figure B.2: Normalized heat flux distribution along flow duct radius. Red lines represent tube inside radius.

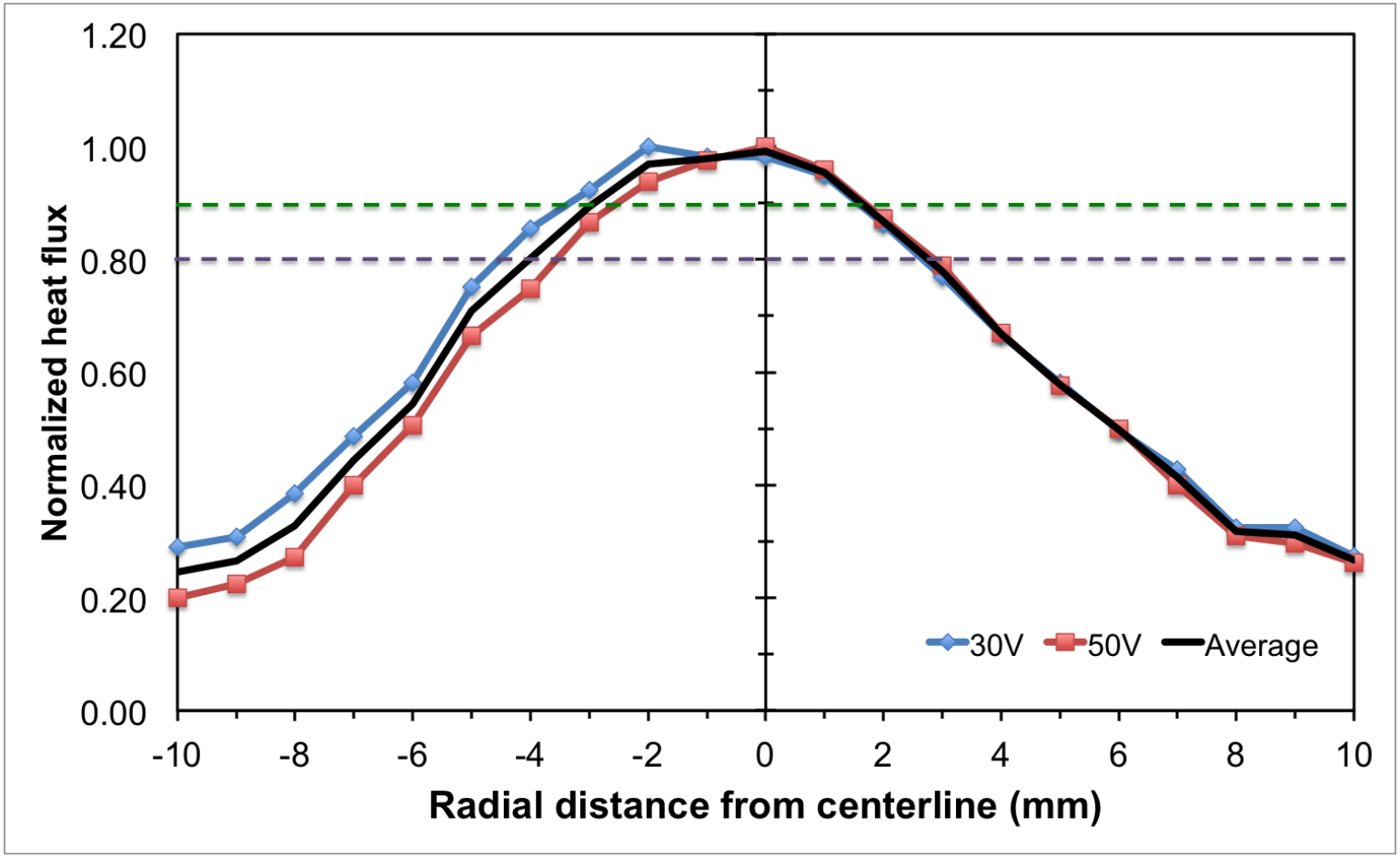

Figure B.3: Detailed normalized heat flux distribution along flow duct radius.